Sumea Klokic, BSc.

Investigations and process development for an efficient poly(oxymethylene dimethyl ether) (OME) fuel production

Master's Thesis

to achieve the university degree of

Master's degree program: Chemistry

Master of Science

submitted to

Graz University of Technology

Supervisor

Ao. Univ.-Prof. Mag. rer. nat. Dr. phil. Martin Mittelbach

Institute

Institute of Chemistry, University of Graz

Graz, June 2019

Eidesstaatliche Erklärung

Ich erkläre an Eides statt, dass ich die vorliegende Arbeit selbstständig verfasst, and als die angegebenen Quellen/Hilfsmittel nicht benutzt und die den benutzten Quellen wörtlich und inhaltlich entnommene Stellen als solche kenntlich gemacht habe. Das hochgeladene Textdokument in TUGRAZonline ist identisch mit der hier vorliegenden Masterarbeit.

Graz, am_____ Unterschrift_____

Affidavit

I declare that I have authored this thesis independently, that I have not used other than the declared sources/resources, and that I have explicitly indicated all material which has been quoted either literally or by content from the sources used. The text document uploaded to TUGRAZonline is identical to the present master‘s thesis.

Graz, the_____ Signature_____

Acknowledgements

Firstly, I want to thank Ao. Univ.-Prof. Mag. rer. nat. Dr. phil. Martin Mittelbach as my master thesis advisor for the innovative topic, great assistance and understandings regarding my practical work, thesis or any personal issues. Moreover, I want to thank him, who supported and steered me during this work in the right direction and encouraged me to successfully finalize my master thesis.

I would like to thank DI Markus Hochegger for his expertise in almost any trouble spot I ran into regarding synthesis or autoclave technique, his exceptional support during the writing of the manuscript and my master thesis. Further I want to thank Dr. DI Philipp Neu for his great support regarding analytical issues providing great support for whichever question I had. I also want to thank Mag. Dr. rer. nat. Sigurd Schober for his helpful contributions during discussions of my thesis as well as for his support regarding analytical tasks.

Finally, I want to express my profound gratitude to all members of the working group *NAWARO* for their kind welcome and assistance regarding any difficulty arising especially during my practical work of my thesis. Thank you all very much for the encouraging talks, great know-how and a helping hand when needed. At this point, I want to thank my parents for their support who enabled, encouraged and supported me.

Abstract

Oxygenates such as poly(oxymethylene dimethyl ethers) (OME) with the structure $H_3C – O – (CH_2O)_n – CH_3$ are attractive as an alternative diesel fuel especially for OME_n with chain lengths n = 3 – 5 due to their applicability for direct blending with conventional diesel fuel. Hence, large-scale pilot plants especially in Germany and China produce OME compounds, which are mainly driven by the development of economically feasible processes based on renewable feedstocks utilizing acidic catalysts for the at present most detailed investigated educts dimethoxymethane, trioxane, methanol and para-formaldehyde. In this regard, kinetic studies on the production of OMEs are crucial for their application as environmentally benign and promising components for designing diesel fuels focusing on high $OME_{3–5}$ yields, low side-product formation and plain synthetic procedures.

For the first time a detailed kinetic investigation was conducted for the anhydrous OME synthesis starting from dimethoxymethane and trioxane at ambient conditions catalyzed by sulfuric acid, methanesulfonic acid (MSA) and a formerly commercially available solid acid, Deloxan®. Thus, the influence of different reaction parameters such as temperature, molar educt ratio, reaction time and finally reaction pressure on the OME_n yield (with n = 2 – 12) were surveyed. It was found that the highest OME_{2-8} yields were obtained at catalyst loadings of 1.0 wt% sulfuric acid (60.0 wt%), 3.5 wt% MSA (64.9 wt%) and 1.7 wt% Deloxan® (60.3 wt%) for the anhydrous synthesis under atmospheric conditions, 80°C reaction temperature and 60 min reaction time.
At these reaction conditions, the $OME_{3–5}$ product yields were found the highest for MSA with 32.7 wt%, for sulfuric acid with 32.1 wt% and for Deloxan® with 30.1 wt%. Results obtained for pressurized reactions (9 bar N_2) were found to exhibit a deviant product distribution for the respective catalysts. However, following the aqueous OME production pathway at pressurized conditions using the educts methanol/trioxane and dimethoxymethane/para-formaldehyde comparably low $OME_{3–5}$ yields (3 – 9 wt%) were achieved.

Hence, the OME synthesis performed at ambient pressure was found to enable a quick product formation, high OME_{3-5} product yield for the corresponding catalysts, low side product formation for the anhydrous reaction pathway following a Schulz-Flory distribution leading to sequential formaldehyde incorporation into the growing OME chain. These results obtained herein were found promising compared to other acidic catalysts for OME synthesis reported in literature.

Kurzzusammenfassung

Sauerstoffhaltige Verbindungen wie beispielsweise Poly(oxymethylene dimethyl ether) (OME) mit der chemischen Struktur $H_3C\text{-}O\text{-}(CH_2O)_n\text{-}CH_3$ erlangten an Bedeutung aufgrund ihrer ausgezeichneten Mischbarkeit mit konventionellem Dieseltreibstoff. Vor allem OME_n mit der Kettenlänge n = 3 – 5 erwiesen sich in ihren physikalischen und chemischen Eigenschaften als besonders geeignet als Dieseladditive. Motiviert durch ökonomisch nachhaltige Prozesse produzieren einige große Pilotanlagen in Deutschland und China OME im großen Maßstab, basierend auf erneuerbaren Ressourcen ausgehend von Dimethoxymethan, Trioxan, Methanol oder para-Formaldehyd. In dieser Hinsicht sind kinetische Studien von äußerster Wichtigkeit in Bezug auf die Produktion von OME und ihre Anwendung als alternative, nachhaltige Dieseltreibstoffe. Besondere Beachtung wird auf hohe $OME_{3–5}$ Ausbeuten, geringe Bildung von Nebenprodukten und einfache Synthesen gelegt.

Erstmalig wurde eine Synthese sowie eine detaillierte kinetische Studie von OME katalysiert mit Schwefelsäure, Methansulfansäure (MSA) und einem ehemals kommerziellen heterogenen Katalysator, Deloxan® bei Atmosphärendruck durchgeführt. Für die Synthese ausgehend von Dimethoxymethan und Trioxan wurde die Änderung der Reaktionsparameter Temperatur, das molare Eduktverhältnis, Reaktionszeit und Reaktionsdruck auf die OME_n (mit n = 2 – 12) Ausbeute untersucht. Die höchsten $OME_{2–8}$ Ausbeuten für die wasserfreie Synthese bei Atmosphärendruck wurden mit den Katalysatormengen von 1.0 wt% Schwefelsäure mit 60.0 wt% Ausbeute, 3.5 wt% MSA mit 64.9 wt% und 1.7 wt% Deloxan® mit 60.3 wt% erzielt. Bei den entsprechenden Katalysatormengen ergaben die entsprechenden $OME_{3\text{-}5}$ Ausbeuten für MSA den höchsten Produktanteil mit 32.7 wt%, für Schwefelsäure mit 32.1 wt% und für Deloxan® mit 30.1 wt%. Im Vergleich, unter Anlegen eines Reaktionsdrucks (9 bar N_2) für die OME Synthese mit den entsprechenden Katalysatoren resultierte in einer abweichenden Produktverteilung. Diese Ergebnisse für die wässrige OME Synthese ausgehend von Methanol oder para-Formaldehyd sind weniger vielversprechend und ergaben nur 3 – 9 wt% an $OME_{3–5}$ Produktausbeute.

Somit ergab die hiermit untersuchte OME Synthese eine schnelle und einfache wasserfreie Syntheseroute mit geringer Nebenproduktbildung und hohen OME Ausbeuten für die entsprechenden homogenen und heterogenen Katalysatoren. Zudem folgt die Produktbildung der Schulz-Flory Verteilung und folglich einer sequentiellen Formaldehyd-Monomer Inkorporation in die wachsenden OME Kette. Demnach sind die experimentell gefunden Produktausbeuten für die entsprechenden Katalysatoren äußerst vielversprechend im Vergleich zu in der Literatur untersuchten sauren Katalysatoren für die OME Synthese.

BuOH	butanol
cat.	catalyst
CDF	conventional diesel fuel
CH_2O	formaldehyde units
CO	carbon monoxide
DEE	diethoxyethane
DMF	dimethylformamide
DMM/OME_1	dimethoxymethane, methylal
DOC	diesel oxidation catalyst
DPF	diesel particulate filter
EF	ethylformals
EGR	exhaust gas regulation
ETBE	ethyl-*tert*-butyl ether
ETIC	external temperature sensor
FA	formaldehyde
FAME	fatty acid methyl esters
GC-FID	gas chromatography with flame ionization detector
GC-MS	gas chromatography with mass spectrometry
GHG	greenhouse gas
Gly	glycols
HF	hemiformals
HHV	higher heating value
HJ	heating jacket
HVO	hydrogenated vegetable oils
ICP-MS	inductively coupled plasma mass spectrometry
ISTD	internal standard (THF, dioxane)
ITS	internal temperature sensor
LHV	lower heating value
MeOH	methanol
MSA	methanesulfonic acid
MTBE	methyl-*tert*-butyl ether
n	number of CH_2O units
NO_x	nitrogen oxide (NO, NO_2)
OEE	oxyethylene ethers
OESI	oxygen extended sooting index

OME	poly(oxymethylene) dimethyl ether
pFA	paraformaldehyde
PM	particulate matter
PN	particulate number
RRF	relative response factors
RT	room temperature
SCR	selective catalytic converter
ST	storage tank
T	temperature (in degree, °C, or Kelvin, K)
THF	tetrahydrofuran
TRI	trioxane
V	valve
wt%	weight fraction
X	conversion in %
Y	mass selectivity in wt%

Content

1.Introduction

Combustion of diesel fuel is proven to lead to the formation of hazardous exhaust gas emissions, which contribute vastly to air pollution. At present, one of the main struggles which have to be overcome to pave the way for future fuels is the combination of sustainability, reduction of emissions focusing particularly on CO_2-neutrality, technical functionality and hence the environmentally feasible development of such (*1–3*). The desire for alternative fuels was encouraged with the major objective to overcome difficulties known for petrol-based diesel fuels (*1, 3*). According to the International Agency for Research on Cancer exhaust emissions from petrol-based diesel fuels are classified as carcinogenic to humans. Thus, current climate protection legislations stress the importance of estimating real driving emission regulations (RDE) focusing particularly on NOx, soot and other pollutants (*3–5*). Bio-based diesel fuels as an alternative to fossil fuels were examined extensively by various researchers concluding that biodiesel can reduce life-cycle CO_2 emissions (*3, 6*). The combustion of biodiesel was furthermore found to reduce carbon monoxide emissions (CO) with respect to fossil fuel (*3, 7*). However, since the soot reduction is strongly correlated to the oxygen content, fatty acid methyl esters (FAMEs) exhibiting an oxygen content of about 10% (*3, 7–10*) are referred to control soot reduction (*3, 8*). Hence, the survey for alternative diesel fuels is still a major issue regarding exhaust emissions.

In recent years, synthetic fuels derived either synthetically or from biomass attracted particular attention, such as poly(oxymethylene) dimethyl ethers, also known as OME, POME, POMDME or DMM_n (*1, 3*). OME, as oligomeric homologues of dimethoxymethane (DMM) with the structure H_3C-$(OCH_2)_n$-O-CH_3, n = CH_2O being the formaldehyde (FA) repeating unit, received increasing importance based on their chemical composition and their advantageous physical properties making them applicable as diesel additives and alternative for diesel fuel (*1*). Compared to biodiesel, the oxygen content of OMEs has been found in the range between 42 and 53 wt% (*3, 11*). The high oxygen content enhances an increased soot reduction compared to both, biodiesel and diesel (*3, 4, 11*). In this regard, the optimum chain length *n* of OME_n for blending into diesel fuel is n = 3 – 5 (*11*). Various studies showed that under some particular combustion conditions blending of diesel fuel with OME_{3-5} decreases furthermore unburned hydrocarbons (HC) and CO emissions compared to non-blended diesel fuels (*1, 3, 5, 8, 12–14*).

At present several industrial processes were developed based on acid catalyzed anhydrous or aqueous OME synthesis either by homogeneous liquid catalysts such as sulfuric acid or heterogeneous catalysts e.g. various ionic resins, zeolites and others (*15*). There are some issues that have to be addressed for the synthesis of OME, which are (i) inexpensive catalyst, (ii) promotion of high conversions of educts (iii) high selectivity of $OME_{n>1}$ advantageously n = 3 – 5, (iv) simple removal of the catalyst from the reaction mixture, and last but not least, (v) recyclability (*2, 3*). Thus, much attention has been devoted to heterogeneous catalysts regarding catalyst characterization, kinetic studies and recycling performance upon OME synthesis. However, no detailed kinetic studies for the liquid catalysts sulfuric acid and

methanesulfonic acid were reported for OME synthesis performed at ambient conditions (*3*). Moreover, Deloxan® ASP as a formerly commercially available solid-acid catalyst, consisting of polysiloxanes bearing alkylsulfonic acid groups was utilized for OME synthesis. This was supported due to some of its advantageous properties (*16*) such as for example the excellent activity for this type of solid acids compared to polystyrene based cationic resins (*17*).

The main focus in this work was a kinetic study for the catalysts sulfuric acid, MSA and Deloxan® based on the work reported by Li and co-workers (*18*) comprising a reaction procedure for the synthesis of OME catalyzed by sulfated titanium conducted at ambient pressure. The stoichiometric ratio of DMM and trioxane (TRI) as starting educts for the OME synthesis at ambient conditions was varied as well as the catalyst loading, reaction time and reaction temperature focusing on differences of the OME_n yield with n = 2 – 12 (*3*). Under pressurized conditions methanol (MeOH), DMM, TRI and para-formaldehyde (pFA) were investigated for a study on reaction pressure and educt variation (*3*). Moreover, apart from investigations on OME synthesis, a detailed approach for OME quantification by GC-FID was developed including a multi-step distillation of the OME product mixture for purification of OME_n required for internal standardization. The latter was motivated due to rather vague procedures in literature regarding OME quantification.

2.1. Diesel fuels

At present, diesel powered engines are most commonly used in on-road (vehicles, trains, ships) as well as in off-road transporting (industrial machinery) (*19*). Although diesel engines have been employed in many different fields such as power generation, farming and constructing, diesel engines are accounted as major contributors to environmental pollution with particulate matter (PM) and nitrogen oxides (NO_x) as the major contributors (*19*). Today's diesel engines are designed with engines exhibiting a high number of revolutions and high torque at low fuel consumption (*20*) and therefore, 'cleaner' fuels are in demand with comparable efficiencies to conventional fuels producing lower emissions upon combustion (*21*). Exhaust gas regulations for the emission of carbon monoxide (CO) and unburned hydrocarbons (HC) were established in the 1970s by the European community. At present, emission regulations were set by the Euro-Norm VI as provided in **Table 1**, whereas in the USA both, the EPA- and CARB – legislations regulate diesel emissions (*22, 23*).

Table 1 Euro VI compression ignition emission limits for passenger cars (up to 9 persons) (*23*)

Emissions	Euro VI[a]
NO_x [mg/km]	80
HC + NO_x [mg/km]	170
CO [mg/km]	500
Particulate matter (PM) [mg/km]	4.5
Particulate Number (PN) [Nb/km]	6.0*E11[b]

[a] Euro 6b, 6c, 6d
[b] E11 fuel

In Europe, diesel fuel is regulated by the EN 590 (*24*), whereas in the USA the AST D975 regulates the fuel properties (*25*). An excerpt of some regulated requirements for conventional diesel fuel is provided in **Table 2**. Thus, much effort has been done for the reduction of hazardous pollutants, such as the reduction of the carcinogenic pollutant NO_x by the Selective Catalytic Converter system (SCR) employed by injection of urea (*20*). Moreover, at present the reduction of particles is possible up to 99% by siliciumcarbide based particle filters, which can moreover be regenerated (*20*). A brief overview of the existing technologies for the reduction of diesel engine exhaust gases will be covered in section *2.1.1*.

Diesel as a fuel comprises a mixture of different hydrocarbons and can be blended by various additives such as amylnitrate, ethylhexylnitrate, biodiesel and others (*26*). The prior bearing reactive nitrate or nitrite functional groups were especially utilized as ignition accelerators, whilst other additives can be employed to enhance other properties such as the cold filter plugging behavior (*27*).

Table 2 Selected requirements for diesel fuels by EN 590 (*24*))

	EN 590 (*24*)
Boiling range [°C]	170 – 390
Cetane Number	> 51
Density [g/cm³]	0.82 – 0. 84
Flash point [°C]	> 55
Lubricity [µm]	< 460
Viscosity [mm²/s]	2.0 – 4.5
Polycyclic aromatic hydrocarbons (PAH) [% wt%]	< 11
Total contamination [mg/kg]	< 24
Distillation recovered at 250°C and 350°C, 95% [vol%]	< 65 to 85
Carbon residue of 10% distillate residue [% wt%]	< 0.3

Oxygenated diesel fuel additives such as methyl-*tert*-butylether (MTBE) and ethyl-*tert*-butylether (ETBE) are commonly used as they are low-costing, easy to synthesize, non-toxic and renewable (*20, 28, 29*). Moreover, oxygenated fuel additives are highly desired since their emission-reducing properties are strongly correlated to the amount of oxygen (*20*). Other oxygenated compounds for blending with diesel fuels including ethers, acetals and a novel type of compound, namely oligomeric poly(oxymethylene dimethyl ethers) (OME). The prior mostly lack to fulfill diesel specification such as ignition temperature, viscosity or toxicity (*20*). Especially higher homologues of dimethoxymethane (DMM), as the smallest representative of the OME compounds, were found to exhibit several advantageous properties, which will be described and discussed in detail in the next sections.

2.1.1. Diesel engine exhaust gas aftertreatment

Diesel exhaust comprises gaseous, liquid and solid components, with some being referred to have significant environmental and health implications (*30*). In general, diesel emissions originate from incomplete combustion producing carbon monoxide (CO), soot and unburned hydrocarbons (HC), which can react further forming both, polynuclear aromatic hydrocarbons (PAH) and volatile organic compounds (*30*). Furthermore, NO_x emissions produced during combustion originate mainly from the nitrogen in air, with smaller contributions from the fuel-bound nitrogen (*30*). Hence, diesel engines require multiple exhaust gas aftertreatment systems with the diesel oxidation catalyst (DOC) typically being the first component, followed by a diesel particulate filter (DPF) and selective catalytic converter (SCR) (see **Figure 1**) (*30*). The respective exhaust gas aftertreatment units will be described in the following.

Diesel oxidation catalyst (DOC)

The diesel oxidation catalyst (DOC) was introduced in the 1960s and since then various catalytic systems were investigated including platinum, palladium, rhodium, copper, nickel and others. At

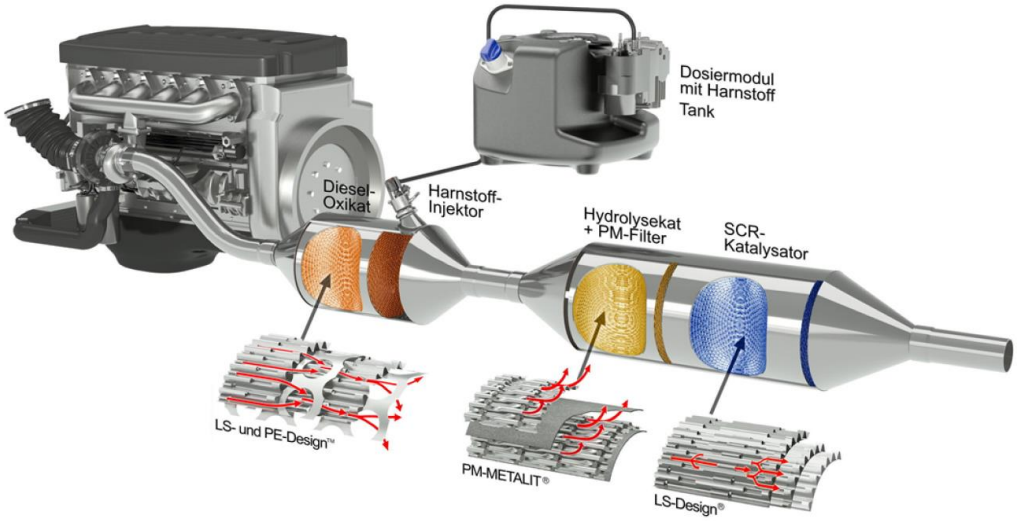

Figure 1 Schematic representation of the exhaust gas aftertreatment units of a diesel engine (image retrieved from ref. (*31*))

present, DOCs are typically based on ceramic monoliths with a washcoat stabilized on the monolith's surface. The latter is employed to disperse the catalytic metal due its high surface area (*30*). Typically, alumina (Al_2O_3), silica (SiO_2) and zeolites are common washcoat materials, whilst the active site of the catalysts is regarded to the metal. It must be considered that different oxidation states of the metals lead to different activities for the hydrocarbon oxidation reactions. In general, for the metal catalyst, a highly dispersed state of the metal is desired to achieve a higher surface area which is available for the reaction (*30*). A comprehensive discussion of the different catalyst types, DOC reactions including reaction kinetics and other aspects of this technology are reviewed in detail by Russel and co-worker (*30*). Briefly, the catalytic site will undergo the following stages, namely (i) oxygen being bound to the catalytic site with the (ii) reactants diffusing to the surface and reacting with the bound oxygen and lastly, (iii) the reaction products such as CO_2 and water vapor desorb from the catalytic site and diffuse to the exhaust gas. The oxygen absorption on the catalyst surface is increasing with temperature. Hence, HC and CO are oxidized producing the product gases carbon dioxide (CO_2) and water (H_2O), as described by **Eq. 1** and **Eq. 2**, respectively (*30, 32*).

$$C_nH_{2m} + 0.5\,(n+m)O_2 \longrightarrow n\,CO_2 + m\,H_2O \qquad \textbf{Eq. 1}$$

$$2\,CO + O_2 \longrightarrow 2\,CO_2 \qquad \textbf{Eq. 2}$$

However, it must be considered that the oxidation catalyst will promote the oxidation of any compound exhibiting a reducing character, such as SO_x and NO_x. Hence, oxidation of sulphur oxides (SO_x) leads to the undesirable product sulphuric acid, which in its gaseous state in combination with water molecules nucleates under certain conditions to particles, also termed sulfate particulates. These were reported to contribute to the total particulate matter emission of the engine exhaust (*32*). Furthermore, the reaction product SO_3 was found to deactivate the catalyst by reacting with the active sites of the metal catalyst

forming sulfates. In contrast, the oxidation of the nitrogen oxide exhaust gas (NO) to nitrogen dioxide (NO_2) is advantageous as the NO_2 is required to (i) enhance the performance of the selective catalytic converter catalyst (SCR), as well as (ii) to promote the regeneration of diesel particulate filters (DPF), which will be discussed in the following (*30, 32*).

Selective catalytic reduction (SCR)

The term selective catalytic reduction (SCR) refers to the conversion of nitrogen oxides (NO_x) present in exhaust gas into water and nitrogen (*30*). At present, the SCR system is the dominant technology exhibiting good NO_x reduction efficiency. For mobile SCR applications, urea as an aqueous solution ('Ad Blue') is employed as the reducing agent due to safety and toxicity issues. Upon injection of urea in the hot exhaust gas streams, the evaporation, the thermal decomposition of finely sprayed urea into ammonia (NH_3) and isocyanic acid (HNCO), and moreover hydrolysis are occurring. As the NO_x diesel exhaust comprises >90% NO, the main reaction of the SCR with NH_3 provided by **Eq. 3** is the well-known standard SCR reaction.

$$4\,NH_3 + 4\,NO + O_2 \longrightarrow 4\,N_2 + 6\,H_2O \qquad \textbf{Eq. 3}$$

To meet the Euro VI regulations, the titanium dioxide (TiO_2) supported vanadium oxide catalyst (V_2O_5) is utilized in SCR systems exhibiting a higher temperature tolerance with the advantage to be essentially insensitive to sulphur (*33*). Moreover, to meet the more stringent emission legislations an integrated catalytic system for the removal of NO_x and particulate matter (PM) will be required. Thus, an exhaust gas recirculation (EGR) engine and an aftertreatment system comprising a DOC, a SCR and a diesel particulate filter catalyst (DPF) placed in a specific order are required to achieve the desired emission reduction performance (*33*).

Diesel particulate filter (DPF)

In general, the composition of diesel particulate matter depends on the combustion temperature. In regions with high temperatures, most of the volatile materials (HC, sulfuric acid, etc.) are in their gaseous state (*34*). Upon cooling and dilution of the exhaust gas by ambient air, other processes are occurring such as nucleation, condensation and adsorption transforming the volatile material to solid and liquid particulate matter. Furthermore, when emitted to the environment the particle properties might be additionally altered due to condensation and solar radiation (*34*). A diesel particulate filter (DPF) removes soot particles produced during the combustion process in the diesel engine by a fine-pored ceramic, with typical catalysts being V_2O_5, MoO_3, Na/CuO, and various others. Moreover, the removal of the collected particulates (regeneration) from the filter must be performed to restore the filters soot collection capacity, which can be performed thermally. During the thermal regeneration, the collected particulates are oxidized by oxygen or NO_2 to gaseous products containing mainly CO_2. Details

on the different soot-oxidation catalytic systems are out of the scope of this work but were summarized excellently by van Setten and co-workers (*34*).

Exhaust gas recirculation (EGR)

In diesel engines, recirculation of the exhaust gas is typically performed to reduce the NO_x production, which is mainly produced during combustion processes in the presence of oxygen and nitrogen in regions with high flame temperature. When the exhaust gas regulation (EGR) is applied, the engine intake stream consists of fresh air and recycled exhaust gas (*35*). The percentage of recycled gases is defined by the EGR ratio, which in other words is the mass ratio of recycled gases to the whole engine intake. Typically, the EGR ratio is measured by comparing the CO_2 concentrations between the intake of the engine and the exhaust gas as provided by **Eq. 4**. Moreover, several test results showed that thigh EGR ratios should be applied at low load, whilst low EGR ratios are favoured at high load (*35*).

$$\text{EGR ratio} = \frac{\text{intake } CO_2 \text{ concentration}}{\text{exhaust } CO_2 \text{ concentration}} \qquad \textbf{Eq. 4}$$

2.2. OME – properties as synthetic fuel

2.2.1. Physicochemical and fuel properties

At present, internal combustion engines rise concerns as exhaust emissions were found to contribute significantly to environmental pollution (*21*). Especially, greenhouse gas (GHG) reduction has become the major objective for novel technological developments in the transportation sector. Thus, to develop cleaner fuels producing less pollution than conventional fuels, new emission standards for diesel engines (e.g. Euro VI) and a significant reduction of exhaust gases have to be met, such as hydrocarbons, CO, nitrogen oxide (NO_x) as well as the particle number (PN) (*21*, *36*). However, to fulfill the regulations, the exhaust gas aftertreatment must be established, which comes along with high costs (*36*). An alternative to reduce the formation of pollutants during combustion in diesel engines can be achieved by blending of additives in diesel fuel. This implies, that this novel type of fuels must be carefully selected to reach a compromise between the reduction of problematic emission issues of present fuels and low investment and vehicle modification costs (*37*).

A novel representative in the category of alternative fuels are poly(oxymethylene) dimethyl ethers (OME). In **Figure 2** the simplified synthesis flow-scheme is depicted for the acid catalyzed production of OME compounds, which are suitable diesel fuel additives due to their favorable physicochemical properties. OME compounds can be derived e.g. from methanol (MeOH) as the methyl-cap provider, which serves as the methyl end-group during the OME product formation, whilst formaldehyde (FA) is used as the repeating unit for the OME chain growth reaction (*36*). Methanol itself can be produced from synthesis gas obtained from renewable resources *via* e.g. gasification (*38*) and can be subsequently

converted to FA (see section *2.3*), since a reduction of the total CO_2 emissions can only be achieved if OME production is based on renewable resources (*39*).

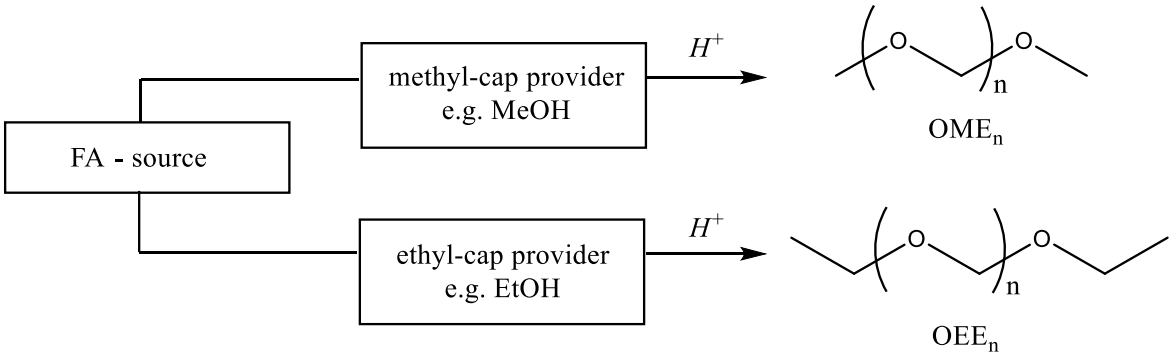

Figure 2 OME_n and OEE_n formation from a formaldehyde (FA)-source and methyl- or ethyl-cap provider (*36*)

In 1960, Boyd's pioneering investigations on physicochemical properties for OME_n with n = 1 – 5 comprising boiling and melting points, viscosity and density determinations were extended several years later by German and Chinese authors (*11, 36, 40–44*). Ever since, detailed investigations on OME compounds have been conducted by various authors in literature (*11, 40, 41, 43, 44*) as extensive interest has arisen in OME_n compounds with the chain length n = 3 – 5, due to the suited boiling points, high flash points and Cetane Numbers for their blending in diesel fuel (*36*). Lautenschütz (*36*) reported the analogous poly(oxymethylene) diethyl ethers (OEE), which can be derived using an ethyl-cap providing source (e.g. ethanol (EtOH)) as depicted in **Figure 2**. These compounds were reported to be another category of promising oxygenated fuels (*20, 36*).

An overview of physicalchemical and fuel properties is provided in **Table 3** for pure OME_n with n = 2 – 6, OEE_n with n = 1 – 4, $OME_{3\text{-}5/6}$ and $OME_{3\text{-}8}$ mixtures compared to conventional diesel fuel (EN 590). The melting points of the OME and OEE compounds were found below 0°C for shorter-chain oligomers, indicating that OME_n/OEE_n with n < 5 are liquids at ambient conditions, whereas n > 5 solidify at temperatures lower than 18°C, which might lead to the blocking of the fuel filter and are thus highly undesired for diesel engines (*1, 36*). The densities of the desired $OME_{3\text{-}5}$ compounds are higher than required by EN 590, compounds of these chain lengths are desired regarding their application in fuel blends (*36*). Physicochemical properties of longer-chain OME_n compounds with n > 6 can be derived *via* extrapolation from pure OME compounds with lower chain length (n = 1 – 5) (*36*). Longer-chain OME homologues fulfill the EN 590 flash point requirements, whilst $OME_{2\text{-}3}$ would lead to a significant decrease of the flash point of diesel when employed as additives (*36*).

The boiling points of OME/OEE compounds were found to depend solely on the chain length matching the requirements of EN 590 for the provided compounds (see **Table 2**) (*24, 36*).

Table 3 Physicochemical and fuel properties of DMM, OME_n with n = 2-6, OEE_n with n = 1-4 and diesel (EN 590) (MW – molecular weight, m.p. – melting point, b.p. – boiling point, LHV – lower heating value, HHV – higher heating value (*11*, *36*, *40*, *41*, *43*, *44*)

Molecule	MW [g/mol]	Density at 25°C [g/cm³]	m.p. [°C]	b.p./range [°C]	Cetane Number	Flash point EN ISO 2719 [°C]	Oxygen content [wt%]	LHV [MJ/kg]	HHV [MJ/kg]	Autoignition point EN 14522 [°C]	Kinematic viscosity at 25°C [mm²/s]	Lubricity at 60°C ISO 12156-1 [µm]	Surface tension ISO 6295 [mN/m]
DMM	76	0.86	-105	42	29	-32	42.1	22.4	25.6	237	0.36	759	20.4
OME_2	106	0.96	-65	105	63	16	45.3	20.3	---	---	0.64	---	---
OME_3	136	1.02	-41	156	78	54	47.1	19.1	22.0	235	1.08	534	28.8
OME_4	166	1.06	-7	202	90	88	48.2	18.4	21.5	235	1.72	465	30.7
OME_5	196	1.10	18.5	242	100	115	49.0	17.9	20.9	240	2.63	437	32.6
OME_6	226	1.13	58	280	104	---	49.6	17.5	---	---	---	---	---
OEE_1	104	0.83	-67	88	32	-5	30.7	28.5	31.0	174	0.49	n.d.	20.6
OEE_2	134	0.91	-45	140	64	36	35.8	25.7	25.8	195	0.79	576	24.3
OEE_3	164	0.97	-24	185	80	68	39.0	23.7	28.0	195	1.22	504	25.0
OEE_4	194	1.01	4	225	103	95	41.2	22.3	24.4	205	1.83	418	28.2
diesel (C_{16}-C_{23}) (EN 590)	---	0.83	-20 to 0	170 – 390	>51	> 55	---	42.7	45.4	~220	2.0 – 4.5	< 460	26
$OME_{3\text{-}5/6}$ mixture	---	1.01	---	157 – 259	75	70	47.9	18.8	---	230	0.34	514	30.7
$OME_{3\text{-}8}$ mixture	---	1.07[a]	---	150 – 257	85.3	62	---	---	---	---	2.17[a]	---	---

[a] determined at 20°C

Moreover, the autoignition points of the diesel additives OME and OEE were found to be in the range of 235 – 250°C and 174 – 205°C, respectively. Thus, OEE compounds exhibit lower values as these compounds undergo radical decomposition in the presence of oxygen (*36*). One of the most promising characteristic properties of diesel fuel is the Cetane Number, which should exceed 51 according to EN 590 (*24*). The Cetane Numbers of OME_n and OEE_n (n = 1) being in the range of 29 – 32 do not fulfill this requirement as too low Cetane Number would lead to a decrease in the operating efficiency of the diesel engine (*36*). However, for both OME_{3-5} and OEE_{3-5} the Cetane Numbers were reported to match those of conventional diesel fuel (*36*). Most of the requirements by EN 590 are not satisfied for dimethoxymethane (DMM) and OEE_1, the shortest OME and OEE compounds, such as the flash point, which must be fulfilled as a security criterion (*11, 36*).

Further physical properties such as lubricity, kinematic viscosity or surface tension are important, as moving parts in modern engines require diesel fuel with self-lubricating properties to ensure proper working conditions (*36*). Thus, it was determined that the lubricity of OME and OEE compounds decreases with increasing chain length. Considering pure OME fuel, the desired OME_{3-5} products fulfill the EN 590 requirements only partially (*36*). The viscosities for the listed OME and OEE compounds are in accordance to EN590 (*36*).

Conventional diesel fuel typically lacks oxygen almost completely as alkanes with $C_{16} – C_{23}$ are the major constituents. OME or OEE compounds are promising diesel fuels due to their relatively high oxygen content, which was associated to their beneficial property in particulate matter reduction (*8, 11, 36*). However, the oxygen content is correlated with the lower heating value (LHV) of a fuel, which corresponds to 42.7 MJ/kg for pure diesel fuel (*11*). Therefore, with increasing chain length and consequently with an increasing oxygen content of OME or OEE compounds the LHV is decreasing (*11*), which as a consequence would lead to higher fuel consumption, if OME or OEE would be added to diesel fuel at an identical engine point (*8, 36*).

Thus, short-chain OME and OEE compounds with n = 3 – 5 met for most fuel properties the EN 590 requirements, matching therefore those of conventional diesel fuel, and confirming that these are suitable diesel fuel additives (*36*). Especially higher viscosities and higher boiling points enable the application of OME compounds in diesel fuel supply systems without the necessity to undertake changes on such (*11*).

Dimethylether (DME) and trioxane were found to exhibit similar properties to conventional diesel fuel (**Table 4**), which were considered in literature as potential diesel additives due to their lower production costs compared to OME (*11*). On the example of DME, the major drawback accompanying this additive in diesel fuel blends is the significantly lowered viscosity. This would lead to a change in the fuel injection behavior thus requiring certain engine and injection system modifications leading to higher investment costs (*11*).

In this context, whilst the technological relevance of OEE compounds was not pursued further in literature, much effort has been done concerning production, purification and process developments of

the homologous OME compounds (*1, 11, 20, 31, 45*). Moreover, several studies on different OME blends with conventional diesel fuel will be discussed in the following. In this regard, since the development of an environmentally benign OME synthesis was the main focus within this work, synthetical approaches for OEE compounds will be treated in detain in the section *4.7*.

Table 4 Physical properties of conventional diesel fuel (CDF), dimethyl ether (DME), trioxane (TRI), dimethoxymethane (DMM) at atmospheric pressure (*11*)

	CDF	DME	TRI	DMM
Melting point [°C]	-	-141	64	-105
Boiling point [°C]	170 – 390	-25	115	42
Viscosity (25°C) [mPa s]	2.71	-	-	0.58
Density liquid (25°C) [kg/L]	0.83	-	-	0.86
Cetane Number	55	55	-	29
Oxygen content [wt%]	-	34.7	53.3	42.1

2.2.2. Combustion engines for OME fuel emission investigations

Various test engine set-ups for combustion tests on pure OME fuel or as an additive in diesel blends have been developed and reported in literature (*5, 8, 40, 46*). Most of these test engines consist of a single-cylinder research engine operating under compression-ignition (*5, 8, 46*) or forced-induction (*40*). An example of the latter type, namely a single-cylinder forced-induction based on the MAN-D20 engine was developed by Härtl and co-workers (*40*) utilizing two fuel tanks for the diesel and OME fuel, with the detailed engine set-up shown in **Figure 3**. Measurement of volatile particles was performed by a condensation particle counter, whilst the amount of soot was determined by a Microsoot sensor based on the photo-acoustic principle. Determination of gaseous exhaust components was characterized and quantified by a FT-IR thus enabling the possibility to distinguish between burnt and unburnt components (*40*). It must be noted, that this technique (FT-IR) was as well reported for various other combustion engine set-ups (*47*). The mixing region of diesel fuel with OME fuel requires some considerations, since differences in viscosity, lubricity and others were found to arise (*5*). Hence, a higher flow velocity of diesel fuel compared to OME_n fuel (n > 1) during injection was reported by Richter and co-workers (*5*) for diesel/$OME_{3\text{-}6}$ blends leading to differences in mass flow and mixing properties. Moreover, an increase of the OME ratio in diesel blends lead to a combustion delay due to the increasing Cetane Number of the mixture (*48*). On the contrary, increasing of the diesel engine loading was found to promote the injection of larger amounts of fuel in the combustion chamber leading to fuel-rich zones, which are favorable for pyrolysis and thus for soot-particle formation (*8*, *13*).

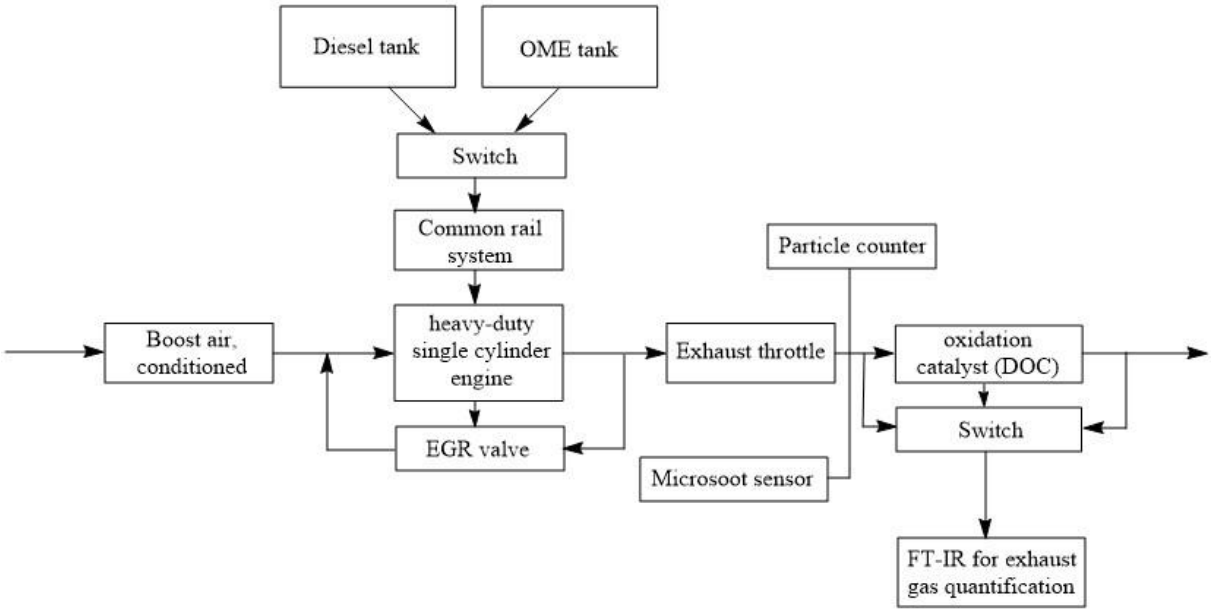

Figure 3 Experimental test set-up for combustion experiments of fuel (developed by TU Munich; engine characterization: oxidation catalyst, DOC 1641.40 g/ft³ platinum; engine speed 1000 – 1750 rpm; injection pressure 180 bar (pre- and main injection); air temperature, 40°C) (redrawn from ref. (*40*))

However, as discussed in *2.2.1 (8)*, OME compounds were found to reduce soot formation allowing thus higher engine loadings and exhaust gas recirculation rates (EGR), which are associated in reducing NO_x emissions (*47*). Regarding formaldehyde emissions upon OME fuel combustion no FA could be measured under certain engine conditions. According to this, FA in the exhaust gas was reported to be successfully removed by exhaust gas aftertreatment and will not be discussed further herein (*49*). In this regard, although the experimental test-engine set-up is of great importance regarding the emission characteristics, the investigated fuel ratio diesel/OME and moreover the OME mixture was found to have an even more pronounced influence on the emission characteristics (*1*).

However, as various engine modifications were reported utilizing different OME blends with e.g. diesel, biodiesel, etc. at different OME to fuel ratios under again different combustion conditions, a comparison of the results regarding emission characteristics is out of scope for this work (*1*). Therefore, in the upcoming section a more general approach will be derived for OME/diesel blends and pure OME fuel regarding CO_2, NO_x and soot emissions upon combustion.

2.2.3. Soot characteristics of pure OME fuels or in diesel blends for internal combustion engines

Oxygenated hydrocarbons as additives for diesel fuels, such as alcohols (*50*), ethers (*51, 52*), esters (*51*) and carbonates (*52*), were found to decrease the formation of soot emissions during fuel combustion in compression engines (*13*). It has been shown, that soot reduction is based on both, the oxygen content in the fuel (*9, 53*) and the structure of the oxygenated compounds (*53, 54*), since alcohols and ethers are more efficient in soot reduction than esters and carbonates exhibiting oxygens bound in a $-COO^-$ moiety, which upon combustion is prone for CO_2 elimination (*54*).

In this regard, OME compounds were found in different engine modifications to effectively reduce soot production without increasing the emission of other pollutants (*13, 14, 55*). In the section *2.2.1* the physicochemical properties of OME compounds regarding different chain lengths were discussed concluding that the optimal chain length regarding OME fuel properties is in the range n = 3 – 5. However, the question if the OME chain length is influencing the soot characteristics was elucidated by Tan and co-workers (*13*) by investigating different volume percentages of OME_1, OME_2, OME_3 and OME_4 in conventional diesel fuel (see **Figure 4**, *left*). They found out, that the oxygen extended sooting index, OESI, a property which is proportional to the sooting propensity, was invariant for different OME chain lengths (*13*). This result indicates that increasing the oxygen content by adding of one additional $-CH_2O$ repeating unit (for more clearance see *2.4*) does not result in remarkable differences in the soot characteristics for fuel mixtures. In **Figure 4** (*right*) the OESI is provided for different oxygenated compounds as a function of the oxygen content in the diesel blend (*13*).

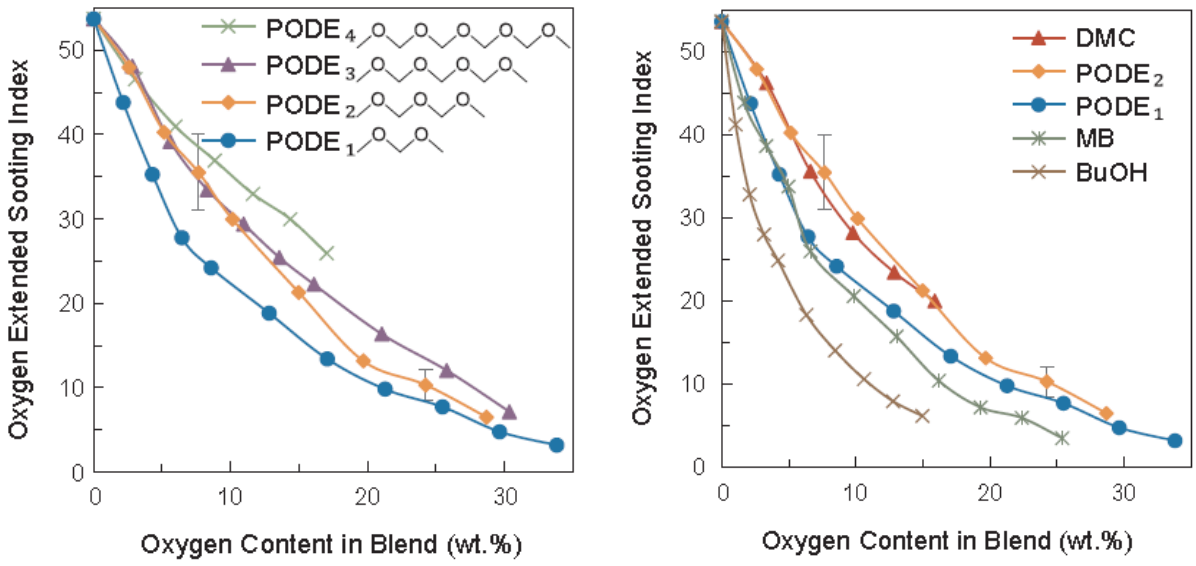

Figure 4 *Left*: OESI as a function of oxygen content in blends of OME_n/diesel (n referring to the number of CH_2O units,; 97% OME purity); *right*: OESI as a function of oxygen content in diesel blends of different oxygenated fuels (dimethyl carbonate, DMC; methyl butyrate, MB; butanol, BuOH) (images retrieved from ref. (*13*))

At a certain oxygen content in the fuel mixture, the OESI was found to decrease for certain OME chain lengths corresponding to a decreasing soot tendency of the respective fuel (*13*). This property can be rationalized based on an ether decomposition model developed by McEnally and Pfefferle (*56*). According to that, OME decomposition can either happen by a two-step chain scission producing a methyl radical, $\cdot CH_3$, upon releasing of a methoxy radical, $CH_3O\cdot$, or *vice versa* by producing formaldehyde as an intermediate product (*13, 56*). Moreover, for longer-chain OME_n compounds (n > 1) the amount of formaldehyde (FA) production was reported to increase with decreasing methyl radical formation (*57*). This was found to have an influence on the soot reduction properties as FA is less efficient in soot reduction, whereas radicals produced upon OME decomposition can be subsequently converted to oxidizing species important for OME soot reduction (*13*). Hence, increasing the OME chain

length leads only to a promoted production of formaldehyde and consequently lower soot reduction. Therefore, the soot reducing ability of OME compounds was found to obey the trend OME_1 > OME_2 > OME_3 > OME_4, with the oxygen contents 42 wt%, 45 wt%, 47 wt%, 48 wt%, respectively (*13*).

As already noted OME compounds are suited for soot reduction, however alcohols are superior in this regard due to the -OH functionality which is prone to the formation of ·OH radicals. The latter is a strong soot repression species compared to the methoxy radical, $CH_3O·$, which is formed upon OME decomposition (*13*). Similar was found for dimethoxymethane, DMM or OME_1, the shortest representative of OME compounds. In this regard, blending diesel fuel with alcohols or dimethyl ethers was investigated extensively leading to an almost smokeless combustion (*13, 56*).

However, minimization of the soot reduction property was found even for non-oxygenated hydrocarbons (HC), which was attributed to the 'dilution effect' (*13*). This property refers to sooty aromatics in diesel fuel, which are less abundant in diesel fuel compared to linear or branched carbon chains, which are diluted upon addition of unbranched HC, e.g. heptane, thus reducing the diesel soot production upon combustion (*13*). In contrast, addition of the linear oxygenated OME compounds to diesel fuel led to a combined soot reduction comprising both the dilution effect, as observed upon addition of linear hydrocarbon chains to diesel fuel, and the 'oxygen content effect' (*13*). However, most compounds exhibiting good soot reduction properties require engine modifications in order to eliminate problems arising due to vapor lock, low viscosity and lubrication properties (*11*). The term vapor lock refers to failures occurring in the automobile during the transfer of the required amount of fuel from the fuel-tank to the engine inlets. Vapor lock can be a caused either by poor design and installation of the fuel system leading to e.g. boiling of the gasoline in the fuel-feed system thus causing excessive vapor pressure, or due to atmospheric conditions. Whilst the latter cannot be influenced, the fuel vapor pressure is typically regulated by the fuel heating to minimize the vapor pressure (*58*).

As discussed in section *2.2.1* these problems are overcome for OME compounds with a chain length of n = 2 – 5 (*47*). Moreover, since the fuel combustion was found to be much better they are superior to the volatile DMM (*5*). However, to achieve a soot-free combustion pure OME fuels are required (*5*). Nevertheless, an addition of 5% oxygenated fuel to commercial diesel fuel was found to lead to a soot reduction of 30% at certain test engine conditions (*47*). A summary of various volumetric percentages for either pure or OME blends with diesel fuel with the corresponding emission characteristics are provided in **Table 5**. The general conclusion regarding soot formation drawn from different experimental set-ups and blending ratios is related to the oxygen content as the most important factor regardless of combustion temperature, as low volumetric OME blending ratios in diesel fuel were found to lack the reduction of soot formation (*47*).

Table 5 Soot formation characteristics for pure OME (DMM, OME_2) and OME/diesel blends in different volumetric percentages (5%, 30%, 50%) according to ref. (*47*)

Fuel investigated (% vol. percentage in diesel fuel)	Emission characteristics
DMM[a]	smoke formation, but less than OME blends in diesel fuel
OME_2[a]	almost smokeless combustion; better than pure DMM
OME_2 (5%)	2.6% presence of oxygen content reduces soot formation by 30% (in soot mass)
OME_2 (30%) and OME_2 (50%)	with increasing OME_2 content, increased soot reduction; still higher than pure OME_2
OME_n mixture (n = 2 – 4)[a]	almost smokeless combustion; better than pure DMM

[a] pure fuel, no blending with diesel-fuel

2.2.4. OME – fuel or blends?

Typically, NO_x exhaust gases are combustion products of fuels with an increased residence time at high temperature regions (*59*). In general, the residence time is related to the mixing time, whilst the engine temperature is dependent on several parameters such as the compression ratio, pressure rise due a to premixed combustion and others. Thus, a direct comparison of the NO_x emissions from diesel fuel to OME fuel is complicated since most of previously mentioned parameters are changed simultaneously (*59*). Furthermore, exhaust gas recirculation, EGR, is typically used in diesel engines to reduce NO_x production and consequently to increase the efficiency of spark-ignition engines (see *2.1.1* for more details) (*60*). As OME fuel decrease the soot formation more efficiently compared to diesel fuel high EGR rates are applicable, which further decrease the NO_x formation, as depicted in **Figure 5** (*1*).

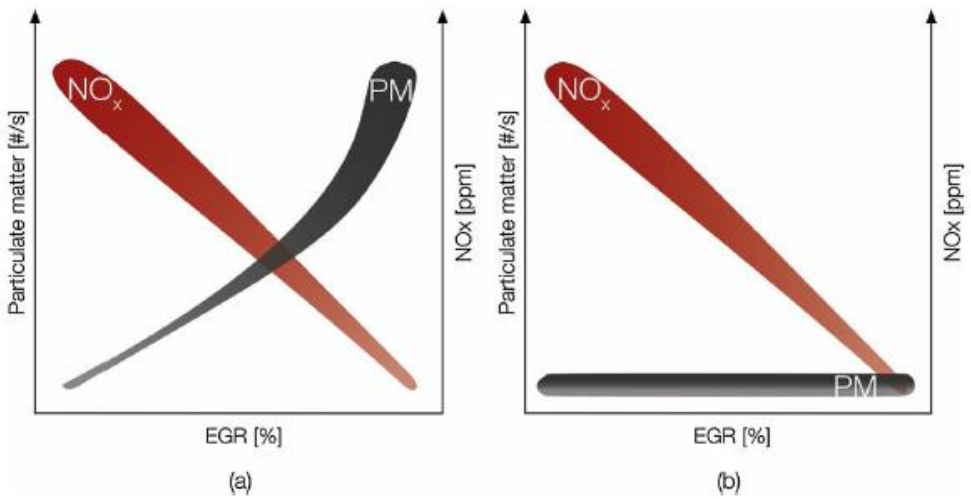

Figure 5 Particulate matter (PM) and NO_x as a function of the exhaust gas recirculation (EGR) for the combustion of (a) diesel fuel and (b) pure OME (in a compression ignition engine; image retrieved from ref. (*1*))

Investigations performed in absence of EGR were found to exhibit a strong correlation of NO_x emissions and oxygen content (*5*). It was found by Ianuzzi and co-workers (*61*) that low NO_x values are achieved typically with fuels containing molecular oxygen. However, they concluded that the NO_x emissions were not significantly reduced for diesel blends with a 5% and 10% volumetric amount of OME_{2-5} (*61*). Since higher blending ratios were found to slightly increase the NO_x emission the optimal OME blending ratio for diesel fuels regarding NO_x reduction was found with 20% (vol.) leading to acceptable soot reduction properties (*1, 40*).

It must be considered, that an optimal balance between oxygen content and EGR rates must be found since higher percentages of oxygen at higher EGR rates were found to result in an increase of CO emissions (*5*). According to Barro et al. (*59*) CO and unburned HC emissions from diesel engines can be due to (i) fuel dripping from injector nozzles after the fuel injection, (ii) from overmixed regions during ignition delay, which are typically non-flammable or (iii) from combustion zones in fuel rich conditions. The emissions of CO were found to increase with an increase in the EGR rate as previously stated and are on average decreasing upon combustion of OME fuel (*59*). Moreover, it was found that combustion of pure OME lead to even lower CO emissions and the formation of short unburned HC, such as methane (*59*).

Hydrocarbon emissions are mostly due to under-mixing regions with insufficient oxygen amount for fuel oxidation (*8*). For OME_{3-4} in 10% and 20% volumetric addition to diesel blends, the HC emissions were found to decrease with increasing blending ratio. This result was attributed to the higher volatility and ignitibility of the oxygenated additive, as the prior leads to the preferred formation of over-mixed fuel regions and the latter promotes the combustion of such (*8*).

To draw a concluding view on the CO, NO_x and HC emissions upon fuel combustion, pure OME compounds were found to exhibit advantageous properties such as an almost soot-free combustion and decreasing CO and HC emissions. However, employing pure OME fuel e.g. OME_2 or OME_n mixtures with $n = 2 – 6$ would still require further engine modifications compared to engines operating with OME blended in diesel fuel. Nevertheless, OME as an additive in diesel fuel was found to decrease soot, CO and unburned hydrocarbon emissions, thus requiring less engine modification and lower investment costs. In this regard, also the production costs of the different OME compounds must be considered which will be discussed in the next sections.

2.3. Relevant starting educts

Poly(oxymethylene) dimethyl ethers (OME) exhibit advantageous physical properties matching those from fossil fuel derived diesel fuels (see chapter *2.2*). In **Figure 6** two OME synthesis routes are schematically depicted as employed for large scale production starting from the methyl-cap source methanol and formaldehyde (FA), which are both inevitable for OME synthesis (*11, 15, 62–65*). The pathway **R1** is employed in a non-aqueous environment employing trioxane and DMM as educts for OME synthesis. Trioxane represents a cyclic trimer of FA whilst DMM is regarded as the shortest OME_n

representative with the chain length n = 1 (*11*, *62*, *66*). However, both educts can as well be considered as reaction intermediates from methanol and FA in a first upstream reaction step, which upon subsequent distillation can be employed for the OME synthesis in the absence of water (*67*, *68*).

Another OME production route can be employed from an aqueous FA/MeOH solution (**R2**) (*62*, *69*–*73*). This reaction does not require the production of trioxane and DMM as reaction intermediates, however, the presence of water reduces the OME product yield leading to the formation of side products (see chapter *2.4.2*) and thus complicating the downstream processing (*62*, *74*). Nevertheless, preparation of OME *via* pathway **R2** has considerable advantages and much effort has been done on this synthesis route, as MeOH has become a platform chemical and is commercially available in large quantities (*62*). Moreover, MeOH can be directly employed in the production of OME products without converting it upfront to DMM (*70*, *75*). In this regard, the most promising starting educts for OME synthesis will be discussed in the following sections elucidating their industrial production routes.

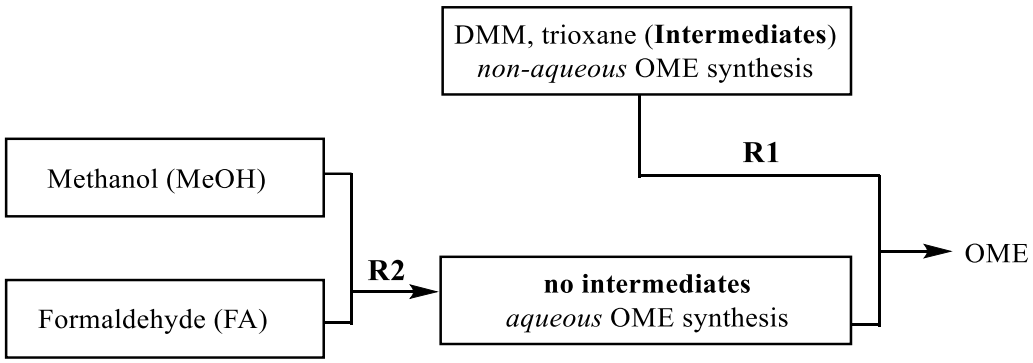

Figure 6 Different routes for the production of OME (large scale) from methanol or formaldehyde following two different routes - **R1**: OME synthesis in non-aqueous environment with trioxane or DMM as intermediates; **R2**: OME synthesis in aqueous environment with no intermediates (*62*)

2.3.1. Trioxane

In 1885 the cyclic trimeric FA compound, trioxane (TRI), was originally reported as a colorless solid stable at basic and neutral conditions (**Figure 7**). Trioxane is hydrolyzed in the presence of acids in aqueous media, whereas in absence of water the polymerization to poly(oxymethylene) (POM) is catalyzed by strong acidic catalysts (*76*).

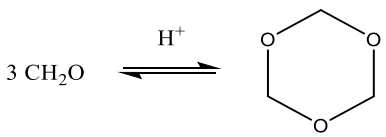

Figure 7 Reaction to produce trioxane from FA (*67*)

The conventional trioxane production process was developed in 1960s comprising a series of steps as depicted in the simplified flow-sheet in **Figure 8** (*67*, *77*). Firstly, an aqueous FA solution is distilled to reduce the water content for subsequent steps (*67*). Subsequently, the FA-enriched stream is catalyzed

by sulfuric acid to trioxane at temperatures < 373 K, whereas the outgoing trioxane-rich stream is further concentrated by distillation and extracted by halogenated solvents (e.g. methylene dichloride, 1,2 – dichloroethane) (*67*). Further purification steps such as solvent removal by distillation are required, which are provided by numerous additional units to obtain pure trioxane (*67*, *77*). However, this process requires chlorinated solvents, which are undesired due to environmental concerns (*62*).

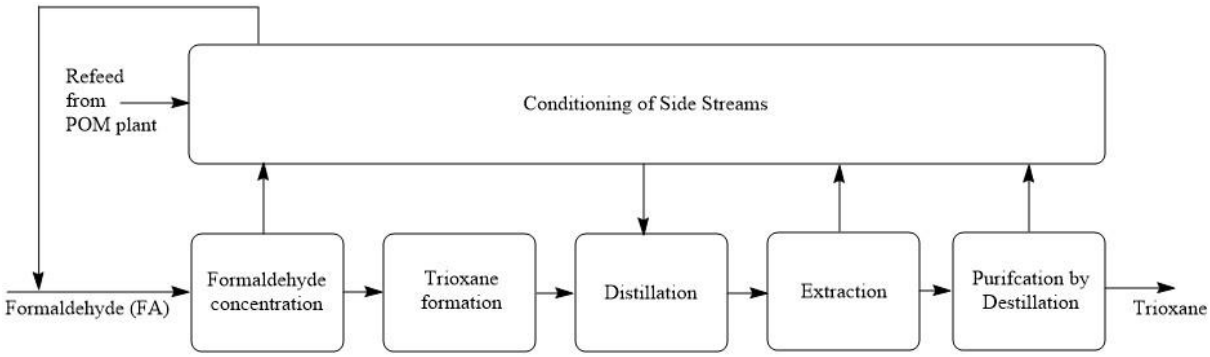

Figure 8 Simplified flow-sheet for the production of trioxane (image retrieved from ref. (*67*))

Employing chlorinated solvents is circumvented by the novel TRI process, which is based on consecutive distillation processes comprising three distillation columns operating at different pressures as depicted in **Figure 9** (*67*). Equally to the old process, an aqueous FA solution (stream 2) is fed into the reactor (R1), which is producing inefficient quantities of trioxane. Thus, the outgoing stream (stream 3) is fed into the first distillation column (K1) operating at low pressure and high temperature (e.g. 1 bar) to prevent solid precipitation (*67*). A trioxane rich overhead stream (stream 5) is produced, which is subsequently fed into column K2 operating at higher pressure (e.g. 4 bar) to obtain trioxane as the bottom product (stream 7) (*67*). The bottom stream of the first column (stream 4) containing high amounts of FA is recycled and combined with stream 2 (*67*). Furthermore, the overhead stream of column K2 (stream 8) is fed into the third column K3 operating at intermediate pressure to separate water from the remained mixture (stream 9), whereas the overhead product is recycled into column K1 (*67*).

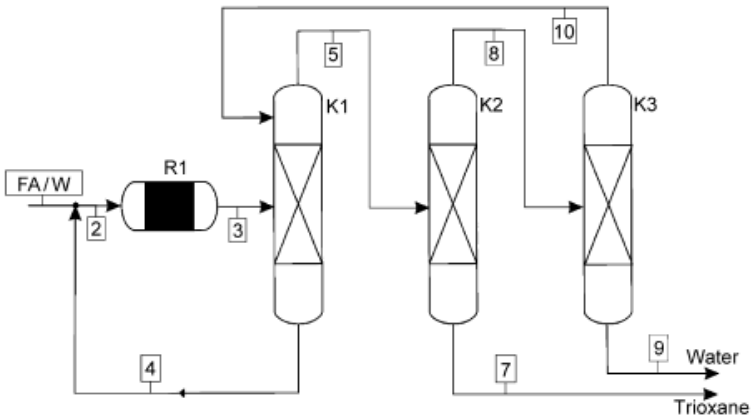

Figure 9 Flow-sheet for the novel trioxane production process based on reactive distillation (image retrieved from ref. (*67*))

Thus, this process was based on various patents (*78–81*) with their technology verified by various pilot-plant activities (*67, 78–80*). For both processes, the conversion of FA to trioxane is very low, thus downstream processing is necessary (*67*). However, the novel trioxane production process is cheaper as several purification steps are omitted (*62, 67, 77*). Moreover, trioxane is obtained with a water content in the ppm range, which is highly desired for OME production (*62, 64*).

2.3.2. Dimethoxymethane (DMM)

Dimethoxymethane (DMM), also known as methylal in literature, is a colorless and volatile liquid at ambient conditions with an etheric smell (see **Table 3** for physicochemical properties). Moreover, DMM exhibits a low viscosity and can be used as a solvent especially in extraction procedures for pharmaceutical products (*82*).

The first commercial production of methylal was developed by Masamoto et. al (*83*) based on reactive distillation. Thus, as depicted in **Figure 10**, DMM is produced from a solution of MeOH and FA over different catalysts such as e.g. zinc chloride, ferric chloride, hydrochloric acid and others in a distillation tower connected to reactors containing the catalyst (*84*). More specifically, the liquid educt stream is fed into the reactors whereas the DMM vapor stream is passing several stages of the gas-liquid contacts leading to enrichment of DMM, which is obtained in 95% yield (*84*).

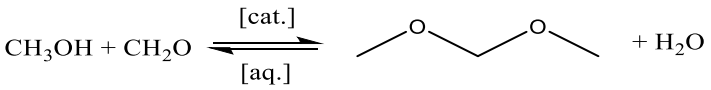

Figure 10 DMM production from MeOH and FA in aqueous solution (*83*)

As depicted in **Figure 11**, the MeOH/FA solution is fed closest to the top of the distillation tower to ensure that only the DMM-rich vapor is subsequently circulated (*84*). Preferentially 3-5 reactor units are employed which are packed with the catalyst, as previously described, operating typically in the range of 45 – 90°C (*84*). The distillation tower is operated at 1 – 3 atm pressure in a temperature range of 60 – 100°C (*84*). However, the described DMM production is strongly dependent on the FA feed and hence the purity for this process is capped with 98% (*84*).

A novel process developed by Hasse et. al (*85*) yields high-purity DMM based on a continuous process as depicted in the flow-sheet in **Figure 12**. Again, a MeOH/FA mixture is fed into a reactor (A) to form partially DMM and water as the side product (stream 2), which is subsequently fed into the first distillation column (B) (*85*). Reactor A can be a tubular reactor comprising the solid catalyst as a fixed bed (*85*). In column B, the mixture is split into the overhead DMM-rich stream (stream 5), the middle MeOH-rich stream (stream 3) and the bottom stream containing almost pure water (stream 4) (*85*). However, stream 5 is an azeotrope of DMM/MeOH, which is subsequently fed into the second distillation column (D) operating under higher pressure, preferentially 100 kPa higher than B which is operating mostly at ambient pressure (*85*). Thus, the sump product of column D (stream 6) is DMM

with a purity of at least 99.5%. The overhead stream 7 is recirculated into column containing mostly MeOH (*85*).

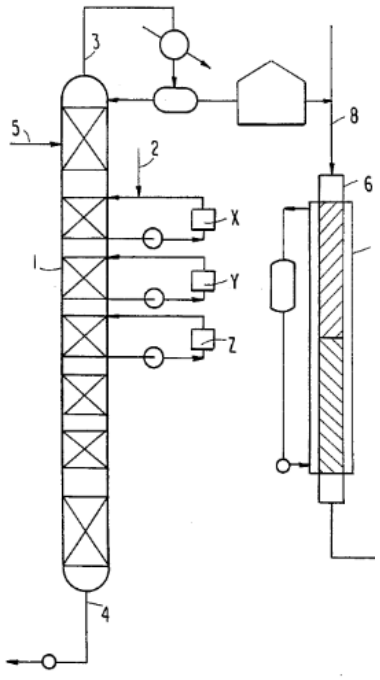

Figure 11 Flow-sheet for DMM production by reactive distillation (image retrieved from ref. (*84*))

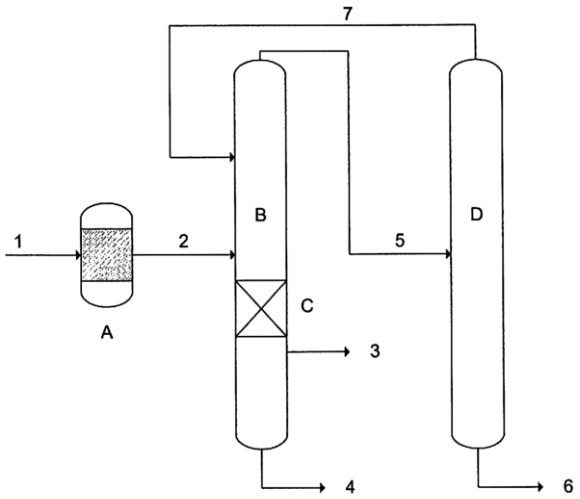

Figure 12 Flow-sheet for continuous DMM production (image retrieved from ref. (*85*))

2.3.3. Methanol (MeOH)

Methanol is a widely applied chemical compound in technological processes either as a solvent or reactant for the synthesis of more complex substances. As the smallest representative of aliphatic alcohols, MeOH is known as a volatile, flammable and toxic compound. First commercial production of MeOH was developed in 1932 by BASF from synthesis gas *via* high, medium or low-pressure processes (**Figure 13**).

$$CO + 2\,H_2 \rightleftharpoons CH_3OH$$

Figure 13 Reaction of synthesis gas ($CO + H_2$) to MeOH (*20*)

As provided in **Table 6**, depending on the process type the different reaction parameters have to be adjusted (*86*). In industrial processes the low-pressure process is employed due to economic reasons (*20*). However, MeOH can be produced from renewable feedstocks *via* various techniques (*38*) as depicted in **Figure 14** and moreover the production costs of MeOH compared to DMM are advantageously lower for OME production (*62*).

Table 6 Technological processes for the production of MeOH from synthesis gas (*86, 20*)

Process	T [°C]	Pressure [bar]	Catalyst	Inventor
High pressure	320 – 450	250 – 300	$ZnO\text{-}Cr_2O_3$	BASF
Medium pressure	250 – 350	100 – 250	$Cu\text{-}ZnO\text{-}Al_2O3$	Vulcan
Low pressure	200 – 300	50 – 100	$Cu\text{-}ZnO\text{-}Al_2O_3$	ICI

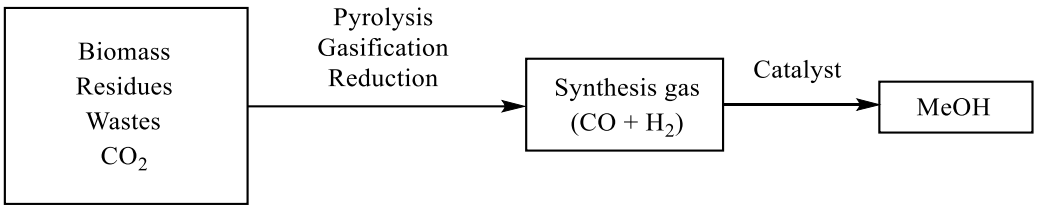

Figure 14 Strategies for the production of MeOH from renewable resources (redrawn from ref. (*87*))

2.3.4. Formaldehyde (FA)

Historically, formaldehyde (FA) was first synthesized in the 1895 as a hydrolyzation product of methylene acetate, and later on upon passing of methanol vapor and air over a hot platinum wire, was found to produce FA (*88*). The latter reaction was further pursued employing different catalysts for the manufacturing of FA with one of the first production plants established in 1889 in Germany. This smallest representative of aldehydes exhibits a pungent odor irritating eyes, nose and in the throat (*89*). Conventionally, FA is produced *via* a three-step process including the steam reforming of natural gas at 700 – 1100°C over a nickel catalyst to syngas (**Figure 15**, reaction (1)), which is converted methanol at lower temperatures at 200 – 300°C over a copper catalyst supported on ZnO (*89*).

$$CH_4 + H_2O \xrightleftharpoons[\text{[Ni]}]{700\text{ - }1100°C} CO + 3\ H_2 \qquad (1)$$

$$CO + 3\ H_2 \xrightleftharpoons[\text{[Cu/ZnO]}]{200\text{ - }300°C} CH_3OH \xrightleftharpoons[\text{[Mo/Fe-Oxide]}]{T_{FA};\ 0.5\ O_2} CH_2O + H_2O \qquad (2)$$

Figure 15 Reaction for the production of formaldehyde (FA) from methanol (*89*)

Formaldehyde can be produced from methanol by the silver catalyst process I (BASF process) conducting a partial oxidation and dehydrogenation with air in the presence of a silver catalyst to achieve high methanol conversions (97-98%) (**Figure 15**, reaction (2)). With the silver catalyst II process lower methanol conversions are achieved (77-78%), hence the product stream is distilled, and unreacted methanol is recycled to the oxidation process. In the Formox® process, methanol is oxidized with air over a molybdenum-iron-vanadium or molybdenum-iron oxide complex, with the flow-sheet depicted in **Figure 16** (*88*). The MeOH feed is entering an evaporator (a) and the exiting gaseous MeOH stream

is injected the heat-exchanging reactor (c), which comprises catalyst filled tubes. Recirculating oil maintains the operating temperature of 340°C with the exiting gas being cooled to 110°C in another heat exchanger (e). The FA rich product stream is obtained from the bottom of the absorption column (f) containing 55 wt% FA and 0.5 – 1.5 wt% MeOH (*88*).

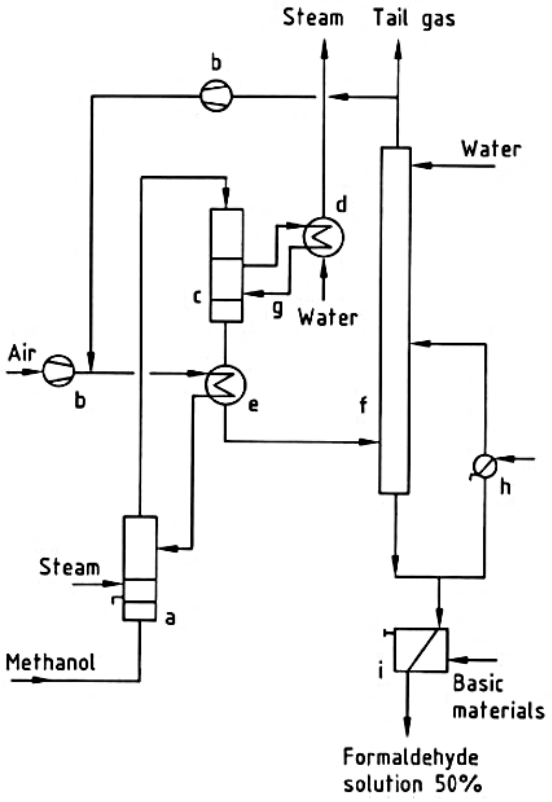

Figure 16 Flow-sheet for the FA production by the Formox® process with (a) evaporator, (b) blower, (c) reactor, (d) boiler, (e) heat exchanger, (f) FA absorption column, (g) circulation system for heat-transfer oil, (h) cooler, (i) anion-exchange unit (image retrieved from ref. (*88*))

Although all three process yield a methanolic FA solution with a relatively low water content with the process operating parameters provided in **Table 7** (*88*), they are energy and cost intensive on a large scale (*89*). In 2017, >35% of the world methanol production was used for the FA synthesis, hence natural gas is needed to be replaced by an alternative feedstock for FA production (*89*).

Table 7 Industrial processes for the production of FA from MeOH (*88*)

	T_{FA} [°C]	Catalyst	Methanol conversion
Silver catalyst process I	600 – 720	Ag on Al_2O_3 support	97 – 98%
Silver catalyst process II	590 – 650	Ag on Al_2O_3 support	77 – 78%
Formox process	270 – 400	FeMoV oxide	98 – 99%

Since synthesis gas can be produced from various biomass sources (*90*), direct conversion of synthesis gas into FA would be a sustainable synthetic approach. Bahmanpour et. al (*91*) reported the first direct

conversion of syngas to FA in aqueous phase employing a Ru-Ni/Al_2O_3 catalyst yielding a 19% CO-conversion, which can be increased if methanol is utilized as the solvent (*92*). Other more sustainable approaches include (i) direct conversion processes of CO to FA employing various catalysts (*89*), (ii) utilizing FA derivates such as bis(boryl)methylene acetal from CO_2 reduction (*93*) and (iii) employing methanol derived *via* pyrolysis or gasification from renewable resources (*38*).

2.3.5. para-Formaldehyde (pFA)

Pure formaldehyde (FA) as a gaseous compound requires certain safety demands regarding handling, transportation and storage (*20*). Moreover, FA exhibits great water solubility thus a 37% by weight FA/H_2O solution can be prepared commonly known as formalin (37% FA, 10% methanol, 53% water). However low concentration of FA and higher water contents are mostly disadvantageous for certain reactions. The major drawbacks of formalin solutions are the high corrosiveness and instability at temperatures differing from the ambient (*94*). Thus, to overcome such difficulties the development of a polymeric FA compound, namely para-formaldehyde (pFA) was invented by Galat et. al in 1953 (*94*). Its commercial production is conducted by evaporation of an aqueous formaldehyde solution under reduced pressure to remove water (*94, 95*). Para-formaldehyde is obtained as a colorless solid product with no characteristic odor from the polymerization of formaldehyde with the number of monomers n = 8 – 100 (*20, 31*).

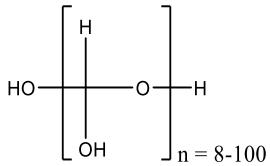

Figure 17 Para-Formaldehyde with n referring to the number of monomers

2.3.6. Assessment of OME production costs

The production costs of a process are regarded as the lower limit for a market price of the product including costs concerning raw materials, energy, personnel and any annual capital related costs (*62, 96*). According to the study survey of Festel et. al (*97*), based on reference scenarios of crude oil prices of €50, €100, €150 and €200, in **Table 8** an excerpt is summarized referring to different fuel-feedstocks, namely fossil fuel, ethanol produced from maize or lignocellulosic waste material), biodiesel from rapeseed oil or waste oil and hydrotreated vegetable oil (HVO) from palm oil. In 2015, the total production costs of most biofuels were estimated to exceed those for fossil fuel with (€cent 68/l) (*97*). At present, the most promising biofuel can be regarded to biodiesel derived from waste with €cent 71/l, which exhibits the smallest gap compared to fossil fuel. However, the production costs of any type of fuel are determined by the market price of the corresponding raw material, with fossil fuel being the cheapest fuel regarding total production costs (*97*).

Table 8 Production costs assessment for 2015 under the assumption of a crude oil price of 730 €/t (*97*)

(Bio-)fuel	conversion factor [l/t]	raw material [€cent/l]	total costs [€cent/l]
Fossil fuel	---	62.89	67.89
Ethanol (maize)	400	53.21	117.13
Ethanol (from lignocellulosic waste material)	250	21.29	161.96
Biodiesel (rapeseed oil)	1100	115.70	135.43
Biodiesel (waste)	1000	36.53	71.17
HVO (palm oil)	1100	66.41	232.44
BTL (wood)	158	464.69	891.29

Conclusively, the production costs for OME fuel should not exceed those of conventional diesel fuel. The OME synthesis from DMM and trioxane (approached by **R1**, see *2.3*, **Figure 6**) can be regarded as highly advantageous leading to high OME yield, low side product formation thus simplifying downstream processing and are referred in literature as the benchmark process chain (*62*). Estimating a methanol price of €261/t and for formaldehyde €15/t, the total production costs of OME comprising a mixture of OME_{3-6} were reported with €535/t of OME by Schmitz and co-workers (*62*). However, these costs are based on existing methanol and formaldehyde processes relying at present mostly on non-renewable feedstocks, which could be replaced by biomass as a renewable resource in the future. For comparison, for an oil price of €49/t and €98/t crude oil, the diesel fuel production costs were estimated with €409/t and €774/t, respectively (*62, 98*). Thus, the production of OME was assessed to be competitive or even cheaper compared to diesel fuel and biofuels (*62*).

OME products with the chain length of n = 3 – 5 are especially employed for diesel fuel blending and scarcely other applications of OME have been reported in literature (*1*). One of such was proposed by Shen et. al (*99*) reacting phenol with OME catalyzed by phosphoric acid to phenolic resins (BPF), which is an important chemical intermediate for further production of epoxy resins and polycarbonates. Short chain OME compounds can be substituents for common organic solvents especially in pharmaceutical production (*100*). Nevertheless, at present the most promising employment of OME compounds is their applicability in novel type of diesel fuel (*65*).

2.4. Synthesis routes and reaction mechanisms for OME production

The two most important production routes of OME products have been introduced in the previous chapter (see *2.3*, **Figure 6)**. Synthesis of OME compounds can in principle be performed starting with different educts such as MeOH, DME, DMM, p-FA, trioxane or formalin (*45*). In literature, the educts MeOH, DME and DMM are commonly referred as methyl-group providing sources for OME production, whereas p-FA, trioxane and formalin are regarded as inevitable FA-sources as they comprise the monomer units of OME compounds (*1*). Different homogeneous and heterogeneous acidic catalysts were reported in literature for the production of OMEs, such as ion-exchange resins, zeolites and sulfuric acids, which will be discussed in chapter *2.6* (*1*). The educts trioxane and DMM can be produced as intermediates from MeOH and FA leading to an economically feasible and highly applicable non-aqueous OME production, as previously discussed (see *2.3*). Both reaction routes build the basis of this work employing DMM/trioxane or MeOH/pFA as starting educts. In this regard, in the following sections only synthesis routes and reaction mechanisms for OME production will be discussed for educts relevant in this work.

2.4.1. Non-aqueous synthesis of OME

Dimethoxymethane (DMM) represents the simplest and smallest OME_n compound with a chain length of n = 1. DMM as a stable yet highly volatile liquid is obtained under neutral and ambient conditions (see *2.2.1*). Trioxane as a colorless stable solid at ambient conditions can be employed as the anhydrous FA source yielding monomeric FA upon acidic depolymerization or upon thermal treatment depicted in **Figure 18**, reaction (1) (*45, 64*). Considering this reaction, one may assume that the trioxane ring is broken at one position and the linear chain is subsequently inserted into the OME chain. However, kinetic experiments did not yield evidence for this mechanism, thus the FA incorporation into the OME chain is referred as sequential (reaction (2)) (see *2.5.1*) (*1*). In the presence of the acidic catalyst further FA incorporation is possible as shown in (3) (*45, 64*). The non-aqueous reaction route, if carried out under the exclusion of water, does not exhibit any water formation during OME synthesis, thus water-induced side reactions can be neglected. However, reaction (4) and (5) show two side reactions, which were observed to occur independently of the reaction route, namely methyl formate (MF) and dimethyl ether formation (DME) (*64*). Hence, MF is produced *via* a Tischchenko reaction from FA in acidic environment, whereas DME is a decomposition product of DMM (*64*). All reactions are typically equilibrium reactions, except the MF formation (4), which was reported to occurs in low quantities (< 1 wt%) (*45*).

Representative acidic catalysts reported in literature for the non-aqueous OME synthesis are sulfuric acid, trifluorosulfonic acid (CF_3SO_3H), ion-exchange resins such as Amberlyst® 36 and different zeolites (HZSM-5, ZSM-5) (see chapter *2.6*) (*1, 64*).

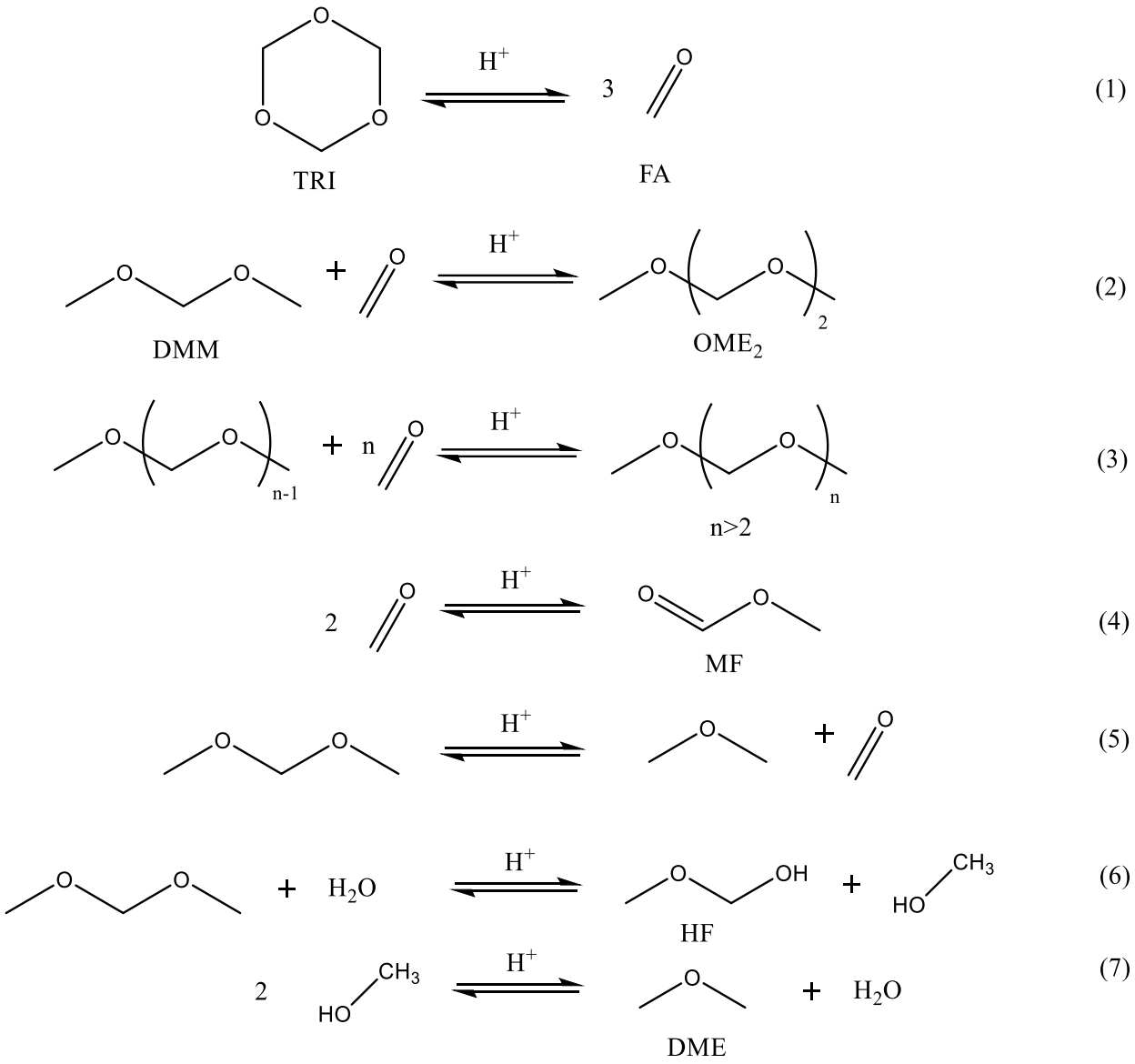

Figure 18 Reactions for the non-aqueous OME reaction pathway starting from trioxane and DMM catalyzed by H^+ (referring to acid catalyst) – (1) Trioxane decomposition to monomeric FA – (2) OME_2 formation from incorporation of FA into DMM – (3) OME acid catalyzed chain growth reaction – (4) Methyl formate (MF) side-product formation – (5) Dimethyl ether (DME) side-product formation – (6) Hydrolysis of DMM – (7) DME formation from MeOH (*45*, *64*)

Although, if water is present in the reaction, DMM is prone to hydrolyze yielding hemiformals (HF) and MeOH as provided in reaction (6) (*1*). Both products can undergo further reactions leading either to HF chain growth, or to DME formation from MeOH (7) (*45*, *64*). Moreover, hydrolysis of OME products can occur leading to lower product yield, shorter OME chain lengths and increased side product formation as depicted in **Figure 19** (*1*, *74*). Therefore, the major objective for this reaction route is the maintenance of a water-free environment in order to yield high educt conversions and consequently satisfying OME yields, which justifies trioxane as the more expensive FA source (*101*).

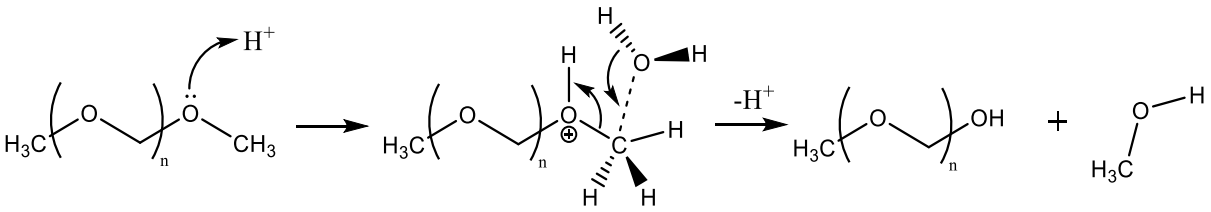

Figure 19 Hydrolysis of OME products in acidic environment (reaction redrawn from ref. (*1*))

2.4.2. Aqueous synthesis of OME

In **Figure 20** an overview is provided of the possible acid catalyzed reactions for the aqueous OME synthetic pathway (*45*). Formaldehyde (FA) in aqueous or methanolic solutions is mostly bound in oligomeric glycols (Gly, (1)) or hemiformals (HF, (2)) (*45, 64*). Both compounds can grow under acidic conditions according to reactions (3) and (4), which can as well proceed upon incorporation of monomeric FA. It is conclusive, that these reactions are inevitably producing either water (H_2O) or MeOH as by-product which induce formation of DME (8), enhance the formation of Gly (1) and HF (2) and most importantly promote OME product hydrolysis as described in *2.4.1* (*1, 45*). However, OME is formed either from HF and MeOH *via* reaction (5) or by transacetalization reactions of different OMEs (reaction (6)) (*45*). The latter has been proved only for DMM and is of low relevance for OME production. Again, all reactions except (7) are equilibrium reactions with reaction (9) being the trioxane formation side-reaction as already introduced in the non-aqueous synthesis route (see *2.4.1* for more clearance, **Figure 18** (1)) (*45*).

Employing pFA as the FA source produces water according to reaction (10), thus the aqueous synthesis route can be employed starting with the educt combinations MeOH/trioxane, pFA/MeOH or pFA/DMM catalyzed by different acidic catalysts such as sulfuric acid, ion-exchange resins (NKC-9), zeolites or heteropolyacids (see *2.6*) (*45*). However, as already discussed the undesired side-product formation reduces the OME product yield thus complicating the product purification. Nevertheless, MeOH is a desired inexpensive educt justifying this reaction route (see *2.3.6*).

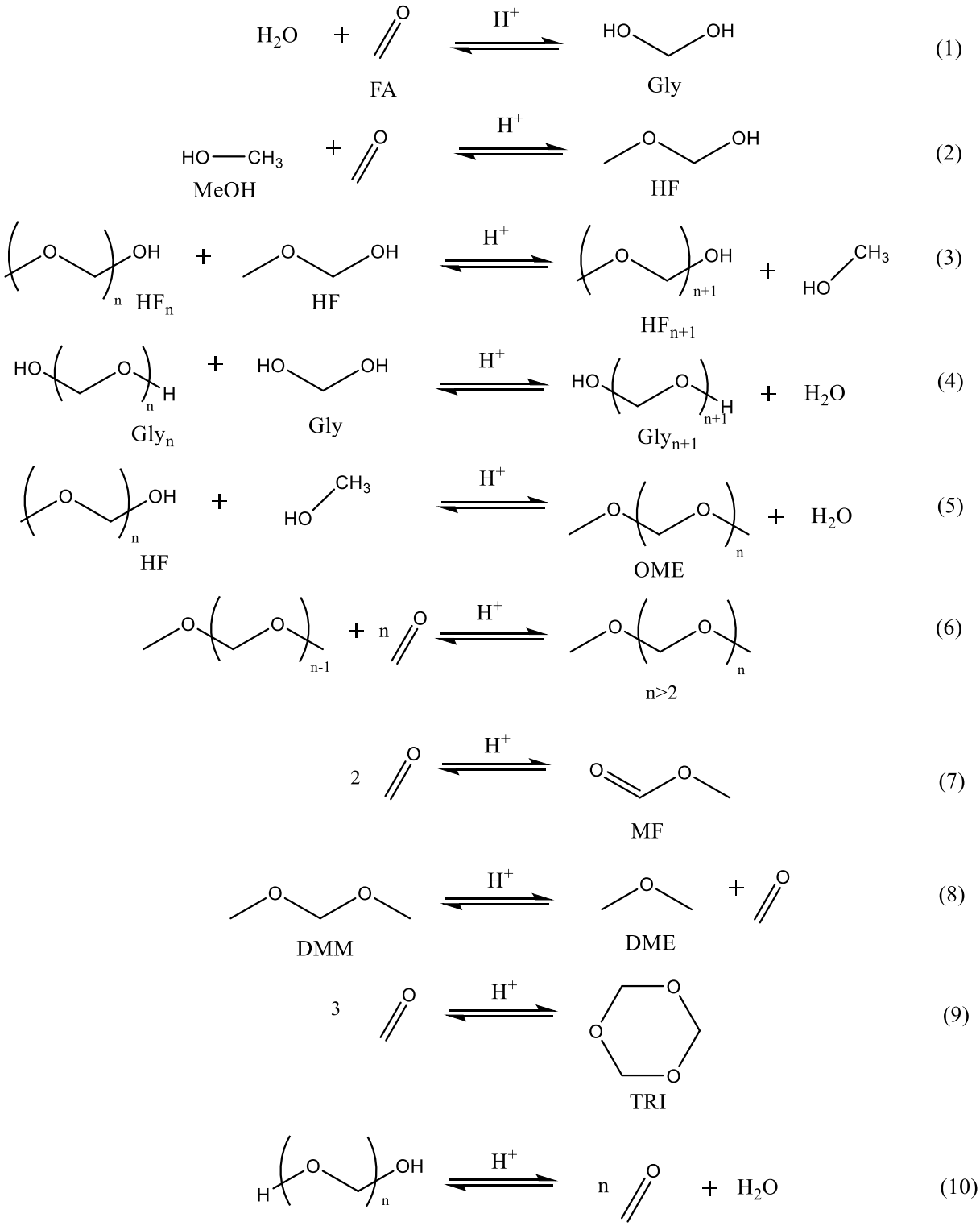

Figure 20 Reactions for the aqueous OME production starting from MeOH and formaldehyde catalyzed by H^+ (referring to acid catalyst) – (1) Glycol (Gly) formation – (2) Hemiformal formation (HF) – (3) HF chain growth reaction – (4) Gly chain growth reaction – (5) OME formation from HF and MeOH – (6) Transacetalization of OME – (7) MF side-product formation – (8) DME side-product formation – (9) Trioxane formation from monomeric FA – (10) pFA depolymerization (*45*)

2.4.3. Other synthetic routes for the production of OME

Utilizing DME and trioxane as starting educts catalyzed by heterogeneous acid catalysts for OME synthesis was reported by Haltenort et. al (*102*). Although this route can be categorized to the non-aqueous OME reaction pathway (*1*), the reaction mechanisms are significantly different from those discussed in *2.4.1*. Here, trioxane is opened at one side and the linear chain is directly incorporated into DME yielding comparably high OME_3 product fractions and almost no longer-chain products. Variation of the reaction temperature or stoichiometric educt ratio lead to the formation of longer and shorter-chain products, which can be explained due to transacetalization reactions (2) (**Figure 21**) (*102*). However, especially high temperatures are undesired since MF formation is enhanced with increasing reaction temperature. However, at present the single-step reaction pathway for OME diesel fuel production is not feasible, due to the low OME_{3-5} product fractions with 8.2 wt% (*102*).

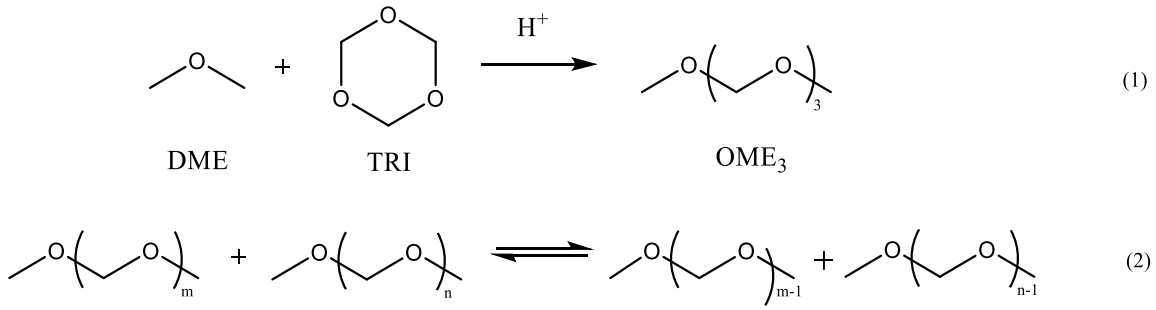

Figure 21 Reactions for the aqueous OME production starting from DME and trioxane catalyzed by H^+ (referring to acid catalyst) – (1) OME formation – (2) transacetalization reactions (*102*)

2.5. Reaction mechanisms

2.5.1. *Chain growth mechanism – simultaneous or sequential OME formation*

In chapter *2.4* the different synthesis routes for OME production were introduced following either the non-aqueous or aqueous pathway. However, both routes require FA as the inevitable monomer for OME chain growth reactions whereas the methyl-source provides the OME methyl-cap (*1*). The term sequential OME formation has been introduced in chapter *2.4.1* referring to the decisive questions: (1) do polymeric FA-sources such as trioxane and pFA decompose under acidic conditions, (2) how do they react with the methyl-cap providers (e.g. DMM, MeOH) and last but not least (3) how does the chain length propagate during OME synthesis? (*103*).

Insight into the chain growth mechanism was conducted by Wang and co-workers (*103*) using DFT calculations and ionic liquids as acid catalysts concluding, that the FA-sources (e.g. TRI) will firstly decompose to monomeric FA and subsequently react with the methyl-cap providers (**Figure 22**, reaction

(1)). It must be considered, that the methyl-cap determines the formed intermediate of this reaction: Employing MeOH as the reactant leads to the formation of a hemiformal (HF) intermediate (reaction (2a)), which subsequently reacts either again with MeOH producing DMM and subsequently longer-chain OME_n products (reaction (2b)), or with FA thus undergoing chain-growth of the hemiformal (*103*). These reactions were already discussed in chapter *2.4.2* (see **Figure 20** for more details) for the aqueous OME production pathway.

Choosing DMM as the methyl-group source, in the first step the decomposition to MeOH and a carbocation will occur catalyzed by the present acid. Subsequently, sequential insertion of FA to the growing carbocation chain produces longer-chain OME_n products, which will be terminated by MeOH again (reaction (3)) (*103*).

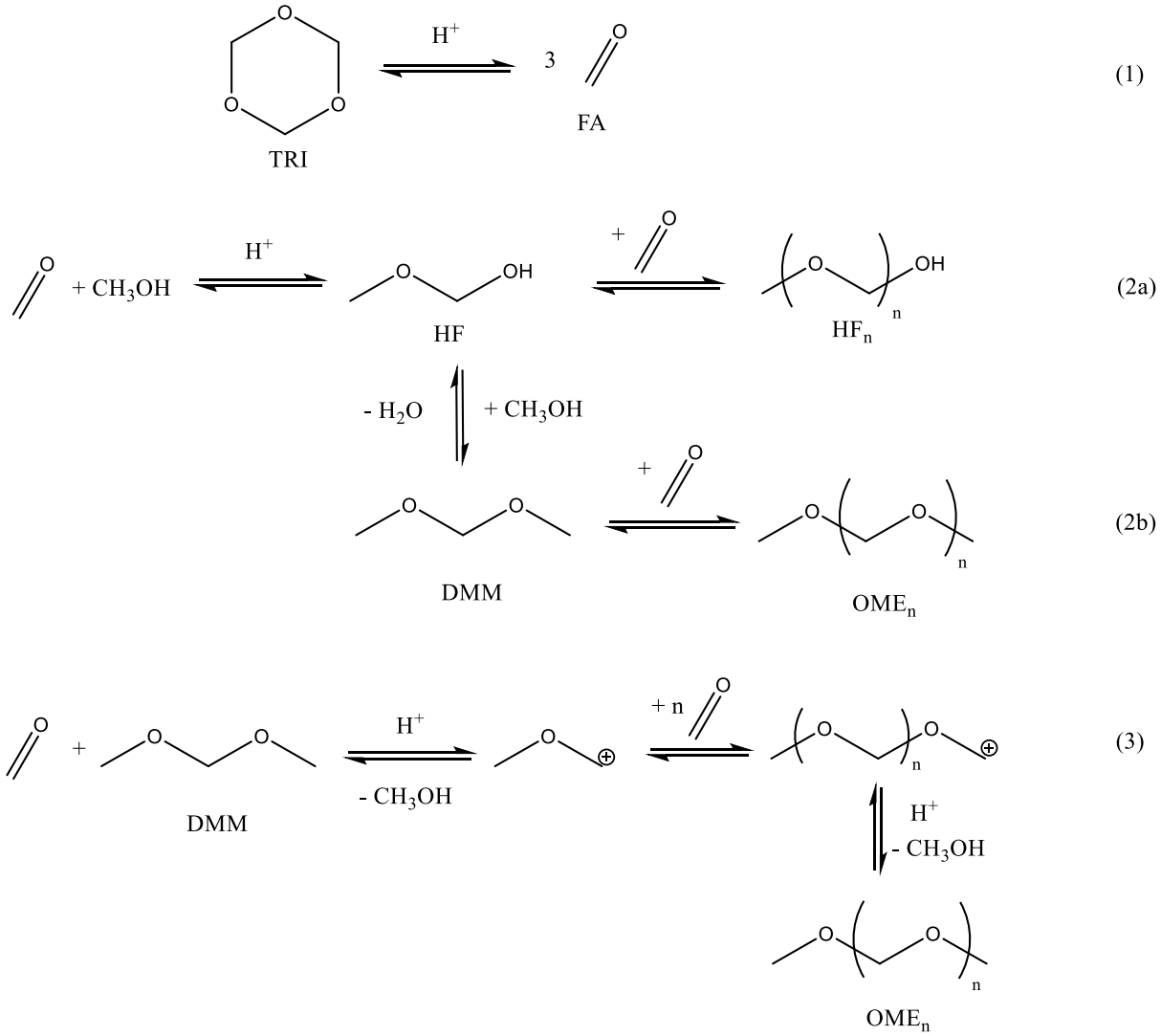

Figure 22 (1) Decomposition reaction of TRI to monomeric formaldehyde (FA); (2a) Chain-growth reaction of hemiformal (HF) under acidic conditions employing methanol as methyl-cap provider; (2b) DMM and OME_n formation from methanol and FA; (3) OME chain-growth employing DMM and FA as educts via radical cation intermediates (*103*)

Although both reactions can be attributed to the sequential OME chain growing, in literature another mechanism has been reported namely the initiation, growth and termination mechanism (IGT) (*1*). Thus,

this type of mechanism was reported to be dependent on the phase, reactants and the catalyst utilized for OME synthesis. Therefore, in non-aqueous liquid phase employing any catalyst except ionic liquids, OME chain growth is following the sequential growth mechanism. In aqueous liquid phase employing ionic liquids as acidic catalysts, the IGT mechanism can be assumed, which is in accordance to the DFT calculations reported by Wang et. al. (*1*, *103*).

To distinguish between the sequential or simultaneous OME reaction pathway, the shape of the product distribution as a function of reaction time may offer deducibility. According to Baranowski and co-workers (*1*), in **Figure 23** a plot is depicted of the OME_{5-8} product mass fractions for reactions reported by various authors. Thus, the main difference between the sequential or simultaneous product formation pathway is determined by the observed product mass fractions: The prior does not yield longer-chain OME products at the reaction start, whereas the latter produces all OME chain-lengths right from initializing of the reaction (*1*).

In this context, OME production employing DMM, pFA or trioxane as educts was found to follow the sequential pathway as reported by Burger et al. (*64*), Zheng et al. (*101*) and Zheng et al. (*74*). Moreover, longer OME products are obtained when using trioxane as the FA-source (*1*). The simultaneous reaction pathway was reported by Schmitz (*69*, *104*) for aqueous MeOH and aqueous FA OME synthesis. Therefore, the simultaneous pathway might not imply any disadvantage compared to the sequential OME chain growth, however, an aqueous reaction medium leads to an increased side product formation and thus lower a OME product yield as previously discussed (see *2.4.2*).

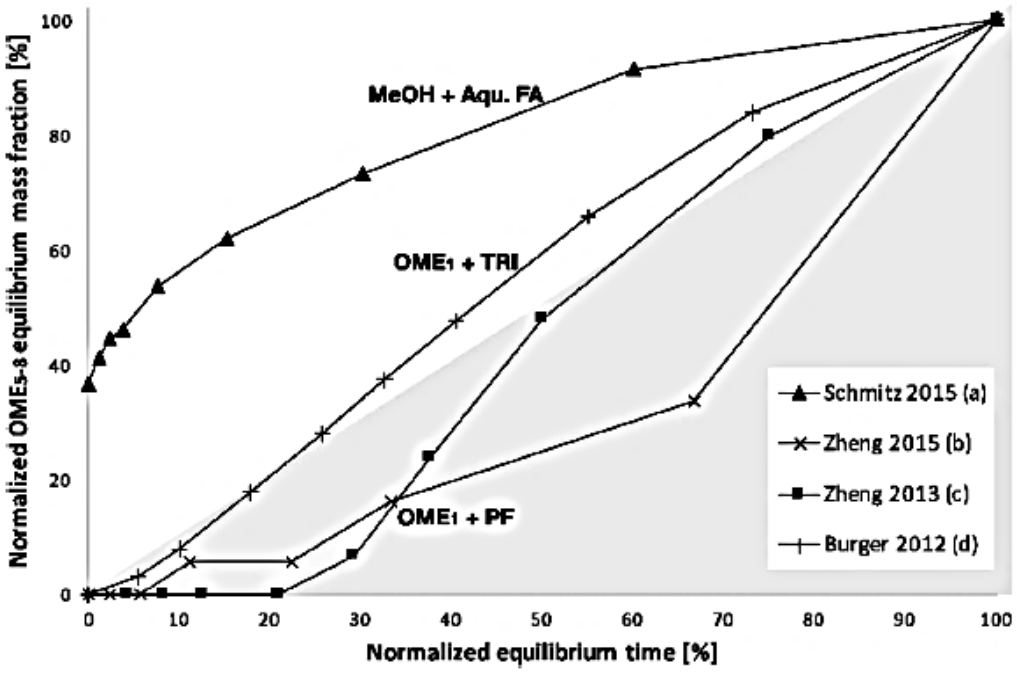

Figure 23 Normalized OME_{5-8} product mass fractions as a function of normalized equilibrium time according to Branowski et. al. (*1*); reaction conditions: (a) Schmitz 2015, T = 90°C, MeOH/FA = 1:1, 12.73 g A46 – (b) Zheng 2015, T = 60°C, DMM/pFA = 2:1, 5 wt% NKC-9 – (c) Zheng 2013, T = 80°C, DMM/pFA = 3:1, 1.0 wt% NKC-9 – (d) Burger 2012, T = 50°C, DMM/TRI = 2.42:1, 0.91 wt% A46

2.5.2. Molecular size and Schulz-Flory distribution

Regarding industrial processes. optimization of process conditions is inevitable for OME production to adjust the molecular size distribution of the products towards chain-lengths of n = 3 – 5 (*11*, *91*). Moreover, studies on the molecular size distribution offer the possibility to adjust or predict properties of a compound undergoing chain growth (*105*), thus providing more insight into the reaction mechanism (*106*). Especially in polymer chemistry molecular size distribution is widely studied using the theoretical distributions by Schulz-Flory and Poisson (*107*). The prior assumes (i) that the probability of a group to react will be independent on the chain length (*108*), (ii) as is the probability of chain termination, (iii) the concentration of the chain propagating species remaining constant as well as of any other agent probably affecting the molecular weight of the products (*109*). The Poisson distribution is typically used, when a constant number of polymer chains begin to grow simultaneously, and the addition of the monomeric unit is independent on the previously added monomers (e.g. living polymerizations) (*110, 111*).

Zhao et. al (*112*) found that the OME production for pFA/DMM follows the Schulz-Flory distribution, which can be applied for OME compounds considering the following variables: The chain propagation probability, *α*, can be derived if the rates of chain propagation and termination are known, r_p and r_t, respectively (**Eq. 1**). Typically, the higher the probability factor the larger the average molecular OME weight production (*112*). For longer-chain OME products with *n* denoting the product chain length, the corresponding mass is given by **Eq. 2**. Further normalization of all OME products produced, integration and linearization **Eq. 2** lead to the more convenient linear form given by **Eq. 3** (*112*).

$$\alpha = \frac{r_p}{r_p + r_t} \qquad \textbf{Eq. 1}$$

r_p…chain propagation rate

r_t…chain termination rate

$$W_n = N_n n\, M = C_2 n\, \alpha^n \qquad \textbf{Eq. 2}$$

$$\text{with } N_n = C_1 \alpha^n$$

n… OME chain length

N…number of FA units in the OME chain

W…corresponding OME_n mass

C_1, C_2…proportion coefficients

M…molecular weight of FA

$$\ln\left(\frac{W_n}{n}\right) = n\ln(\alpha) + \ln(\ln^2(\alpha))$$ **Eq. 3**

Hence, plotting of the $\ln\left(\frac{W_n}{n}\right)$ as a function of $\ln(\alpha)$ enables the determination of the probability factor, α, as depicted in **Figure 24** (*112*). If a linear relationship is obtained, then the OME compounds are produced following the Schulz-Flory law indicating that the insertion the FA monomers proceeds *via* the sequential reaction pathway. Moreover, obtaining larger values for α indicates preferred longer-chain OME product formation, and vice versa. The prior is typically expected for DMM/trioxane OME synthesis (**Figure 24**) (*112*).

In this regard, Zheng and co-workers (*107*) developed a detailed response surface methodology for OME process optimization for DMM and pFA as educts verifying that the OME synthesis follows the sequential reaction mechanism. Therefore, considering the reaction pathway for OME production, which can be derived from the OME product mass distribution (see *2.5.1*), the Schulz-Flory plot can be utilized as a verification tool for the determination of such.

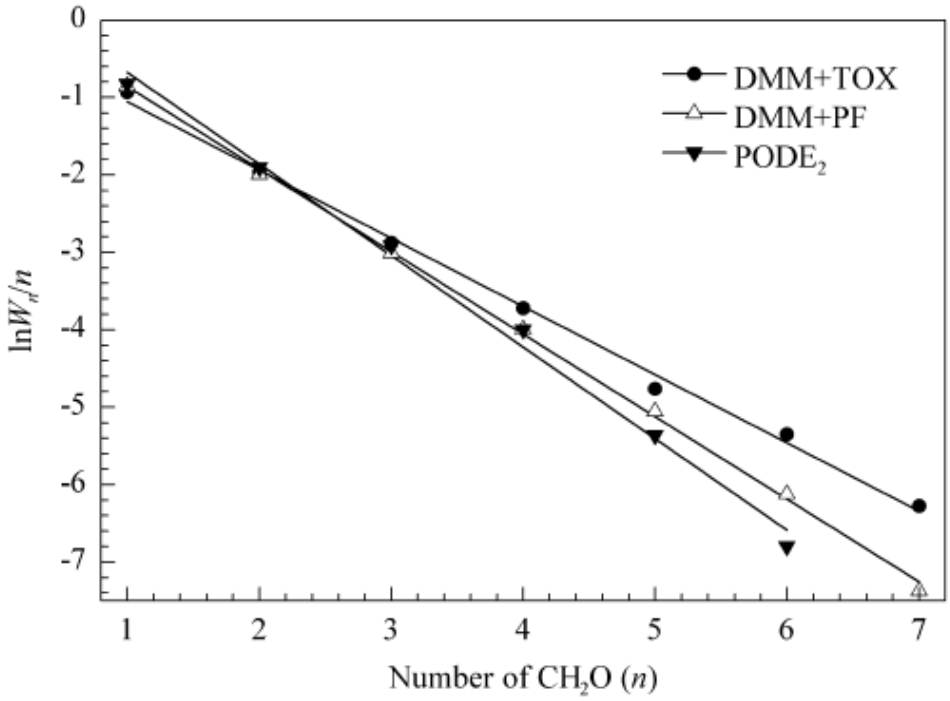

Figure 24 Schulz-Flory distribution of OME_n synthesized from different educts (image retrieved from ref. (*112*))

2.6. Catalysts for OME synthesis

A *homogeneously* catalyzed reactions refers to both, catalyst and substrates being in the same (liquid) phase for the reaction, whilst during the *heterogeneous* catalysis the reaction is taking place at the surface of the (solid) catalyst (*113*). For the synthesis of OME, there are mainly three issues that have to be addressed: Firstly, a catalyst that is inexpensive, less-corrosive and easily prepared, secondly the catalyst should promote high conversions of educts and high selectivity of $OME_{n>1}$, and thirdly, which is not less important, is the preparation of OME as a green reaction process with a plain product purification procedure with the catalyst exhibiting good recyclability and reusability (*114*).

Synthesis of OME requires acidic catalysts, either homogenous (mineral acids) or heterogeneous (ion-exchange resins, zeolites, solid superacid catalysts and others) as described in scientific literature (*1*). Although, homogenously catalyzed OME synthesis enables a good distribution of the catalyst in the reaction mixture with all catalytic sites being available for the reaction, homogenous catalysts exhibit the disadvantage that the catalyst remains in the reaction mixture, which have to be either removed or deactivated (neutralized) in order to halter the reaction and keep side-product formation low (*1*). In this context, Wang et al. (*115*) tested various homogenous catalysts exhibiting different functionalities such as carboxyl, carbonyl, hydroxyl and sulfonyl groups. For catalysts carrying hydroxyl, carboxyl or carbonyl groups, conversions of the formaldehyde source (trioxane) and the methyl-end-cap providing source (methanol) were reported to be very low, whereas the conversions with liquid catalysts carrying sulfonyl or sulfate groups were much higher (see **Table 9**) (*115*). Good results were obtained with sulfuric acid, for which a TRI conversion of 72.2% (MeOH with 64.2%) and an $OME_{2\text{-}8}$ selectivity of 19.3% were achieved (*1, 115*). An even higher $OME_{2\text{-}8}$ selectivity was observed (82.6% of DMM) with rare-earth co-catalysts (La^{3+}) comprising sulfate as counter anion (*116*).

Since mineral acids are corrosive, harmful with some representatives exhibiting low OME selectivity (*1*), ionic liquids as homogenous catalysts were reported to promote high OME selectivity, which contributed to their great interest for scientific research on OME synthesis (*1, 117, 118*). Ionic liquid catalysts were reported to exhibit several advantages compared to other liquid catalysts, such as high tunability of acidic properties, high thermal stability, simple separation from reaction products and even recyclability (*1, 117*). Additionally, they lead to high conversions of the formaldehyde source and to even higher selectivities of $OME_{3\text{-}8}$ products compared to sulfuric acid as homogeneous catalyst (*1*). However, many ionic liquids containing N-alkylimidazolium, N,N-dialkylpyrazolyium and similar cations, exhibit several disadvantages such as toxicity, post-synthesis purification steps and change of chemical and physical properties due to impurities. Therefore, these catalysts will not be further discussed in the scope of this work (*1, 119*).

Synthesis of OME *via* heterogeneous catalysts simplifies the removal of the catalyst, either by filtration or other separation techniques, which is highly advantageous compared to liquid catalysts. In contrast to homogeneous catalysts, acid strength, pore volume, surface area and exchange capacity can

be tuned (*101, 120*). According to Zheng et. al (*101*), cation-exchange resins were referred to exhibit a better selectivity to OME compared to homogeneous catalysts. Especially ion-exchange resins are of great interest comprising well-defined and uniform active sites thus leading to high educt conversions, if the active sites carry sulfonyl groups. Examples of such are Amberlite® IR120, Amberlyst® 36 and 46 and many others (*11, 64, 69, 74, 114, 121*). However, sulfonated resins inside the catalyst micropores, such as Amberlyst® 36 tend to accumulate FA molecules, which exhibit a high probability for the formation of side-products (*64*). In contrast, Amberylst® 46 lacks the sulfonation in its micropores thus leading to a strong decrease in side product formation (*64*). Major drawbacks of ion-exchange resins were found such as their low thermal stability, leaching of active species into the bulk of the solution, catalytic deactivation and swelling especially when using polar solvents (*114, 117*). However, OME_{x-y} (with x – y denoting the selected OME chain length products) is mostly similar or even lower compared to mineral acids as liquid catalysts, as provided in **Table 9** and **Table 10** (*1*). Moreover, in contrast to liquid acids, solid acids display lower activity due to transfer hindrance (*122*).

Other representatives of heterogeneous catalysts are solid acid carbons as reported by Wang et. al. (*115*), such as graphene oxide and HS-C exhibiting high thermal stability and no-swelling behavior showing similar conversions and OME selectivity compared to the previously introduced ion-exchange resins (*1, 115, 101*). Further heterogeneous catalysts, such as zeolites or molecular sieves (HY, HZSM-5, Hβ, HMCM-22) have been investigated on the correlation of their acid strength as a function of both, the conversion of the educts and OME product selectivity (*123*). It was found, that the lower the acidic strength of the heterogeneous catalyst, the higher the selectivity of short-chain products (OME_{1-3}), whilst strong acid sites lead to higher production of OME_{3-8} (*1, 123*).

A different type of heterogeneous catalyst are heteropolyacids (HPAs) as a class of polyoxymetalates with strong Brønstedt acidity. Supported HPAs, stabilized by conjugated polymers as the PVP-HPA, attracted much attention as an environmentally benign acidic catalyst leading to an almost complete conversion of the educts and high OME_{2-5} selectivity. Without any support these catalysts are attributed to the class of homogeneous catalysts as these are difficult to separate from the reaction mixture (*1, 122*).

Since the development of an inexpensive, environmentally friendly catalytic system with high conversions and product selectivity for OME synthesis is still in demand (*1, 115*). However, many heterogeneous catalysts reported in scientific literature do not fulfill this requirement. Especially the costs for the production of such catalysts are mostly quite high and recycling may introduce leaching problems or similar, which makes many of the heterogeneous catalysts not really environmentally friendly (*115, 117*).

Table 9 Overview of homogeneous catalysts for OME synthesis reported in literature; (x – y) referring to the selected OME chain length

Catalysts [catalyst loading wt%]	Reactants	T [K]	Time [h]	Conversion [%]/FA source	Conversion [%]/methyl-cap source	Selectivity [%] to OME_{x-y}	Reference
H_2SO_4 (0.1)	DMM/pFA (4:1)	373	1	68.6	not given	27.6 (3-4)	(*1*)
H_2SO_4 (0.27)	MeOH/ TRI (2:1)	393	10	72.2	64.2	19.3 (2-8)	(*115*)
H_2SO_4 (1)	DMM/ TRI (1:1)	353	1	75.7	66.3	46.6 (3-8)	(*18*)
La^{3+}/SO_4^{2-} (1)	DMM/pFA	398	6	not given	82.6	75.5 (2-8)	(*116*)
CF_3SO_3H (0.01)	DMM/ TRI (4:1)	373	40	not given	not given	22.5 (3-11)	(*1*)
p-Toluenesulfonic acid (5)	DMM/ TRI (3:1)	363	0.5	not given	not given	30.4 (3-8)	(*115*)
1,4-Dihydroxy benzene (5)	MeOH /TRI (2:1)	393	10	14.0	7.2	0.0	(*115*)
1,4-Benzoquinone (5)	MeOH/ TRI (2:1)	393	10	11.7	4.0	0.0	(*115*)
1,4-Dicarboxy-benzene (5)	MeOH /TRI (2:1)	393	10	29.1	11.1	0.0	(*115*)
o-Hydroxybenzoic acid (5)	MeOH/ TRI (2:1)	393	10	16.5	15.4	0.0	(*115*)
Phenylsulfonic acid (5)	MeOH/ TRI (2:1)	393	10	51.9	24.3	5.7 (2-8)	(*115*)
Sulfosalicilic acid (5)	MeOH/ TRI (2:1)	393	10	68.4	52.3	10.9 (2-8)	(*115*)

Table 10 Overview of heterogeneous catalysts for OME production reported in literature

Catalysts [wt%]	Reactants	T (K)	Time (h)	Conversion [%]/FA source	Selectivity [%]to OMEx-y	Reference
Ion exchange resin						
A36 (4.2)	DMM/TRI (2:1)	323	0.33	93.5	31.5 (3-6)	(*15*)
NKC-9 (7.0)	DMM/pFA (3:1)	353	1.5	84.6	36.6 (3-5)	(*101*)
Dowex-50Wx2 (1.0)	MeOH/pFA (1:1.6)	353	0.023	not given	29.3 (3-5)	(*45*)
CT175 (7.5)	DMM/TRI (3:1)	363	0.5	89.0	64.2 (3-8)	(*114*)
Zeolite						
ZSM-5 (7.5)	DMM/TRI (3:1)	363	0.5	4.7	22.7 (3-8)	(*115*)
HZSM-5 (5)	DMM/TRI (2:1)	393	0.75	85.3	88.5 (2-8)	(*124*)
Others						
HS-C (undisclosed)	DMM/TRI (undisclosed)	323	48	not given	31.9 (2-7)	(*112*)
graphene oxide (5)	MeOH/TRI (2:1)	373	10	92.8	30.9 (2-8)	(*115*)
PVP – HPAs (2.3)	MeOH/TRI (2:1)	413	4	95.4	54.9 (2-5)	(*122*)

Nevertheless, heterogeneous catalysts comprise different degrees of modification, which can be moreover reused after purification (*1*), whilst in scientific literature the use of homogeneous catalysts is often claimed to be of non-industrial interest (*117, 123*). However, the conversion of the formaldehyde source and the selectivity of sulfuric acid as a liquid catalyst is compared to several heterogeneous catalysts similar or even higher, which made liquid catalysts interesting for industrial processes such as the BASF processes (*64, 118*). Moreover, homogeneous catalysts provide a more uniform distribution of the catalyst and moderate or even better conversions and OME selectivity. However, one of the major drawbacks of mineral acids is their high corrosiveness, which makes them challenging to handle especially at higher temperatures and pressures. To separate homogeneous catalysts such as sulfuric acid from the OME reaction mixture, a neutralization step with an defined amount of base is required to obtain OME_n compounds (*1, 114, 123*).

Extensive kinetic investigations were conducted for many novel homogeneous and heterogeneous catalysts (*1*). Sulfuric acid as one of the firstly reported homogeneous catalyst by Gresham and Brooks (*125*) for OME synthesis was investigated extensively on different educt combinations. Later on, some studies were conducted on varying the stoichiometric ratio of the corresponding educts and reaction conditions (*114, 122*). However, no report could be found for kinetic studies on sulfuric acid catalyzed OME synthesis as well as for methanesulfonic acid (MSA), which is another representative of sulfonic acids. In patent literature one report was found investigating methanesulfonic-pyrrolidonium based ionic liquids as catalysts for OME synthesis (*126*) and as noted, many others refer to other sulfonic type catalysts (*3*). Moreover, patent literature refers rather vaguely to mineral acids for OME synthesis (*127*).

Therefore, in the scope of this work, kinetic investigations were conducted on the homogeneous catalysts, sulfuric acid and MSA, as well as for the heterogeneous solid acid Deloxan®. The latter was a former commercially available solid-acid catalyst, consisting of polysiloxanes bearing alkyl-sulfonic acid groups (*16*). These types of catalysts contain alkyl sulfonic acid groups as anchored ligands, namely $-SO_3H$ (*128, 129*) and they have been described in scientific literature for their excellent activities, compared to polystyrene based cationic resins (*17*). Several other advantageous structural and physical properties of Deloxan® ASP type catalysts were reported, exhibiting no swelling or shrinking behavior, a high selectivity and especially a high catalytic activity, which is comparable to sulfuric or sulfonic soluble acids (*16*). In the past, Deloxan® type catalysts were used as cost-efficient and reliable catalysts for esterification of free fatty acids, alkylation, condensation reactions (*16*) and many others (*3, 130*).

2.7. Processes for the production of OME

In scientific and patent literature much effort has been made for the development of OME production processes. At present, OME are desired components for tailoring diesel substitutes (*11, 15*), since their physical properties were found to satisfy the requirements to become a diesel fuel component (*15*). In this context, pilot-plant projects in Germany were funded, various production methods were patented by BASF (*1*) and since 2016 ton-scale production of OME by OME-Technologies® was started (*131*).

Moreover, Chinese industry and academics are highly ambitious, regarding the number of patents and publications. At present, the BP process (*71*), the BASF process (*70, 73*) and the Lanzhou process (*132*) are the three main process routes as summarized in **Table 11**. These processes focus on the OME_n production with n = 3 – 8 as suitable fuel additives, which were reviewed in great detail by Bhatelia and co-workers (*15*) and will be summarized in the subsequent sections. In **Table 41** an overview of the patents regarding OME production and purification of the OME products is provided in the *Appendix*.

Table 11 Summary of the industrial processes for OME production including process parameters (according to ref. (*15*))

	Reactants	Catalysts[a]	T [°C]	p [bar]	Composition OME [%]
BP process	DME, O_2, FA, MeOH	Ag cat, MFI alumino or borosilcate, cation exchange resin	300-500, 160, 70	15 - 25	OME_2 = 83 OME_{3-4} = 5
BASF process	TRI, DMM	mineral acids, sulfonic acids, heteropolyacids, acidic ion exchange resins, zeolites and others.	50 - 200	1 -20	DMM = 49 OME_2 = 25 OME_3 = 12 OME_4 = 5 OME_5 = 10
	TRI, DME		100	2 - 100	DME = evaporated OME_2 = 18 OME_3 = 58 OME_4 = 16 OME_5 = 8
Lanzhou Inst.	TRI, MeOH,	ionic liquids (quarternary ammonium, phosphonium, imidazolium cation with various sulphonate anion)	80 – 120 or 100 – 130	5 - 50	OME_2 = n.d.[b] OME_3 = 46 OME_4 = 31 OME_5 = 16 OME_6 = 5
	ROH, FA		100 - 130		OME_2 = 4 OME_3 = 51 OME_4 = 30 OME_5 = 11 OME_6 = 3

[a] For the BASF and Lanzhou Inst. processes different educt combinations are employed, but the catalysts are summarized.
[b] not detected

2.7.1. BP process

The BP process, which is often referred as the formaldehyde route for OME synthesis was introduced by BP utilizing a mixture of DME/MeOH and producing FA by oxidative dehydrogenation catalyzed by an Ag-catalyst, as depicted in **Figure 25** (*15*). The subsequent reaction of FA with dimethylether (DME) and MeOH leads to the production of DMM and OMEs catalyzed by the borosilicate catalyst and cation exchange resin, respectively (*15*). Firstly, DME is oxidatively converted to FA over a metal oxide catalyst, e.g. Fe, Mo, V and Ag, as drawn in reaction (1). Subsequently, MeOH or DME is reacting with monomeric FA to DMM (2a, 2b) (*15*). In reaction (3) the chain-growth of OME_n products is shown producing water as a by-product, which was reported to react with FA to form undesired side-products such as glycols (Gly), hemiformals (HF) or others (see *2.4.2*) (*15*, *74*).

Hence, the BP process requires challenging separation procedures hindering techno-economic feasibility thus leading to low yield and as a consequence to high maintenance costs (*15*). Moreover, OME_2 is the main product of the process with 83% in the overall product composition, which is not the target product regarding OME in diesel fuel applications (*11*, *15*). Thus, OME products produced *via* this route are hampered in their direct application in diesel engines.

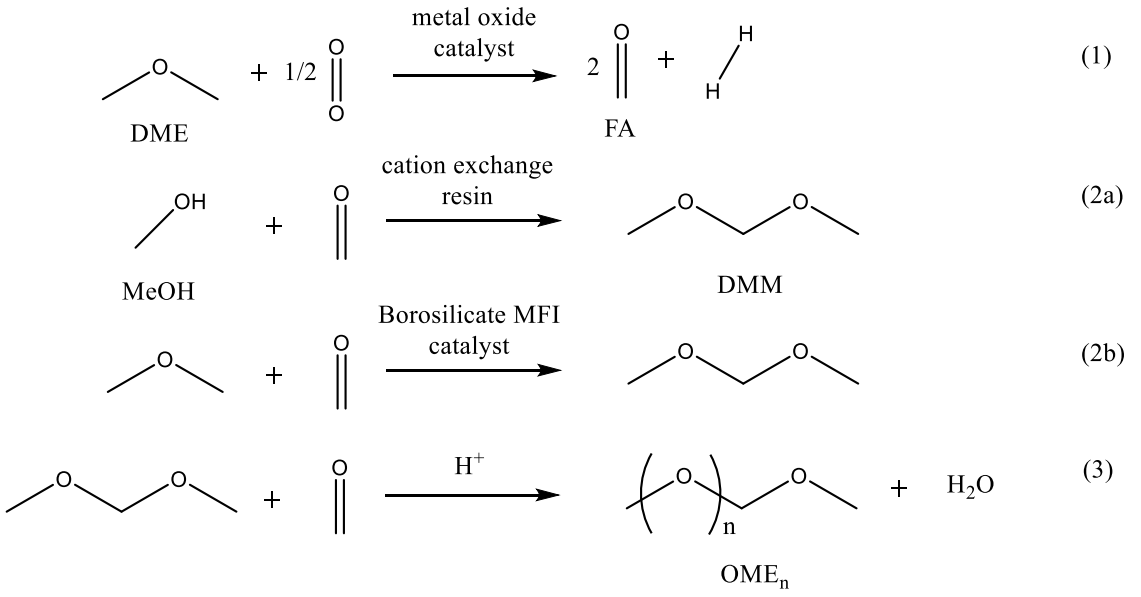

Figure 25 BP process routes for OME_n production (*15*)

2.7.2. BASF process

To overcome water formation upon OME synthesis and to avoid complex purification procedures, BASF patented the reaction depicted in **Figure 26** (*15*). In a first reaction, TRI is opened catalyzed by sulfuric acid (H_2SO_4) to FA monomers (reaction (1)), which are subsequently incorporated into DMM catalyzed by a cation exchange resin thus leading to OME products (reaction (2)) (*15*). Burger et. al (*11*) reported a detailed kinetic study on this reaction pathway proposing a process for OME production catalyzed by

Amberlyst® 46 (*11, 63–65*). The product selectivity is favored for DMM and OME_2 production comprising 73.2% of the overall composition.

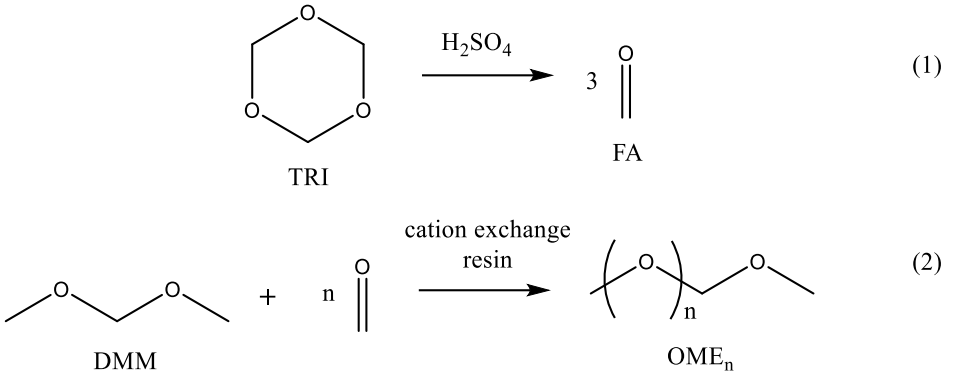

Figure 26 BASF trioxane process route for OME_n production (*66, 73*)

Replacing DMM with DME results in an OME_3 selectivity of 58% of the overall composition, which makes OME fuel more applicable for diesel engines compared to the BP process. Haltenort et. al (*102*) investigated this reaction procedure more in detail proposing an acid-catalyzed trioxane ring-opening and direct incorporation into DME, explains the preferred formation of OME_3 producing other OME products *via* consecutive transacetalization reactions as shown in **Figure 27** (see *2.4.3* for more clearance) (*102*).

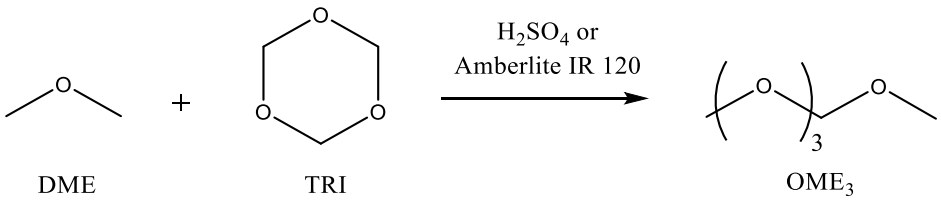

Figure 27 BASF DME process route for OME_3 production (*66, 73*)

2.7.3. Lanzhou Inst. process

In contrast to the BP and BASF process, Lanzhou institute developed an OME production process using ionic liquids as catalyst starting either by TRI and MeOH or other alcohols (*132, 133*). High conversions of the educts and thus high OME product selectivity were reported for this reaction route, similar to many other reports on ionic liquid catalyzed OME synthesis developed preferably by Chinese academics and industry (*117, 118*). Moreover, this type of catalyst was described by Wu and co-workers (*117*) to provide an easy separation from the reaction mixture and to exhibit great recyclability. However, various other authors classify ionic liquids as expensive and toxic materials requiring multiple rectification units for their separation form the product mixture (*15, 119*). As noted previously (see section *2.6*), further discussion on ionic liquids are out of scope within this work.

2.7.4. Application: one-step synthesis route of OMEs

Another approach for the synthesis of exclusively DMM (OME_1) was developed through a selective oxidation of MeOH to firstly FA on the redox sides of the catalyst, which subsequently reacts with another MeOH on the acidic sites of the catalyst producing preferably DMM (**Figure 28**) (*15*, *132*). Representatives of this type of catalyst are e.g. V_2O_5 or V_2O_5/ZrO_2 supported on γ-Al_2O_3 (*15*, *132*). Thus, this reaction route is at present developed to produce exclusively DMM, which cannot be directly employed in diesel engines. More details on the various catalysts and reaction conditions were summarized in great detail by Bhatelia and co-workers (*15*) with the reaction conditions provided in **Table 11**.

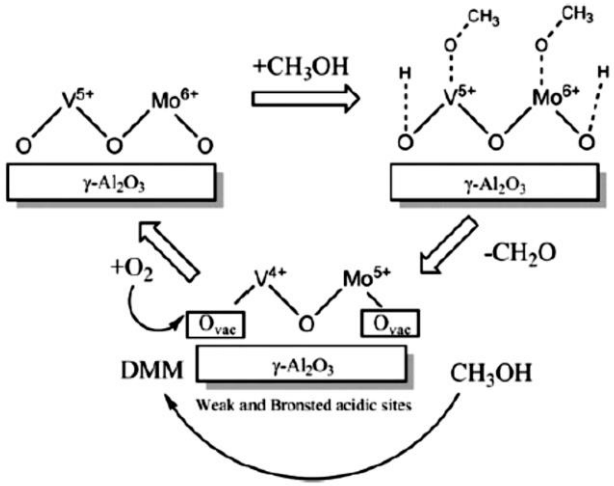

Figure 28 Production of DMM by the selective oxidation of MeOH catalyzed by V-O-Mo oxides *via* one-step OME synthesis (image retrieved from ref. (*132*))

3.1. Materials and Methods

3.1.1. Instruments

In **Table 12** an overview of the technical devices is provided, which were employed for OME synthesis, analysis and quantification. The respective technical settings will be discussed in the next sections in detail. Other tools such as syringes and vials used for GC measurement are provided in **Table 13**. However, glass equipment will not be described in detail and is referred as standard laboratory glassware.

Table 12 Overview of the apparatus required for OME synthesis, analysis and quantification

Device	Classification
Melting point measuring device	SANYO SG99/11/367; Cat. No. MP D350.BM3.5
Infrared moisture analyzer	Sartorius MA 35
Heating and stirring plate[a]	Lactan RCT Basic (IKA Labortechnik)
External temperature sensor[a]	IKA® ETS-R4 fuzzy 2666600
Autoclave (100 mL)	HEL stainless steel (max. 350°C, 100 bar)
Autoclave (40 mL)	HEL stainless steel (max. 250°C, 350 bar)
Heating and stirring plate coupled with an external temperature sensor[b]	Heidolph Hei-Standard (MR Hei-End)
Inductively coupled plasma mass analyzer (ICP-MS)	Agilent 7700
GC-FID	Agilent 6890A gas chromatograph equipped with a 7683 autosampler
GC-MS	Agilent 7890A gas chromatograph equipped with a 7693 autosampler connected to a 5975C mass analyzer
Balance	Sartorius BP 210S
Oven	VWR Venti-Line

[a] Reactions performed at ambient conditions
[b] Reactions performed under pressure

Table 13 Tools necessary for support in OME synthesis, analysis or quantification

Tool	Manufacturer
Plastic syringe	BD-Discordit™ II (2 mL), INJEKT® Braun (10 mL), HENKE SASS Wolf (100 mL)
Glass vials for GC measurement	Thermo Scientific 2 mL (12 x 32 mm)
Caps with rubber septum	LLG Labware® (11 mm)
Metal cannula	FINE-JECT® Braun Sterican® (120 mm), HENKE SASS WOLF (100 mm)

3.1.2. Chemicals and acidic catalysts

3.1.2.1. Employed chemicals

The chemicals employed for OME synthesis, purification and quantification are provided in **Table 14**. All chemicals were used as received without any further pretreatment. The catalysts essential for OME synthesis will be discussed in the upcoming section *3.1.2.2*.

Table 14 Overview of the employed chemicals for the synthesis, purification and quantification/analysis of OME compounds

Chemical	Abbreviation	Application	Purity [%]	Manufacturer
1,3,5 – trioxane	TRI	educt	≥ 99	Sigma Aldrich, Germany
dimethoxymethane	DMM	educt	> 98	Alfa Aesar, Germany
methanol	MeOH	educt, solvent	HPLC grade	Fischer Scientific, UK
para-formaldehyde	pFA	educt	97	Alfa Aesar, Germany
ethanol	EtOH	solvent	99%	VWR Chemicals
dimethylformamide	DMF	solvent	99%	Fischer Scientific, UK
tetrahydrofurane	THF	solvent, internal standard	>99.8% (HPLC grade)	Fischer Scientific, UK
acetone	-	cleaning solvent	HPLC grade	Fischer Scientific, UK
1,4 - dioxane	-	cleaning solvent	HPLC grade	Fischer Scientific, UK
n-hexane	-	extracting solvent	HPLC grade	Fischer Scientific, UK
cyclohexane	-	extracting solvent	HPLC grade	Fischer Scientific, UK
sodium hydroxide	NaOH	neutralization base	99	VWR Chemicals
potassium hydroxide	KOH	titration	99	VWR Chemicals
helium	He	analytics	5.0	Messer, Austria
synthetic air	-	analytics	5.0 – KW free, 20 Vol% O_2, 80 Vol% N_2	Messer, Austria
hydrogen	H_2	analytics	5.0	Messer, Austria
nitrogen	N_2	analytics, reaction	5.0	Messer, Austria
calcium chloride	$CaCl_2$	drying agent	general purpose grade	Fischer Scientific, UK

3.1.2.2. Homogeneous and heterogeneous acidic catalysts

In **Table 15** the utilized acidic catalysts for OME synthesis are provided, classified as homogeneous (liquid) and heterogeneous (solid) catalysts. Furthermore, the manufacturer specifications are given according to the data sheet. The liquid catalysts, sulfuric acid and methanesulfonic acid (MSA) were used as received.

The heterogeneous solid acid catalyst Deloxan® was an old stock of a former commercially available catalyst. At present, this type of solid acid, exhibiting reactive sulfonyl groups, cannot be ordered from chemical manufacturers. Details on the physical properties and the catalyst pretreatment will be discussed in the following section *3.1.2.3*.

Table 15 Homogeneous catalysts (sulfuric acid, MSA) and heterogeneous catalyst (Deloxan®) utilized for OME synthesis – manufacturer specification

Homogeneous catalyst	Manufacturer	Specification
sulfuric acid	Carl Roth	98% [a]
methanesulfonic acid (MSA)	Alfa Aesar	> 98% [a]
Heterogeneous catalyst		
Deloxan®	Degussa Hüls AG	ASP IV/6-2 S-W; suspended water wet; (0.1 – 0.4 mm); 72.2% moisture content[a]

[a] Provided by the manufacturer

3.1.2.3. Deloxan® - specification and pretreatment

Pretreatment of Deloxan® (ASP IV/6-2 type solid acid catalyst) was performed by stirring 150 g of the resin in 200 g of methanol for 15 minutes. The solid was subsequently filtered over a buchner funnel and washed thoroughly with additional methanol. This procedure was repeated twice leaving a colorless wet catalyst, which was subsequently dried at 105°C yielding a brownish powder with a minimum moisture content of approximately 3 – 4%. Prior usage for reactivity experiments, the moisture content was determined by an infrared moisture analyzer.

As no data sheet could be obtained for Deloxan® the exchange capacity was determined by titrating 50 mg of the dry catalyst against 0.005 M KOH base with phenolphthalein as indicator. Thus, approximately 50 mg of dry catalyst were diluted in 5 mL distilled water and two drops of the indicator were added. The titration was performed under vigorous stirring of the catalyst solution and was repeated thrice.

Furthermore, the sulfur content was determined externally by ICP-MS (specified in **Table 12**). For sample preparation, an aliquot of the dry catalyst (100 mg) was digested in 2 mL HNO_3 in an MLS autoclave. The temperature profile was applied by heating the mixture and digesting for 30 min at 250°C. The result was calculated and provided as a mean value of two independent measurements. It has to be noted, that the digesting procedure was incomplete yielding a gel-like residue.

3.1.3. Experimental procedure and reaction set-up

Pre-experiments for OME synthesis

A 40 mL stainless steel autoclave equipped with a magnetic stir bar (10 mm length) was purged trice with N_2 prior loading with 5.5 g of DMM (0.07 mol, 6.4 mL) and 6.0 g of trioxane (0.07 mol). The catalyst sulfuric acid (0.112 g, 1.13 mmol, 60.8 µL) was injected by a plastic syringe to the educts. Subsequently, the reactor was sealed by a rubber O-ring and was pressurized to 9 bar N_2 gas. A control experiment in a second 40 mL stainless steel autoclave employing equal amounts of DMM, trioxane and sulfuric acid was conducted without applying N_2 pressure. Both reaction vessels were placed in a metal heating jacket to ensure a constant heat transfer from the magnetic stirrer to the synthesis autoclave. The temperature of the heating jacket was set to 80°C and was controlled externally for both reactors. Once the temperature was reached, the reaction was run under vigorous stirring for 60 min. After reaction completion, both reactors were quenched in an ice bath for 15 min prior opening. The obtained reaction products yielded for both experiments colorless solids in quantitative yield.

General procedure for reactions performed under ambient conditions

To obtain reliable data, all experiments performed in glass vessels under ambient atmospheric pressure were strictly conducted in a two-neck flask (50 or 100 mL) equipped with a reflux condenser, Teflon® coated magnetic stir bar (15 mm) and a drying tube filled with $CaCl_2$. A schematic representation of the glass equipment is shown in **Figure 29** and the experimental set-up for OME synthesis is depicted in **Figure 30**.

Firstly, trioxane (4.0 g, 0.04 mol) was added in the flask and subsequently DMM (3.4 g, 0.04 mol, 3.9 mL) was injected *via* syringe through the septum, which was exchanged by a glass stopper prior heating to ensure no losses of the reaction mixture through evaporation. Heating of the reaction mixture was ensured by a paraffinic oil bath to a reaction temperature of 80°C under refluxing conditions and vigorous stirring until a homogenous solution was obtained. Once the reaction temperature was reached and stabilized, catalyst dosage for the homogeneous catalysts (MSA, sulfuric acid) was performed by a syringe, whereas the heterogeneous catalyst (Deloxan®) was added with a spatula. Exemplarily, for the optimized catalyst loadings of 1 wt% of sulfuric acid, 0.117 g (1.19 mmol, 63.6 µL), for 3.2 wt% of MSA, 0.241 g (2.51 mmol, 0.163 mL) and for 1.7 wt% Deloxan®, 0.129 g were added. The moment of catalyst addition was considered as the starting time of the reaction (t = 0 min). After 60 min reaction time, a sample of the reaction mixture (t = 60 min) was analyzed by GC-FID or GC-MS. The detailed analytical procedure including quantification of the OME products will be described in chapter *3.1.4*. The remaining reaction mixture was cooled to room temperature, neutralized with the corresponding amount of aqueous NaOH (2.5 M) and if required, further purification steps were performed including distillation and extraction procedures.

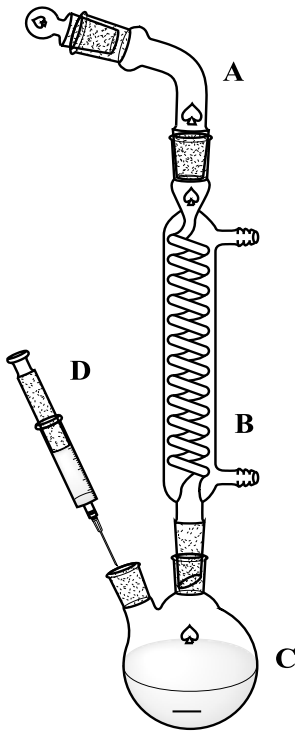

Figure 29 Schematic representation of the reaction set-up for experiments performed at ambient conditions; A = drying tube filled with $CaCl_2$; B = water cooled reflux condenser; C = two-neck 100 mL vessel charged with a Teflon® coated stirring bar and the educts; D = syringe for transfer of DMM, liquid catalyst or sampling of the reaction mixture

Figure 30 Reaction set-up; glass cuts secured with plastic or metal clips; openings are sealed with rubber septum or glas stub; external temperature control of the paraffinic oil bath; tubes for water cooling of the reflux condenser;

Experiments on OME kinetics performed under ambient conditions

The reaction procedure and set-up of the OME synthesis at ambient conditions catalyzed by either sulfuric acid, MSA or Deloxan® were conducted as previously described. For the kinetic studies, the educt loadings were kept in the range of 3.4 g for DMM (0.04 mol, 3.9 mL) and 4.0 g for trioxane (0.04 mol). Once the reaction mixture reached the desired reaction temperature, the corresponding amount of catalyst was added either by syringe (for MSA, sulfuric acid) or by spatula (for Deloxan®), denoting the reaction start (t = 0 min). The investigated reaction conditions are summarized in **Table 16** comprising the variation of the catalyst dosages, reaction temperature, reaction time and molar educt ratio of DMM/TRI.

For studies on the product profile depending on the reaction time, samples of the liquid product phase were drawn by pre-heated glass pipettes (at 105°C) in intervals of 10 – 20 min, collected in glass vials and analyzed by GC-FID. Details on the quantification procedure will be discussed in the section *3.1.4.* After reaction completion, the reaction was stopped by neutralization with aqueous NaOH and the reaction mixture was cooled to ambient temperature.

Table 16 Reactions performed at ambient pressure (educts = DMM, TRI)

	Sulfuric acid	MSA	Deloxan® [a]
Catalyst dosage [wt%]	0.2 – 1.5	1.0 – 3.8	0.1 – 2.0
Reaction temperature [°C]	75, 80, 85, 90	50, 60, 70, 80, 85, 90	50, 60, 70, 80, 85, 90
Reaction time [min]	0 – 90	0 – 100	0 – 100
Molar educt ratio n_{DMM}/n_{TRI}	1.0	0.5, 1.0, 2.0	0.5, 1.0, 2.0

[a] refers to pre-treated solid catalyst, dried to a moisture content of 3 – 4 %

General procedure for reactions performed in autoclaves

The experiments carried out under N_2 pressure were conducted in a stainless-steel autoclave with an internal volume of 100 mL. In **Figure 31** a schematic representation of the autoclave set-up is depicted with the applied experimental set-up in **Figure 32**. For technical details of the autoclave, heating and stirring plate and the temperature control see *3.1.1* (**Table 12**).

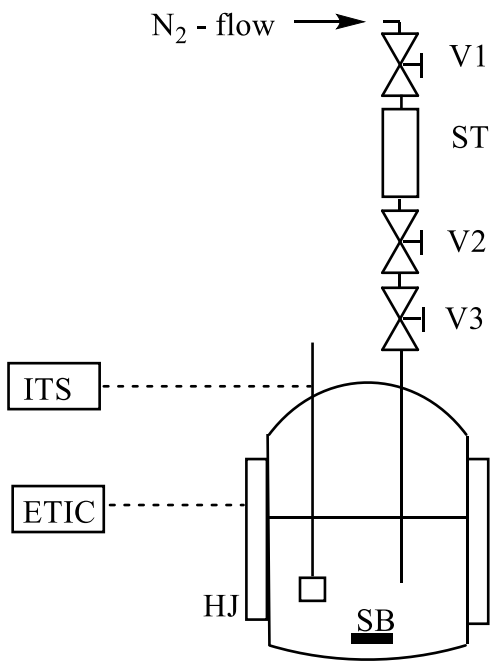

Figure 31 Schematic of the autoclave utilized for the reactions under N_2 pressure. V1, filling valve; V2, control valve; V3, closing valve ST, storage tank for liquid acid; SB, stirring bar; HJ, heating metal jacket; ITS, internal temperature sensor; ETIC, external temperature indicator and control.

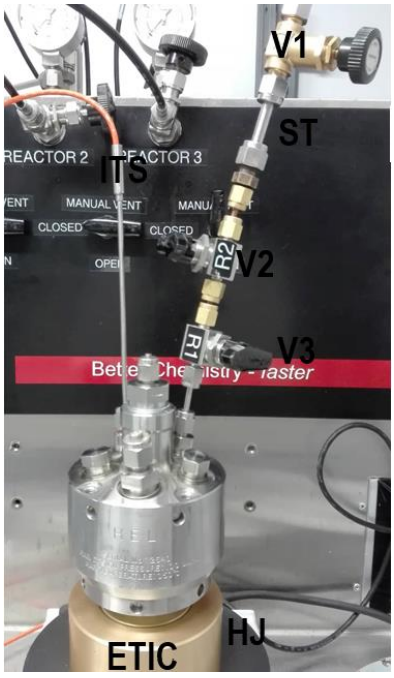

Figure 32 Representation of the autoclave set-up during OME synthesis; V1, filling valve; V2, shutting valve; V3, control valve ST, storage tank for liquid acid; SB, stirring bar; HJ, heating metal jacket; ITS, internal temperature sensor; ETIC, external temperature indicator and control.

The reaction procedure was carried out by loading the methyl-cap providing chemical (DMM, MeOH) and the FA source (pFA, TRI) with a Teflon®-coated magnetic stir bar (15 mm length) in the autoclave. The educt combinations with the corresponding catalyst amounts are provided in **Table 17**. Subsequently, the autoclave was sealed by a rubber O-ring and stirring of the reaction mixture at 250 min^{-1} was started simultaneously as heating of the reaction mixture. The autoclave temperature was

controlled externally (ETIC) with a metal heating jacket (HJ) and the internal temperature was solely measured by a temperature sensor (ITS). Injection of the liquid catalyst sulfuric acid and MSA was performed by a transfer-line, consisting of a N_2 inlet connected *via* a valve (V1) to the catalyst tank (ST, tank volume 0.9 mL) as depicted in **Figure 31**. The latter was further attached in the sequence to one control valve (V2) and one closing valve (V3), which was essential as the transfer-line can be removed from the autoclave without influencing the interior pressure by shutting the closing valve (V3). For the homogenously catalyzed reaction, once the temperature reached 80°C, the required amount of catalyst in the storage tank was quickly pressed with 9 bar N_2 pressure into the reaction mixture referred as the reaction starting time (t = 0). The heterogeneously catalyzed reaction was performed by adding the catalyst to the reaction mixture prior heating and was subsequently pressurized once the reaction temperature reached 80 °C denoting the reaction starting time. Both, the homogeneously and heterogeneously catalyzed OME reactions were stopped after 60 min reaction time by quenching the autoclave with an ice bath to ambient temperature. Subsequently, the liquid phase was analyzed by gas chromatography (see *3.1.4*).

Table 17 Reactions performed in autoclaves under N_2 pressure (molar ratio of educts (DMM, TRI, MeOH, pFA) = 1; pressure = 9 bar; reaction time = 60 min; internal reaction temperature = 80°C)

Educt combinations	m (methyl – cap) [g]	m (FA – source) [g]	m (catalyst) [g]
DMM/TRI	17.9	21.9	0.394 (1 wt% sulfuric acid)
	18.6	22.0	1.312 (3.2 wt%; MSA)
	17.8	21.8	0.673 (1.7 wt% Deloxan®)
DMM/pFA	21.4	10.0	0.351 (1 wt% sulfuric acid)
	20.7	8.41	0.954 (3.2 wt% MSA)
	20.9	8.53	0.534 (1.7 wt% Deloxan®)
MeOH/TRI	5.48	29.2	1.132 (3.2 wt% MSA)
	11.7	31.5	0.766 (1.7 wt% Deloxan®)

Kinetic experiments for reactions performed in autoclaves

To obtain comparable data, the experimental procedure for reactions performed in autoclaves was conducted strictly following the previously described general procedure at an internally controlled reaction temperature of 80°C. The educt combinations DMM/TRI, DMM/pFA and MeOH/TRI with amounts typically in the range as provided in **Table 17** were weighed in the 100 mL autoclave equipped with a magnetic stirrer (15 mm length).

Reactions were performed including variation of the catalyst loads at the fixed stoichiometric educt ratio of 1 both for the reactions with DMM/TRI catalyzed by MSA (1.0 or 3.2 wt%) and Deloxan® (1.0 or 1.7 wt%), and for the reaction with DMM/pFA catalyzed by sulfuric acid (1.0 or 1.5 wt%). Moreover,

the reaction employing MeOH/TRI catalyzed by 3.2 wt% MSA and 1.7 wt% Deloxan® was performed at different stoichiometric educt ratios at constant catalyst loads. In **Table 18** an overview is provided for the varied kinetic parameters for the corresponding educt combinations. All reactions were terminated after 60 min reaction time upon quenching of the autoclave in an ice bath to ambient temperature. Samples were drawn subsequently and were analyzed by GC-FID.

Table 18 Reactions performed in autoclaves under N_2 pressure (educts = DMM, TRI, MeOH, pFA; pressure = 9 bar; reaction time = 60 min; internal reaction temperature = 80°C)

Educt	Parameter	Sulfuric acid	MSA	Deloxan® [a]
DMM, TRI	catalyst dosage [wt%]	1.0	1.0, 3.2	1.0, 1.7
	molar ratio n_{DMM}/n_{TRI}	1	1	1
MeOH, TRI	catalyst dosage [wt%]	---	3.2	1.7
	molar ratio n_{MeOH}/n_{TRI}	---	0.5, 1.0, 3.0, 5.0	0.5, 1.0, 2.0, 5.0
DMM, pFA	catalyst dosage [wt%]	1.0, 1.5	3.2	1.7
	molar ratio n_{DMM}/n_{pFA}	1	1	1

[a] refers to pre-treated solid catalyst, dried to a moisture content of 3 – 4 %

3.1.3.1. Cleaning of the reaction apparatus – glass equipment and autoclaves

Cleaning of the autoclaves prior OME synthesis was performed using 1,4 – dioxane, acetone or MeOH as solvents. The 40 mL or 100 mL autoclaves were charged with solvent accounting max. 80% of the total reactor volume. Prior sealing 1 wt% of H_2SO_4 were added, then the mixture was heated to 120°C or 80°C for 60 min. This procedure was repeated until the interior of the autoclaves exhibited a cleaned steel surface.

Glass equipment was not necessarily cleaned by a specific method prior OME synthesis. However, OME reactions leading to an increased pFA formation resulted in a colorless solid sticking to the flask or reflux condenser walls. Treatment of the glass equipment with a concentrated aqueous NaOH solution in some cases leaving the vessels for one week in basic media removed any impurity. Subsequently, thoroughly rinsing with deionized water had to be ensured to neutralize the equipment.

Both, glass and autoclave equipment were stored at 105°C and cooled in a desiccator prior usage for OME synthesis.

3.1.3.2. Extraction and distillation procedure of OME products

Crude multi-step distillation procedure

The multi-step distillation was performed for the neutralized OME reaction product phases, which were obtained from the educts DMM and trioxane from experiments catalyzed by different sulfuric acid catalyst loadings (0.7 – 1.0 wt%). For the distillation, the neutralized product mixtures were combined in a 100 mL round-bottom flask equipped with a magnetic stirrer, a vigreux column (20 cm length, 1

cm in diameter) and a Liebig-cooler (25 cm length) connected to one or more collecting flasks. Heating was performed by an oil bath under vigorous stirring. After each distillation step the collected distillates were sealed and fresh flasks were utilized for the next distillation step.

In the first distillation the pressure was reduced to 608 mbar at an oil bath temperature of 106°C to remove MeOH and DMM (head temperature 52°C). In the second and third distillation step the pressure was further reduced at an oil bath temperature of 130°C and the column head temperature 62 – 72°C and the distillates rich in TRI and OME_2 were collected. To enhance the distillation progress, the column was coated in aluminum foil. Solids accumulating in the Liebig cooler were heated by a heat gun and collected. Small amounts of OME_3 and OME_4 could be obtained at higher distillation temperatures (122 – 138°C) with the column head temperature being 62 – 68°C (**Table 19**). The crude distillation was stopped after five steps and all intermediate sump products and distillates were analyzed by GC-FID.

Table 19 Distillation parameters including the oil bath temperature, column head temperature and pressure for the multi-step distillation

No. of distillation steps	Distillate content[a]	T (oil bath) [°C]	T (head) [°C]	p [mbar]
1	MeOH, DMM	86 – 106	36 – 52	930 – 608
2	OME_2, TRI	106 – 110	62 – 66	580 – 367
3	TRI (OME_2)[b]	115 – 130	67 – 72	480
4	OME_3, OME_4, TRI	122 – 125	40 – 64	410 – 460
5	OME_3, OME_4	137 – 138	62 – 68	121 – 143

[a] According to GC-FID measurements
[b] traces of OME_2 present after the second distillation step

Distillation procedure to obtain OME_2 and OME_3 standards

From the crude distillation procedure, the distillates after the second step (crude distillation) were combined and cooled in an ice bath for two hours to solidify trioxane. The supernatant was collected in a round-bottom flask equipped with a magnetic stir bar and a vigreux column (20 cm length, 1 cm diameter), which was connected to a Liebig cooler and a collecting flask. The distillation was conducted at an oil-bath temperature of 98 – 94°C at 600 mbar under reduced pressure with a column head temperature of 44°C. The OME_2 product was obtained in >97% purity (200.1 mg), determined by GC-FID.

For the distillation of OME_3 and OME_4, the distillate was employed after distillation step no. 5 of the crude distillation. This was performed at a bath temperature of 130°C, 480 mbar reduced pressure and a head temperature of 70°C. The desired OME_3 being in the distillate and OME_4 in the distillation sump were obtained in >95% purity (167.8 mg) (GC-FID).

Extraction procedure

The extraction of the distilled OME reaction mixture was performed in four consecutive steps. For this, in a 10 mL separatory funnel an aliquot of 2 mL OME mixture was extracted with 2 mL of distillated water and 2 mL of either n-hexan or cyclohexane. The upper organic phase was again extracted with 2 mL of each distilled water and organic solvent. After each extraction step, the organic phase was analyzed by GC-FID. Subsequently, solvent removal was attempted either under vacuum (water bath temperature of 40°C, 235 mbar) or by a crude distillation with an oil bath temperature at 100°C, 400 mbar reduced pressure and a head temperature in the range of 42 – 58°C. The experimental procedure for the distillation was in accordance to the previously described set-up.

3.1.4. Analytical procedure

3.1.4.1. Chromatographic methods

Technical details on the GC-FID and GC-MS including columns, software, temperature profile and gas flows are provided in **Table 20**.

Table 20 Settings for the GC-FID and GC-MS measurements

	GC-FID	GC-MS
Gas chromatograph	Agilent 6890A	Agilent 7890A/5975C
Autosampler	Agilent 7683	Agilent 7693
Column	Agilent HP-5 (30 m x 250 µm x 0.25 µm)	DB-5-MS (30 m x 250 µm x 0.25 µm)
Software	Chemstation	Chemstation
Injection volume	1 µL	1 µL
Column flow	1.0 mL/min	0.5 mL/min
Split ratio	50:1	50:1
Injection temperature	250°C	250°C (transfer-line temperature: 310°C)
Gas flows	H_2 = 30 mL/min synthetic air = 350 mL/min	He = 28.5 mL/min
Start temperature of temperature profile	35°C (for 7 min)	35°C (for 7 min)
Heating ramp	30°C/min	30°C/min
End temperature of temperature profile	280°C (for 10 min)	280°C (for 4 min)
Transferline/Detector temperature	250°C	250°C
Internal Standard	THF	THF

3.1.4.2. Sample preparation and quantification

The sampling procedure which was applied for the liquid phase of the OME reactions was conducted as depicted in **Figure 33**. Firstly, in a GC glass vial a defined mass (m_n = 70 – 100 mg) of the liquid product phase from the OME reaction mixture was weighed in (**A**) and secondly an aqueous aliquot of sodium hydroxide (NaOH) solution was added corresponding to the amount which was required to neutralize the acidic catalyst (**B**). For quickly solidifying samples the glass pipettes applied for sampling were pre-heated prior sampling to 105°C. Subsequently, to the neutralized sample (**C**) a defined volume of the internal standard THF stock solution in DMF (100 mg/mL) was added and weighed for a precise quantification of the OME products (**D**). The amount of ISTD was kept constant for all sampled quantification measurements (m_{THF} = 70 mg). After neutralization and addition of the ISTD, the GC glass vial was sealed and solidified products were dissolved by heating of the sample to 50°C prior quantification by GC-FID (*3*).

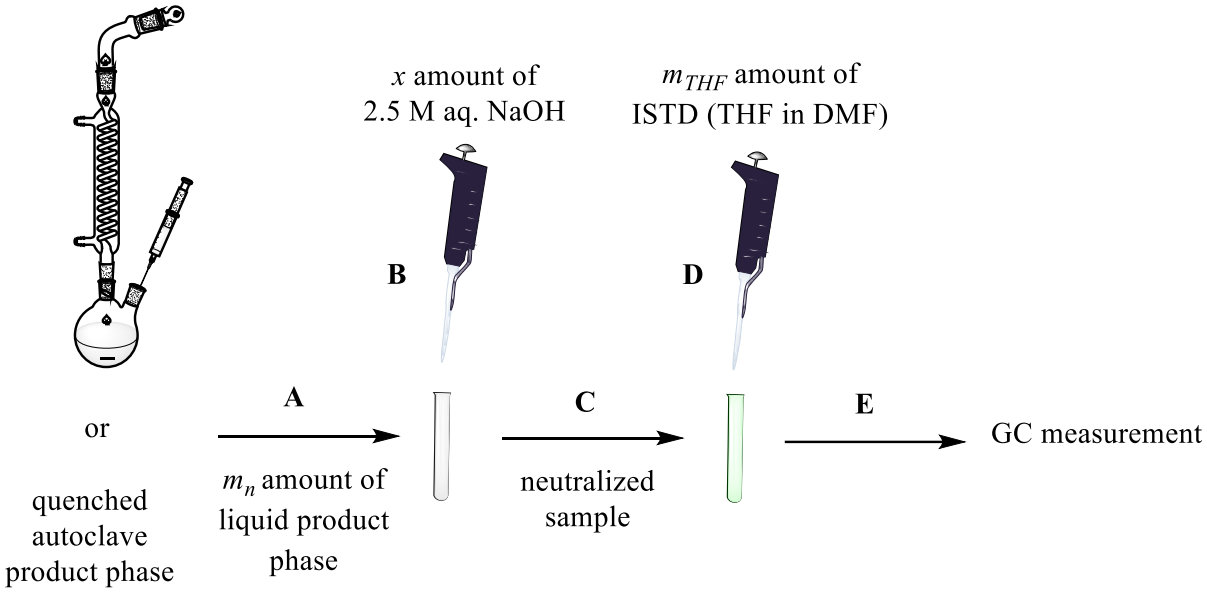

Figure 33 Sampling of the OME reaction for GC measurements for reactions performed at ambient conditions or under N_2 pressure

4. Results and Discussion

As an approach towards the development of OME as alternative synthetic fuels an economically feasible synthesis was the major objective, which was further utilized for a deeper understanding of OME purification and quantification procedures, kinetic understandings and the establishment of a plain synthesis at ambient conditions. Moreover, prior the kinetic investigation a detailed survey of scientific and patent literature was conveyed. Much attention was devoted to the exact procedure including experimental set-up and pre-mixing of educts, catalyst addition, neutralization of the reaction mixture and subsequent sample preparation for quantification since no detailed procedure could be retrieved from literature. Based on the synthetic approach reported by Li and co-workers (*18*), for DMM and TRI as starting educts a pressure-free OME synthesis was developed for the catalysts sulfuric acid, MSA and Deloxan®. Furthermore, pressurized studies were conducted utilizing MeOH, DMM, TRI and pFA as starting educts aiming to determine optimal conditions for (a) a low side-product formation such as formals, glycols and others, (b) high OME_n yields with n = 3 – 5 since these chain lengths were found best suited regarding fuel properties (see *2.2.1*), (c) a plain and quick reaction procedure and finally, (d) a cost-efficient OME synthesis with high educt conversions based on educts derived from a renewable base stock. From the results obtained within this work a manuscript was prepared, which will be cited if necessary (*3*).

4.1. GC-Analysis of reaction products

4.1.1. General remarks

To derive a reaction procedure preferably at ambient conditions, a combination of different reports by various authors including the patent literature of Gresham and Brooks (*125*) was found to lead to the most promising OME synthesis procedure. For this, three important considerations resulted: Firstly, that all glass vessels had to be pre-heated to reduce the water content; secondly, which was moreover the most important finding during the development of the synthetic procedure, all educts had to be charged in the vessel and heated under refluxing conditions to 80°C in the absence of the catalyst and lastly, once the reaction temperature was stabilized, the catalyst was added under vigorous stirring.

Once the experimental procedure was established, a quantification procedure of the OME products was required. The quantification of the OME reaction described by the analytical procedure in chapter *3.1.4* was developed for the liquid OME_n product fraction. For all experiments the influences of free formaldehyde and water in the reaction mixture were chosen as independent variables. Moreover, side-product formation will be treated in a qualitative way, as the production and moreover the quantification of OME_n products was the major objective in the scope of this work. Therefore, information on hemiformals (HF_n, n = 1 – 3) and other by-products were derived from GC-MS measurements. The mass spectra of the corresponding products are listed in the *Appendix*. In this regard it must be considered,

that the ionization source (electron ionization, EI) of the GC-MS was too harsh for the determination of the molecule ion signal in the mass spectra of longer chain OME_n compounds. The retention times of the products were assigned according to their boiling points since the fragmentation pattern exhibits only little differences for $n \geq 1$ OME products. The retention times determined for the OME products and side-products are summarized in **Table 21**. The product distribution of OME, the amounts of DMM, TRI and MeOH were quantitatively analyzed by GC-FID and all products were furthermore confirmed by GC-MS measurement. The GC-areas were determined by automated integration of the signals from the GC-FID – chromatogram for the calculation of the corresponding relative response factors, RRF_n, and subsequently for the determination of the mass selective yields, *Y*, of the DMM, TRI, MeOH and OME_n compounds. Details on the quantification will be provided in the following chapters (*3*).

Table 21 Overview of the retention time of compounds forming upon OME synthesis

	GC-FID retention time [min]	GC-MS retention time [min]
MeOH	3.2	2.1
TRI	6.5	5.0
DMM	3.7	2.6
OME_2	7.2	6.7
OME_3	10.6	10.3
OME_4	12.1	11.7
OME_5	13.0	12.8
OME_6	13.8	13.7
OME_7	14.5	14.5
OME_8	15.1	15.2
OME_9	15.7	15.7
OME_{10}	16.4	16.5
OME_{11}	17.1	17.4
OME_{12}	18.0	18.5
side products		
MF[a]	n.d.[b]	2.3
HF_1	4.0	2.5
HF_2	n.d.	10.5
HF_3	10.8	13.0
Gly_1	n.d.	10.0
Gly_2	n.d.	11.0
Gly_3	n.d.	12.1

[a] Methyl formiate is assumed to form upon OME synthesis confirmed by GC-MS mass analysis
[b] n.d., not detected

In the context of the sampling procedure, it must be considered that the amount of acidic catalyst for the OME production determined the required quantity of base for neutralization, which was calculated for each sampling step prior sampling. Moreover, the consistency of the reaction mixture was directly affected by the catalyst loading. It was experimentally found, as it will be discussed in the next chapters in detail, that higher catalyst loadings lead to the production of longer chain OME products or the side product pFA. Therefore, sampling of these reaction mixtures was challenging as the product phase was solidifying very rapidly upon cooling. As described in section *3.1.4.2*, pre-heating of pipettes was performed to overcome this difficulty. However, some samples could not be drawn even by pre-heated pipettes. For these reactions, a representative amount of the solid product was weighed into the glass vial and further preparation steps were performed as previously described (*3.1.4.2*). The sealed vial was heated subsequently at 50°C until a liquid phase was obtained and the GC measurements were performed immediately.

Furthermore, neutralization of the reaction mixture either for sampling or after reaction completion was performed to prevent the reaction from proceeding. In this regard, for the liquid catalysts sulfuric acid and methane sulfonic acid (MSA) the neutralization step is straightforward. In contrast, the heterogeneous catalyst Deloxan® had to be analyzed upfront for the determination of the exchange capacity by titration against a standard base (see *3.1.2.3*). The results of the titration experiments of the corresponding amounts of dry Deloxan® and the required volumes of KOH for neutralization will be covered in section *4.4.4* (see **Table 27**). Neutralization was tested by both ethanolic and aqueous NaOH in a concentration of 2.5 M, which will be discussed in more detail in the section *4.7*.

Moreover, it was of utter importance to avoid too basic media especially for the subsequent quantification procedure. The solvent of choice which was used for the preparation of the samples or the internal standard (ISTD) stock solution was dimethylformamide (DMF), as an aprotic non-volatile solvent (*134*) exhibiting chemical instability in basic conditions (*135, 136*). Advantageously, the solid side product *para*-formaldehyde (pFA) is prone to form upon OME synthesis which can be dissolved in hot DMF (*137*). Media containing hydroxide ions were reported to rapidly decompose DMF to dimethylamine and formate ion, as shown in **Figure 34** (*138*). Dimethylamine was confirmed by GC-MS measurement of a basic DMF solution at a retention time of 2.2 min (see *Appendix,* **Figure 75** (m/z = 44.1)). A detailed investigation of the signals obtained by GC-MS revealed the formation of N,N,N',N' – tetramethyldiaminomethane (retention time of 4.5 min). This compound might be formed in situ from monomeric formaldehyde (FA) obtained upon acidic breakup of trioxane and dimethylamine *via* a condensation reaction as depicted in **Figure 34** (*139*).

Hence, maintaining neutral conditions of the samples for GC measurements was of great importance and more details on the sample preparation procedure prior quantification by GC-FID measurements will be discussed in the following chapter.

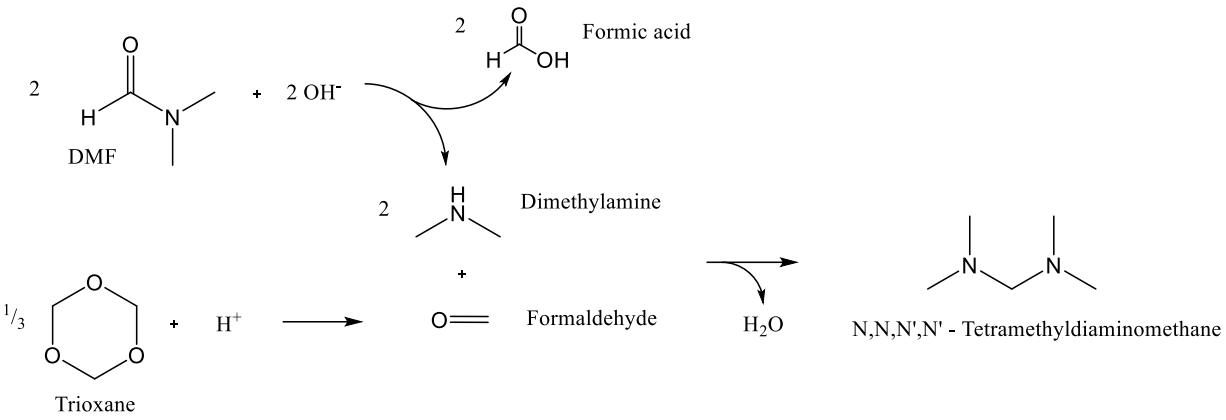

Figure 34 Formation of dimethylamine from dimethylformamide (DMF) by consumption of hydroxyl ions and subsequent condensation with monomeric formaldehyde (FA) to N,N,N',N' – tetramethylamino-methane (*139*)

4.2. Selection of the internal standard (ISTD)

In the prior sections, the sample preparation procedure for the reactions performed within this work was described in detail (see *3.1.4.2*). However, for the quantification of OME products and thus for the determination of the OME_n product distribution for kinetic studies, no details regarding sample preparation could be obtained from literature. Thus, OME_n products were quantified by GC-FID using THF as the internal standard (ISTD). An example of a sample chromatogram measured by GC-MS or GC-FID upon OME synthesis containing the ISTD and DMF as solvent in basic conditions is shown in **Figure 35** and **Figure 36**, respectively.

In literature, several chemical compounds were reported which would be suitable as internal standard for OME product quantification, such as octane (*102*), n-dodecane (*31, 36*), toluene (*31, 36*), nitrobenzene (*31, 36*), 1,4 – dioxane (*69, 140*) and tetrahydrofurane (THF) (*140*). Typically, when an internal standard is used for quantification the standard should be chemically similar to the analytes (*141*). The 1,4 – dioxane and THF as etheric compounds resemble the most to OMEs products. However, the prior could not be applied as an internal standard as the retention time of 1,4 – dioxane was the same as for OME_2 upon measuring with GC-FID. In this regard, THF was chosen as the internal standard (ISTD), which was then applied for the quantification of the products obtained upon OME synthesis, purification or distillation. However, it must be considered that THF is chemically unstable in acidic conditions leading to its polymerization (*142*). Hence, the pH value has to be set to neutral (pH = 6 – 7) to prevent acid catalyzed reactions of the ISTD. Though, upon acid-catalyzed OME synthesis the acidic medium must be neutralized to prevent twice, THF from acid-catalyzed ring opening reactions thus leading to non-accurate quantification results and DMF from hydroxyl anion catalyzed decomposition.

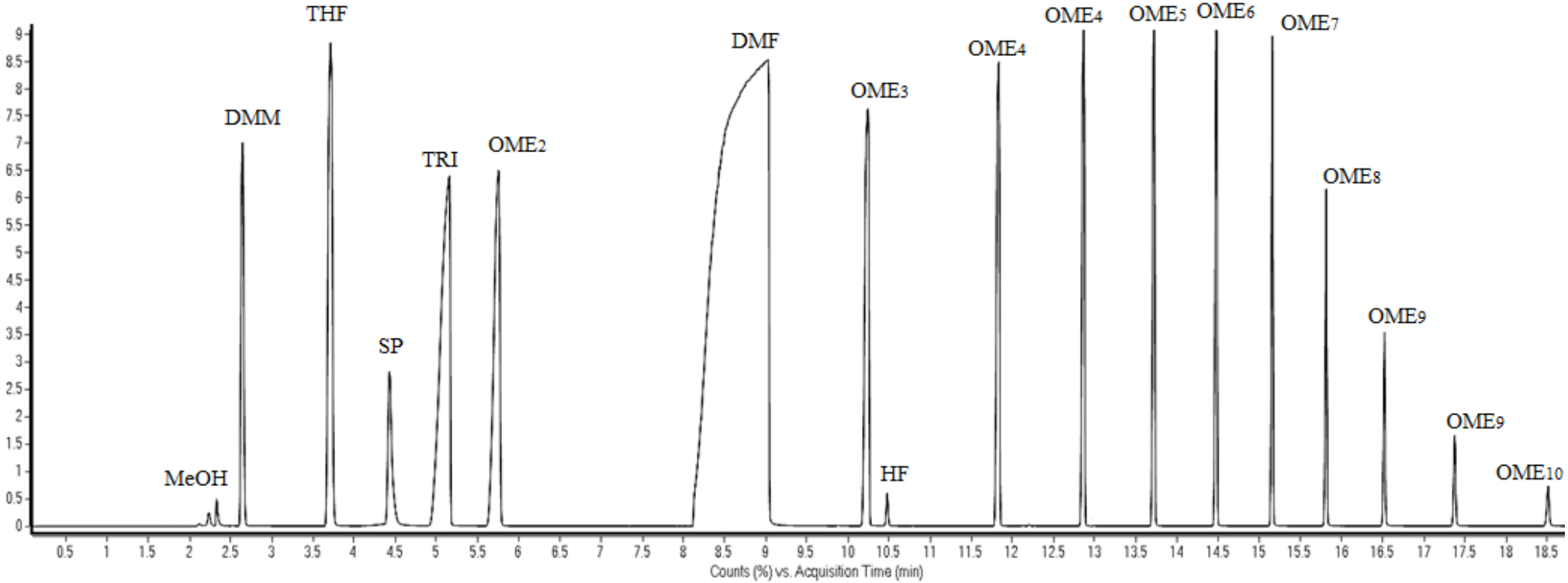

Figure 35 GC–MS chromatogram of a OME sample in DMF (8 – 9 min) and THF (3.7 min) as ISTD after synthesis (4.0 g TRI, 3.4 g DMM, 0.117 g sulfuric acid; 80°C; 60 min reaction time); N,N,N',N' – tetramethyldiaminomethane (SP denoting side-product) at 4.5 min.

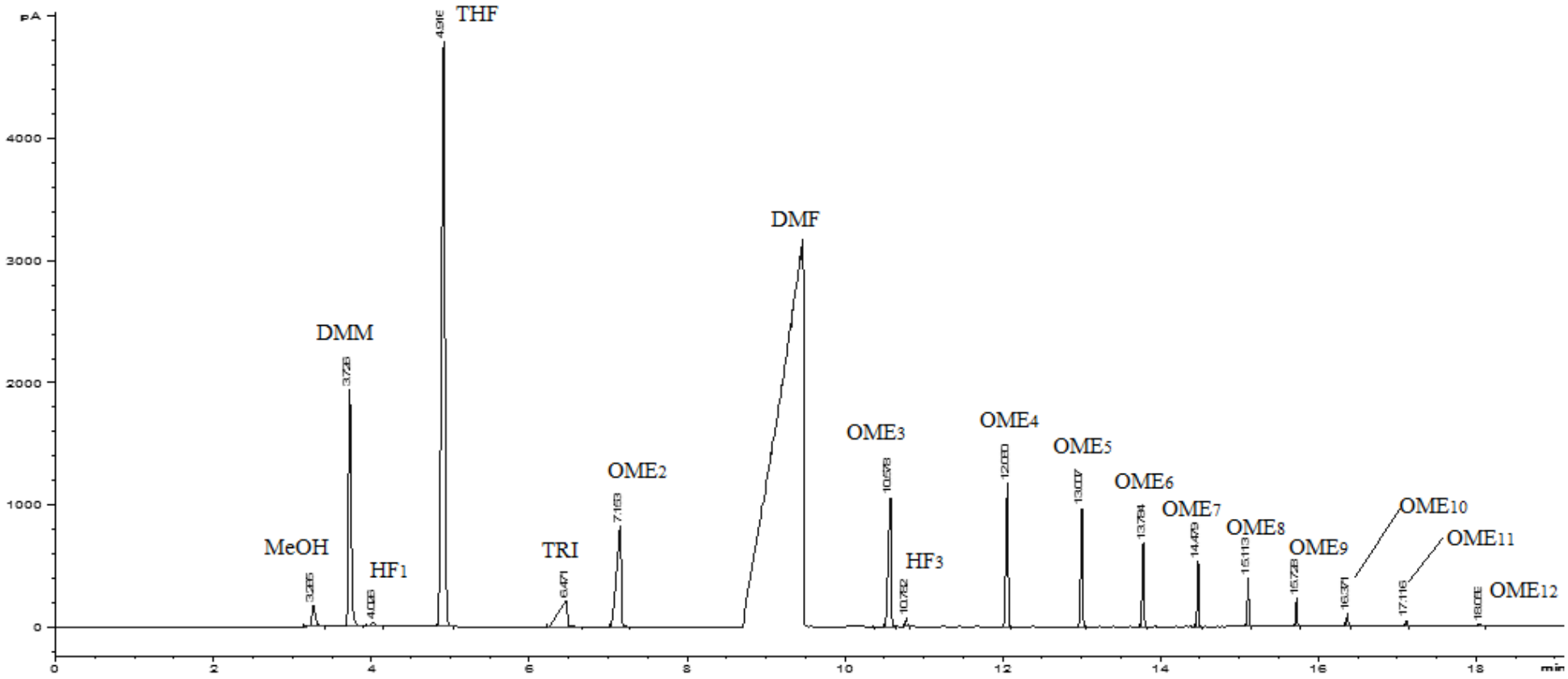

Figure 36 Example of a GC–FID chromatogram of an OME sample in DMF (8.8 – 9.1 min) and THF as ISTD (4.9 min) after synthesis (4.0 g TRI, 3.4 g DMM, 0.117 g sulfuric acid; 80°C; 60 min reaction time)

4.2.1. Calculation of the relative response factors (RRF_n) for OME_n products

In literature, quantification of OME was conducted *via* the internal standardization method (*20, 31*) as this method is mostly used if sample losses are expected (*143*). Utilization of an internal standard as the quantification technique for etheric compounds is favored as an accurate and convenient approach, provided by gas chromatography equipped with a flame ionization detector (GC-FID) (*140*). Calculation of relative response factors, RRF_n, for OME_n compounds was introduced as an accurate method for quantification. However, OME compounds of higher oligomerization (n > 6) are difficult to obtain as these are solids at ambient conditions (*64*), therefore hindering the determination of accurate RRF values (*69, 140*). In this context, Burger et. al (*64*) proposed to linearly extrapolate the RRF values for n < 6 to determine RRFs for longer-chain OME compounds. Furthermore, Zhu and co-workers (*140*) reported a more precise quantification of OME compounds by determination of RRF values *via* the effective carbon atom number increment for multi-ethers using THF as internal standard. These values were used for cross-checking of the calculated RRF_n values determined herein.

Therefore, the relative response factors, RRF_n, were calculated by **Eq. 5** for the educts (TRI, DMM, MeOH) and the OME compounds, with *n* signifying the corresponding OME chain length.

$$RRF_n = \frac{A_{THF}\, m_n}{A_n\, m_{THF}}$$

A_{THF}…peak area of THF (ISTD)
A_n…peak area of the compound
m_n…sample mass
m_{THF}…mass of THF (ISTD)

Eq. 5

The determination of the RRF_n values obligatory for the quantification of the components was conducted using THF as internal standard (see *4.2*). The peak area of THF, A_{THF}, and of the compound, A_n, were derived *via* automated peak integration. The corresponding masses of the internal standard, m_{THF}, and of the compound, m_n, were determined gravimetrically.

For this, pure OME_1, OME_2, OME_3 and OME_4 compounds were distilled to a purity of >97% or >95% GC peak area for the calculation of individual relative response factors ($RRF_{1\text{-}4}$). The educts, TRI and DMM were used as received to obtain the corresponding RRF values. In **Table 22** the experimentally derived RRF_n values are provided for the relative response factors of the educts, DMM

and TRI, and for the pure OME_{1-4} compounds, RRF_{1-4}, which were calculated as a mean value from four independent GC-FID measurements.

Table 22 Experimentally derived values for the relative response factors (RRF_n; n referring to the OME chain length)

	TRI	**DMM**	**OME_1**	**OME_2**	**OME_3**	**OME_4**
RRF_n	7.133	1.851	1.885	2.245	2.424	2.617

For OME with n > 4 the extrapolated RRF_n values with the derived values provided in **Table 23**.

Table 23 Extrapolated values for the relative response factors RRF_n with *n* referring to the OME chain length; n = 5 – 10

	OME_5	**OME_6**	**OME_7**	**OME_8**	**OME_9**	**OME_{10}**
RRF_n	2.684	2.774	2.850	2.916	2.974	3.026

Thus, the experimentally derived RRF_n values with n = 1 – 7 were compared to values reported in literature as shown in **Figure 37** (*140*). The experimentally derived RRF_n values with n = 1 – 4 and the extrapolated values with n > 4 were found to be in good agreement with values reported by Zhu and co-workers (*140*) utilizing THF as internal standard (**Figure 37**).

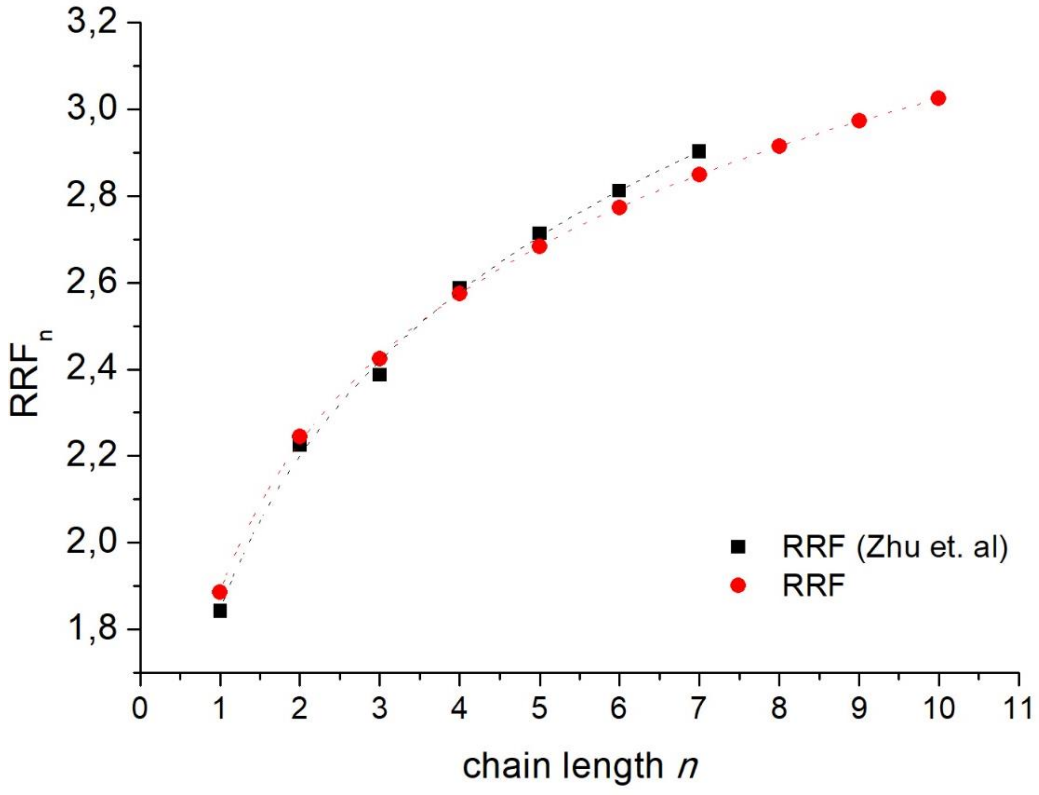

Figure 37 RRF_n (n = 1 – 7) values reported in literature (*140*) and experimentally derived RRF_{1-4} values as well as extrapolated $RRF_{n>4}$ (*140*)

4.3. Pre-experiments for OME_n synthesis

Throughout the early reports based on OME synthesis, purification or process development publications the exact synthesis procedure in most publications or patents is described rather vaguely, mostly referring in the context to firstly load the educts including the acid catalyst and subsequently to heat the reaction mixture to the desired reaction temperature (*11, 64, 107, 112, 114, 123, 125, 144*). However, some recent reports focused on the importance to provide a more detailed experimental procedure (*39, 45, 74, 101, 104*). In this regard, some synthetic OME procedures regarding pressurized reactions propose to pre-heat the autoclave loaded with the educts to the desired reaction temperature and subsequently to release the catalyst to the reaction mixture, denoting the reaction starting time (*64, 74, 145*). Gresham and Brooks (*125*) described in their patent the synthesis of OMEs at ambient pressure. Interestingly, this patent literature as well as some experiments reported by Lautenschütz (*20*) are the only published detailed OME preparation procedures performed at ambient pressure. A survey of the published patent literature is provided in the *Appendix*.

Since the focus of this work was set on the investigation of a more detailed OME_n synthesis performed at ambient pressure, the reaction parameters provided by Li and co-workers (*18*) for the catalyst sulfuric acid (H_2SO_4) served as the basis for the pre-experiments. Nevertheless, Li et. (*18*) al did not state exactly how the reaction was conducted, employing the catalyst sulfuric acid (1 wt%) with the educts DMM and TRI in an autoclave.

Therefore, first experiments for the synthesis of OME products following the experimental procedure according to Li et al. (*18*) were performed in a stainless-steel autoclave (40 mL). The educts, TRI and DMM were loaded in the autoclave, then the catalyst H_2SO_4 was added. Subsequently, the vessel was sealed and pressurized to 9 bar with N_2. As a control experiment, a reaction was performed in a second autoclave (40 mL) with the same amounts of educts and catalyst. However, this reaction was conducted in absence of N_2 overpressure. Both reactions were heated simultaneously to 80°C and by reaching the reaction temperature the mixtures were stirred for exactly 60 min. The corresponding masses and reaction parameters are provided in **Table 24**.

Table 24 Parameters and masses of the educts for the pre-experiments of OME synthesis conducted in autoclaves or glass vessels

Parameters[a]	Ambient pressure or pressurized ($p(N_2)$ = 9 bar)
m(TRI) [g]	6
m(DMM) [g]	5.5
$m(H_2SO_4)$ [wt%]	1.0
reaction conditions	80°C, 60 min

[a] In accordance to Li et. al, with the molar ratio of the educts given as n_{DMM}/n_{TRI} = 1 and the catalyst loading set with 1 wt% (*18*).

After reaction completion, both autoclaves were rapidly cooled in an ice bath. The colorless products for the pressurized and non-pressurized experiment were obtained in quantitative yield as depicted in **Figure 38** and **Figure 39**, respectively. The colorless solid products of both reactions were dissolved in hot DMF for subsequent GC-MS measurement, which confirmed the presence of $OME_{2\text{-}12}$ products. Moreover, the formation of pFA as a side-product in sulfuric acid catalyzed OME reactions was noted by Li and co-workers (*18*), hence its formation was expected, which was proofed by a melting point analysis. The melting region of pure pFA provided by the manufacturer is given in the temperature region of 150 – 180°C, as the solid is decomposing to gaseous FA upon heating (*146*). However, as the colorless solid was containing OME products as well, the measured decomposition region was determined at lower temperature in the range of 145 – 175°C. Hence, the pre-experiments yielded for both reactions majorly pFA as the undesired side product with some amounts of $OME_{2\text{-}12}$. Furthermore, it was concluded that no significant qualitative differences could be found if the reaction pressure was omitted during the OME synthesis. Additionally, since the cleaning procedure of the autoclaves was very time consuming (see *3.1.3.1*), another experiment at ambient pressure was carried out in a two-neck glass vessel. Moreover, reactions conducted at ambient pressure do not necessarily require pressure vessels as the reaction temperature was moderately set at 80°C (*18*). For reactions performed at ambient atmospheric pressure, the utilized masses and reaction conditions were kept invariant (see **Table 24**).

Figure 38 Pre-experiment for the OME synthesis product of the pressurized reaction

Figure 39 Pre-experiment for the OME synthesis product of the non-pressurized reaction

Figure 40 Pre-experiment for the OME synthesis product carried out in glass vessels at ambient pressure

Again, educts and the catalyst were loaded at ambient temperature and were subsequently heated to the reaction temperature of 80°C for 60 min (see *3.1.3* for more details). Similarly, a colorless solid was obtained after completion of the reaction, as shown in **Figure 40**.

At this point, a more detailed reaction procedure was established. Especially Burger et. al (*64*), Oestreicher et. al (*39, 45*) and Schmitz et. al (*69, 104*) provided a detailed description on the synthetic procedure for OME synthesis performed in autoclaves. Hence, the herein conducted reactions in pressure vessels were performed by pre-heating of the educts in the sealed autoclave. The liquid catalyst (sulfuric acid, MSA) was injected by a N_2 pressure of 9 bar once the reaction temperature was reached. The acidic solid catalyst (Deloxan®) was added prior heating and pressurizing of the reaction mixture. Quenching of the reaction by an ice bath was performed to terminate the reaction. Moreover, a technique was developed for reactions performed at ambient conditions employing standard laboratory glass equipment without the necessity to apply a reaction pressure. Briefly, the educts were loaded in a round-bottom glass vessel equipped with a reflux condenser, which were heated to the reaction temperature. The corresponding amount of catalyst was added once the reaction temperature was stabilized and a homogeneous liquid educt mixture was obtained. More details on the neutralization of the reaction mixture to terminate the OME synthesis was covered earlier (see *3.1.3*). Briefly, a defined amount of the reaction mixture was neutralized in a vial by aqueous NaOH (2.5 M). Subsequently, 70 mg of the internal standard THF solution in DMF were added, the sample vial was sealed and measured by GC (*3*).

4.4. Dimethoxymethane (DMM) and trioxane (TRI) as educts

4.4.1. Screening of catalysts

Experiments at ambient pressure were carried out once the reaction procedure was established including the neutralization and subsequent sample preparation steps. Firstly, the homogeneous and heterogeneous Brønsted acid catalysts including concentrated sulfuric acid, MSA and Deloxan® were examined for synthesis of OMEs, according to the reaction conditions at ambient pressure proposed by Li et. al (*18*). These catalysts are known to be highly hygroscopic (*147, 148*), thus water present during OME synthesis hydrolyzes the desired etheric products (*74*). Therefore, for the production of OMEs it was vital that the required amount of the corresponding catalyst was transferred quickly to the reaction mixture. To evaluate the catalytic activity of sulfuric acid, MSA and Deloxan®, a screening of the catalysts was conducted at a catalyst load of 1.0 wt% at 80°C and 60 min reaction time (*3, 18*). It must be noted, that for OME reactions with TRI and DMM as educts, DMM is not included in the OME product yield and is treated solely as educt.

The experimental results of the quantified OME_n product distributions for the corresponding catalysts are summarized in **Table 25**. Obviously, sulfuric acid (H_2SO_4) exhibits at the proposed catalyst load of 1.0 wt% (*18*) and the given reaction conditions compared to MSA and Deloxan® the highest catalytic

activity, producing comparably more OME_{2-8} products. Moreover, MSA catalyzes at the given catalyst load preferably short chain OME_n products, with n = 2 – 5, whilst Deloxan® shows a preferred formation of longer chain OME_n products, with n > 8.

Table 25 Catalytic activity of the different catalysts (loading 1.0 wt%) for the reaction of DMM with TRI (reaction conditions: 80°C, 60 min, $n_{DMM}/n_{TRI} = 1$)

Catalyst load (1.0 wt%)	X_{TRI} [%]	Mass selectivity *Y* [wt%][a]								
		OME chain length *n*								
		2	3	4	5	6	7	8	2-8	n > 8
H_2SO_4	59.8	14.8	13.1	10.8	8.2	5.6	3.4	1.4	57.2	1.1
MSA	11.2	9.00	2.55	0.92	0.19	0.00	0.00	0.00	12.7	0.00
Deloxan[b]	33.0	11.5	10.2	8.36	6.15	4.37	3.02	2.03	45.6	3.03

[a] Mass selectivity *Y* refers to the corresponding OME_n mass fraction according to the amount sample analyzed
[b] Moisture content of Deloxan® 3 – 4 wt%

However, the results for MSA and Deloxan® catalyzed reactions were unsatisfying due to the lower mass selective yields compared to the H_2SO_4 catalyzed OME_n synthesis. Therefore, in the next step a more detailed investigation for different catalyst loadings of H_2SO_4, MSA and Deloxan® for the OME synthesis was conducted. Catalyst screening was performed by a consecutive increase of the catalyst dosage for an initial educt mass of approximately 4 g TRI and 3.4 g DMM with a fixed reaction temperature of 80°C and 60 min reaction time.

In **Table 26**, the OME product yields corresponding to the optimized catalyst loads for H_2SO_4 (1.0 wt%), MSA (3.2 wt% and 3.5 wt%) and Deloxan® (1.7 wt%) are provided. It was found that both MSA and Deloxan® produce more OME_{2-8} products compared to H_2SO_4 at the given catalyst loads.

Table 26 Catalytic activity of the different catalysts for the reaction of DMM with TRI (reaction conditions: 80°C, 60 min, $n_{DMM}/n_{TRI} = 1$)

Catalyst[a]	cat. load [wt%]	X_{TRI} [%]	Mass selectivity *Y* [wt%][b]								
			OME chain length *n*								
			2	3	4	5	6	7	8	2-8	n>8
H_2SO_4	1.0[c]	59.8	14.8	13.1	10.8	8.2	5.6	3.4	1.4	57.2	1.1
MSA	3.2[d]	62.1	12.3	11.5	9.9	7.6	6.0	4.6	3.5	55.5	6.6
	3.5[c]	78.7	12.3	12.1	11.0	9.6	8.1	6.6	5.2	64.9	11.3
Deloxan® [e]	1.7[c]	69.4	11.7	11.1	10.0	8.3	6.6	5.2	3.9	60.3	11.6

[a] Reaction conditions: molar ratio DMM/TRI = 1, 80 °C, 1h, ambient pressure, catalyst load as given for the liquid catalysts H_2SO_4 and MSA or heterogeneous catalyst Deloxan®.
[b] Mass selectivity *Y* refers to the corresponding OME_n mass fraction according to the amount sample analyzed
[c] Optimized catalyst load at the given reaction conditions
[d] Catalyst load which has been used for further investigations
[e] Moisture content of Deloxan® 3-4 wt%

In this regard, it must be considered that a direct comparison of homogeneous and heterogeneous catalysts is more complicated, as for solid catalysts the diffusion of educts and products in the catalytic active sites is highly relevant, which might lead to lower product yields due to transfer hindrance of long-chain OME products (*1*). However, considering the experimental results, Deloxan® exhibits similar catalytic activity to H_2SO_4 and MSA (*16*).

Furthermore, in some reports on OMEs synthesis, the conversion of either the formaldehyde source, X_{CH2O}, or of DMM, X_{DMM}, is given for comparison of the catalytic activity and thus to predict the reaction progress for different liquid and solid catalysts (*114, 144, 149, 150*). However, high conversions of trioxane indicate implicitly formation of side-products (HF, Gly, MeOH), pFA and OME_n products. Li et. al (*18*) reported for the catalyst sulfuric acid at the given reaction conditions both, conversion and selectivity in mol C% towards OME_n products. However, no information could be obtained on the mass selective yields or mass distributions from the results reported by Li et. al (*18*) thus hindering the comparison of the experimental findings. As conducted by various reports in literature on OMEs synthesis (*101, 102, 151*), the experimental results provided herein for catalytic studies are given as mass selective yields, Y_{OMEn}. As the mol C selectivity could not be accurately recalculated into Y_{OME}, for comparative reasons the conversion of trioxane for the catalyst screening on the OME synthesis is given in **Table 26** (*18*). In this regard, Li et al. reported a 75.7% TRI conversion for the sulfuric acid catalyzed reaction with a 30% pFA side-product formation (*18*). The TRI conversion for the 1.0 wt% H_2SO_4 catalyzed OME synthesis was determined with X_{TRI} = 59.8% with almost no pFA formation, which is supporting the imprecision of the conversion as described (*3*).

Hence, the optimized catalyst loadings as previously noted were found at 1.0 wt% for sulfuric acid, 3.5 wt% for MSA and at 1.7 wt% for the solid acid catalyst Deloxan®. In **Figure 41** the experimentally derived $OME_{2\text{-}12}$ mass yield profiles as a function of catalyst loadings are provided. Reactions performed at lower catalyst loadings lead to lower OME product yields. Whilst sulfuric acid (**A**) was found to produce less $OME_{n>8}$ products over the total range of investigated catalyst loads, MSA (**B**) and Deloxan® (**C**) lead to significantly higher yields. Compared to sulfuric acid (1.0 wt%) both catalysts were found to produce higher $OME_{2\text{-}8}$ amounts at their optimized loadings, 3.5 wt% and 1.7 wt%, respectively. Nevertheless, at a catalyst load of 1.0 wt%, sulfuric acid was found to exhibit the highest catalytic activity. A more detailed discussion the OME product distribution for different catalysts and catalyst loadings will be discussed in the following sections.

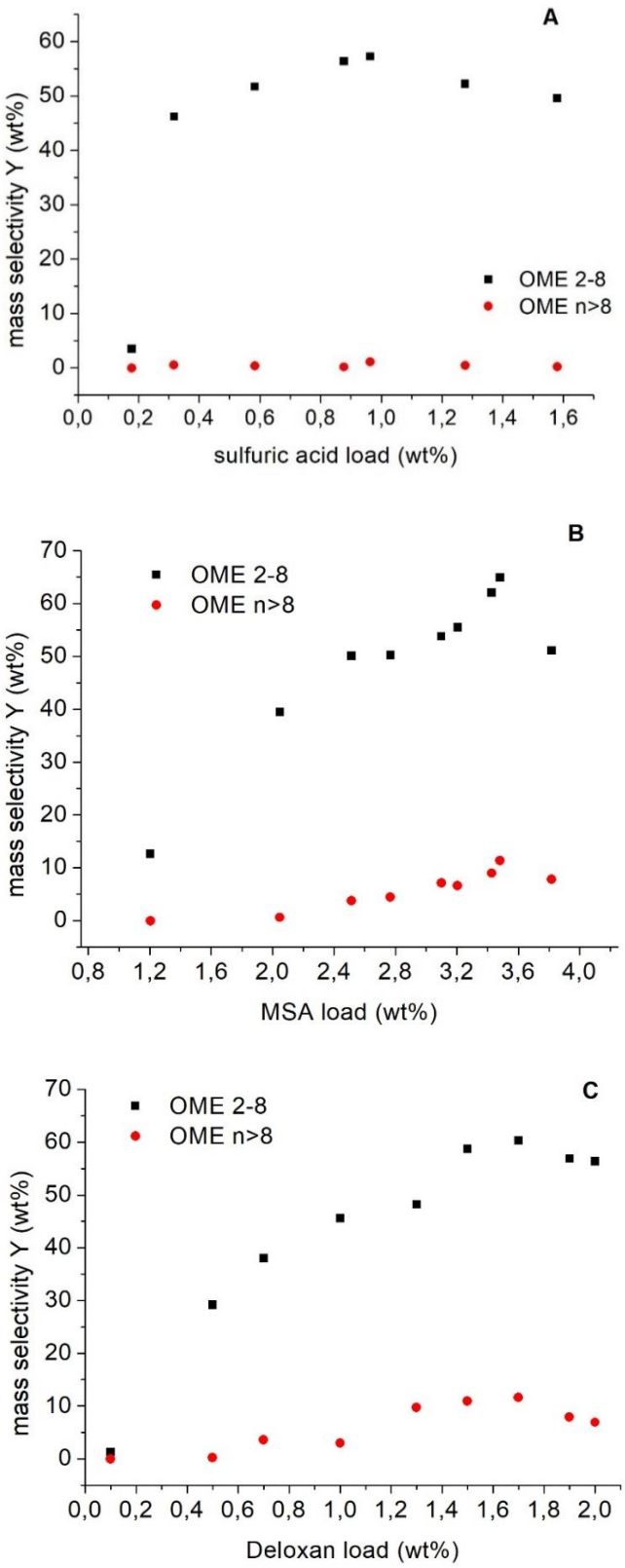

Figure 41 Comparison of the mass selective yield *Y* as a function of catalyst load for the liquid catalysts H_2SO_4 (**A**), MSA (**B**) and the solid ionic resin Deloxan® (moisture content 3-4 wt%; **C**); reaction conditions: 80 °C, 60 min, nDMM/nTRI = 1 (3)

4.4.2. Sulfuric acid (H_2SO_4) as homogenous catalyst

Sulfuric acid as a catalyst for OME synthesis has been reported by several authors, however, the catalytic performance on the reaction is discussed rather vaguely in various scientific and patent literature (*1*, *114*, *125*). The OME_n mass selective product yields were investigated for the catalyst loadings of 0.2 – 1.6 wt% for reactions performed at 80°C and 60 min reaction time at ambient pressure. The determined OME product distribution with n = 2 – 8, 3 – 5 or n > 8 are provided in **Figure 42**. At the catalyst dosage of 1.0 wt%, the mass fraction of both OME_{2-8} and $OME_{n>8}$ were determined to reach the maximum yield at the given reaction conditions. Conclusively, for lower or higher catalyst loadings, less OME production was observed. Interestingly, the OME_{3-5} mass fraction was found to comprise the highest amount with 34 wt% for the reaction catalyzed by 0.85 wt% H_2SO_4 (**Figure 42**, **C**).

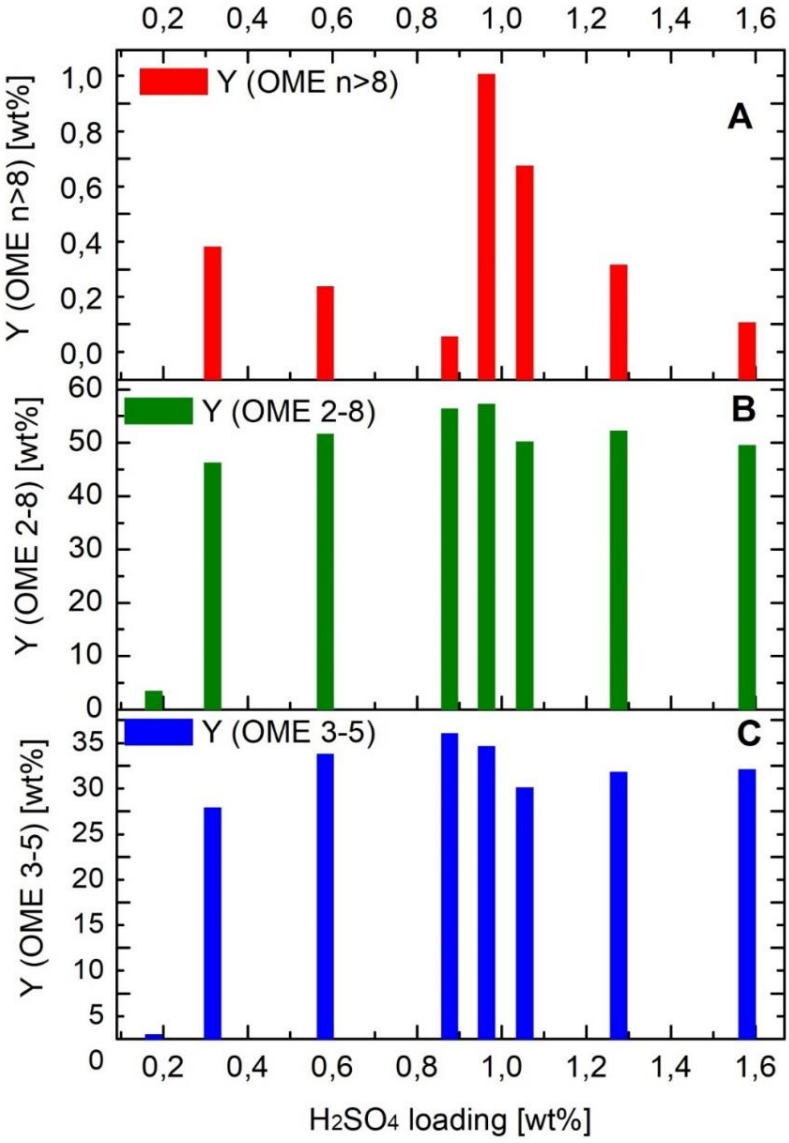

Figure 42 Mass selective yields for the OME_{2-8}, $OME_{n>8}$ and OME_{3-5} products as a function of different H_2SO_4 loadings

Moreover, even at lower catalyst loadings (except 0.2 wt%) the OME_{3-5} product yield was found at values above 25 wt%. Sulfuric acid produces preferably short-chain OME products with the $OME_{n>8}$ product fraction never exceeding 1 wt% (**Figure 42**, **A**). No adequate explanation could be derived for the sudden decrease of $OME_{n>8}$ at catalyst loads of 0.6 wt% and 0.9 wt% (**Figure 42**, **A**).

As previously noted, Li et. al (*18*) reported a pFA formation with 30% for reactions catalyzed by sulfuric acid. Meanwhile, qualitatively lower pFA formation has been found when handling the glass equipment with caution by e.g. storage in a desiccator or oven, transferring educts by pre-heating of utensils and other precautionary steps for experiments performed herein (**Figure 43**). However, at higher catalyst loadings, pFA formation could not be circumvented thus complicating the sampling and quantification procedure (*3*).

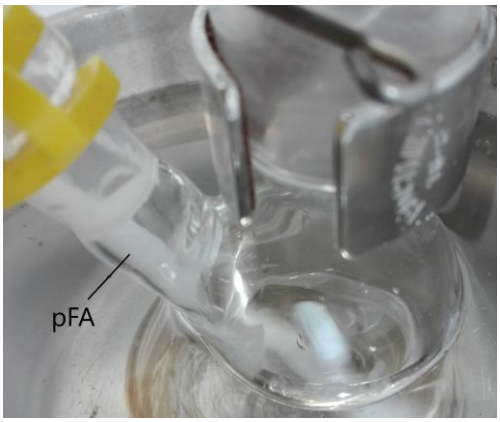

Figure 43 Example of a H_2SO_4 (0.6 wt%) catalyzed OME synthesis

4.4.3. MSA as liquid catalyst

In **Figure 44** three OME product mixtures are depicted after completion of the reactions catalyzed by 2.0 wt%, 3.0 wt% and 3.8 wt% MSA for OME synthesis. Macroscopically, the differences are clearly visible as lower catalytic loadings were experimentally found to produce less longer chain $OME_{n>8}$ products resulting in liquid OME product mixtures.

Figure 44 *From left to right*: OME reactions catalyzed by 2.0 wt%, 3.0 wt% and 3.8 wt% MSA loading (reaction conditions: 80°C, 60 min, $n_{DMM}/n_{TRI} = 1$)

However, higher loadings (> 2.5 wt%) produce significantly more $OME_{n>8}$ products, which are solids at ambient temperature (*64*), thus solidifying the product mixture at catalyst loadings higher than 3.5 wt%. In **Figure 45** the determined OME_{2-8}, $OME_{n>8}$ and OME_{3-5} mass fractions, Y_{OMEn}, are provided. Similar to the sulfuric acid catalyzed reactions, an increase of the OME_{2-12} mass fraction was observed up to 3.5 wt% of MSA loading producing the maximum OME mass yield, which was observed for the given reaction conditions .However, as an increasing $OME_{n>8}$ product fraction complicates the sampling and quantification procedures and additionally an increasing liquid catalyst load comprising $–SO_3H$ groups leads to enhanced corrosion at above ambient temperatures (*152*), the catalyst amount for further kinetic investigations on MSA has been chosen with 3.2 wt% providing nevertheless comparable product selectivity to H_2SO_4 catalyzed OME production (*3*). In this regard it must be considered, that H_2SO_4 as a diprotic strong acid conclusively exhibits an increased catalytic activity compared to the monoprotic MSA.

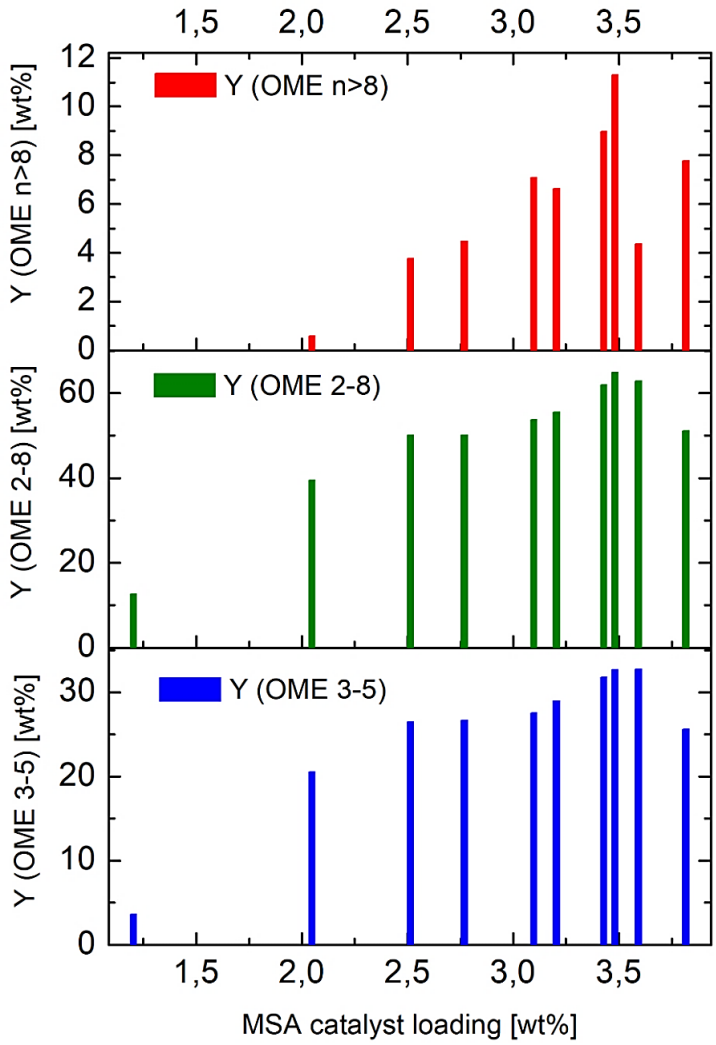

Figure 45 Mass selective yields for the OME_{2-8}, $OME_{n>8}$ and OME_{3-5} products as a function of different MSA loadings (reaction conditions: 80°C, n_{DMM}/n_{TRI} = 1, t = 60 min)

The OME_{3-5} fraction of the 1.0 wt% sulfuric acid catalyzed OME reactions with a OME_{3-5} yield of 32 wt% was found to be slightly less compared to the 3.5 wt% MSA catalyzed reaction exhibiting a OME_{3-5} mass selective yield of 33 wt%. Reaction conducted with 3.2 wt% MSA were found to exhibit with 29 wt% OME_{3-5} still comparable results to sulfuric acid catalyzed reactions.

Although, MSA was determined to lead to a lower catalytic activity compared to sulfuric acid at a given catalyst load, the sulfonic acid lead nevertheless to almost no pFA formation exhibiting additionally a good trioxane conversion and OME product selectivity (*3*). Moreover, the MSA catalyzed reactions lead to promising OME_{3-5} yields, which is the desired production fraction for blends with diesel fuel.

4.4.4. Deloxan® as solid acid catalyst

4.4.4.1. Characterization of Deloxan®

As described in *3.1.2.3*, the mean capacity of the pretreated solid acid catalyst Deloxan® was found with 0.659 mmol H^+/g dry Deloxan®. The sulfur content in Deloxan® was found to be 0.736 mmol S/g dry catalyst (**Table 27**). In theory, the sulfonyl groups, $-SO_3H$, exhibit per sulfur atom one catalytically active H^+ ion. A summary of the determined physical properties of the solid acid Deloxan® (ASP IV/6-2 S-W) are provided in **Table 28**.

Table 27 Titration of dry Deloxan® against KOH (0.005 M) (thrice) and the corresponding exchange capacity of the acidic catalyst

m (dry Deloxan®) [mg]	V (0.005 M KOH) [mL]	Capacity [mmol H^+/g dry catalyst]
51.1	6.80	0.656
50.8	6.45	0.658
50.0	6.40	0.664

Table 28 Determined physical properties of Deloxan® (ASP IV/6-2 S-W)

	Deloxan® (ASP IV/6-2 S-W)
Moisture content suspended waterwet [%]	69
Moisture content after drying [%]	3 – 4
Exchange capacity [mmol H^+/g dry catalyst] [a]	0.659
Sulfur content [mmol S/g dry catalyst]	0.736

[a] Averaged exchange capacities

4.4.4.2. Moisture content

The presence of water during OME synthesis has been reported by Burger and co-workers (*64*) to react with OME in an acid-catalyzed reaction forming hemiformals (HF_n), glycols (Gly) and MeOH, as already described in detail in the sections *2.4.2*. To obtain high OME_{2-8} mass fractions, the moisture

content of the acidic ionic resin Deloxan® has to be reduced to a minimum. The former commercially available heterogeneous catalyst Deloxan® was stored in its suspended water wet form and as the water presence during OME synthesis must be kept low, a catalyst pretreatment was crucial. For this, Deloxan® was washed thoroughly with MeOH in a three-step procedure. The moisture content was kept throughout the kinetic investigations between 3 – 4%. This was achieved upon pre-drying and storing of the catalyst at a temperature of 105°C in a sealed glass vessel as described earlier (see *3.1.2.3*). In **Figure 46** (*left*) the catalyst is depicted prior treatment with a moisture content of 69%, which was determined by the infrared moisture analyzer. In **Figure 46** (*right*) the purified and dried catalyst is shown, exhibiting a characteristic brownish coloring (*3*).

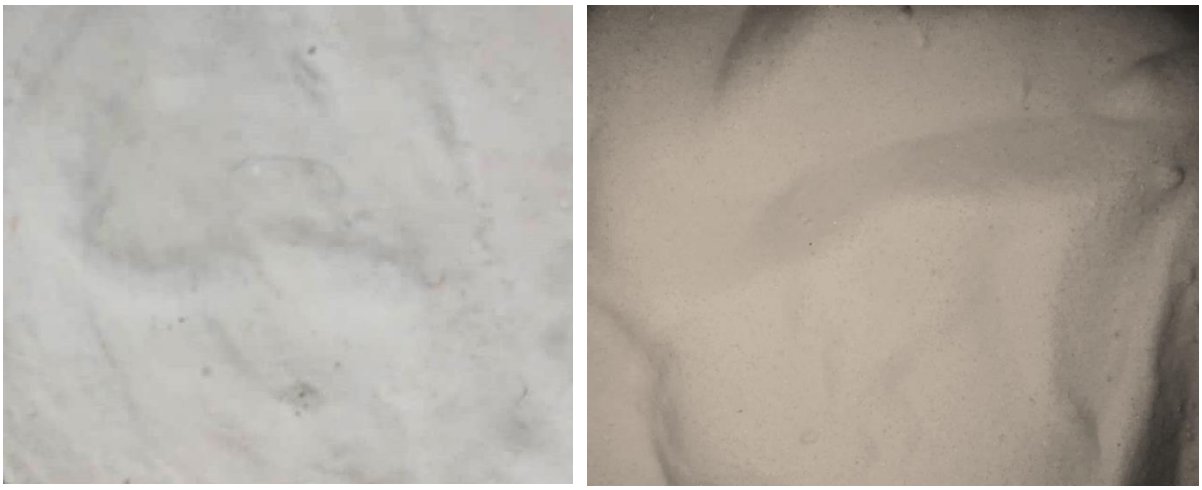

Figure 46 *Left*: colorless suspended waterwet Deloxan® catalyst (ASP IV/6-2 S-W); *right*: brownish Deloxan® catalyst after pretreatment (moisture content 3 – 4%)

The influence of the moisture content on the OME product distribution catalyzed by Deloxan® is shown in **Figure 47**. It was found throughout the catalyst screening experiments, which will be discussed in the following sections (see *4.4*), that higher Deloxan® dosages shift the OME_n distribution towards longer-chain products. However, OME_n with a chain length of $n > 6$ are solids at ambient temperature (*64*), which complicate the sampling procedure (*3*). Therefore, the investigations of the moisture content in Deloxan® and its effect on the OME product distribution were conducted with a catalyst dosage of 1.0 wt% (**Figure 47**).

The results indicate that a low moisture content of the catalyst (4 wt%) increases the OME_n yield, whilst higher moisture contents (8 wt% and 14 wt%) shift the product distribution towards shorter-chained OME products as the presence of water hydrolyzes longer chain OME products (*1*). At a water content of 4 wt%, the OME_1 (DMM) and OME_2 products are produced in similar amounts, namely 12 wt% and 11 wt%, respectively. With increasing water content of the catalyst, the OME_1 content is significantly increasing up to 15 wt%. The OME_2 amount remains almost the same (12 wt%) at higher water contents (8 wt% and 14 wt%), whilst the mass fraction of longer-chain OME ($n > 2$) products are significantly decreasing thus shifting the product distribution towards short-chain OME products. The

observed tendency of the OME products at different moisture contents of Deloxan® during OME synthesis is in accordance to the results reported by Zheng et. al (*74*). In this context, to avoid introducing or generating water during OME synthesis the moisture content of the solid acid catalyst Deloxan® was determined prior every reaction. Therefore, to obtain comparable data all experiments were performed strictly at a moisture content of 3 – 4%, as it was determined that the moisture content of the catalyst influences the OME product formation (*3*).

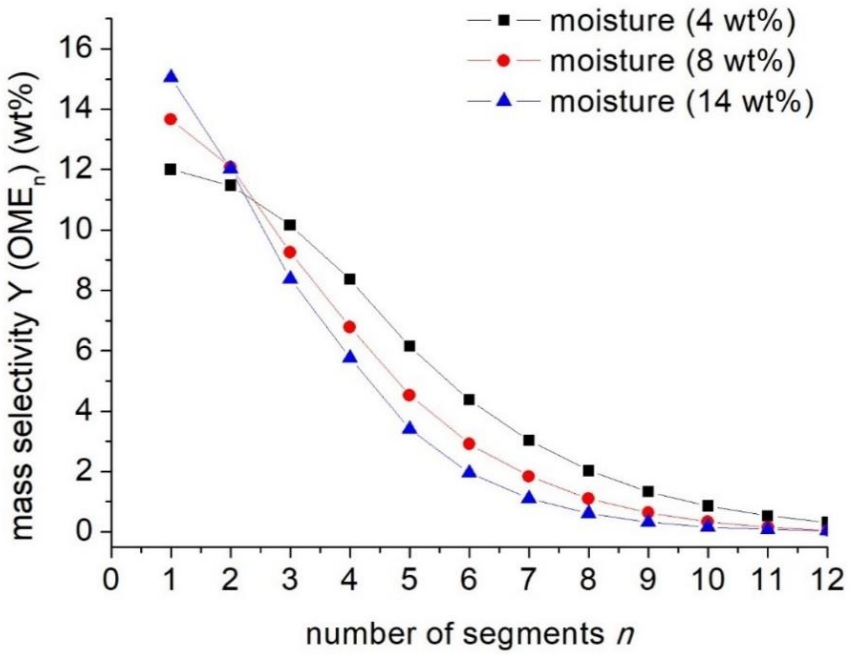

Figure 47 Mass distribution of OME_n product formation as a function of moisture content for the Deloxan® catalyzed reaction (reaction conditions: 80 °C, n_{DMM}/n_{TRI} = 1, 60 min, cat. dosage 1.0 wt%); lines = interpolation

4.4.4.3. Deloxan® catalyst dosage screening for OME synthesis

The -SO_3H comprising solid acid catalyst Deloxan® at a catalyst load of 1.7 wt% was found to produce OME product fractions comparable to results obtained from MSA catalyzed reactions (3.5 wt% and 3.2 wt%) (**Figure 48**). Furthermore, with increasing catalyst loads a higher production of OMEs was observed exhibiting at 1.7 wt% the highest OME yield for the given reaction conditions. At higher catalyst loadings the OME product formation is decreasing as depicted in **Figure 48**. The $OME_{n>8}$ mass fraction was found to be in the mass range as determined for reactions catalyzed by MSA. Moreover, Deloxan® as a monoprotic solid acid exhibits even at low catalytic loadings (1.0 wt%) already comparable OME_{2-8} yields (45.6 wt%) to sulfuric acid (58.9 wt%).

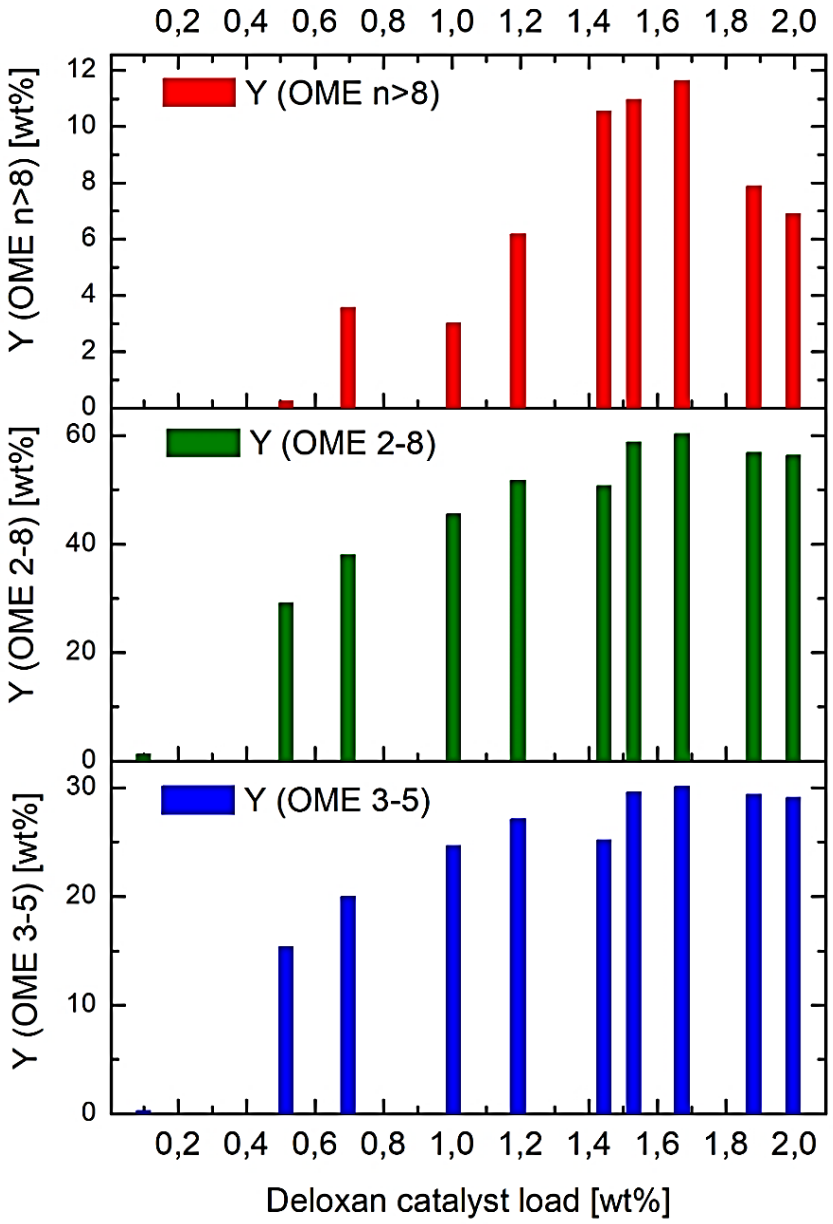

Figure 48 Mass selective yields for the OME_{2-8}, $OME_{n>8}$ and OME_{3-5} products as a function of different Deloxan® loadings (reaction conditions: 80°C, n_{DMM}/n_{TRI} = 1, t = 60 min)

Therefore, the developed mild OME synthesis catalyzed by Deloxan® under ambient pressure led to even higher OME mass fractions compared to other heterogeneous catalysts reported in literature with some examples listed in **Table 29**. Furthermore, Deloxan® exhibits a significantly lower exchange capacity compared to other acidic ionic resins (**Table 29**). This indicates good catalytic performance at the given reaction conditions and moreover a comparable activity to sulfuric acid.

Moreover, the OME_{3-5} product fraction at a Deloxan® load of 1.7 wt% is with 30 wt% comparable to other acids. In this context, sulfonic acid catalyzed reactions lead at the given reaction conditions to an increasing OME_{2-8} and $OME_{n>8}$ yield accompanied with a decreased pFA formation. Further kinetic investigations were conducted with Deloxan® dosage of 1.7 wt%, which will be discussed in the next sections (*3*).

Table 29 Heterogeneous and homogeneous catalysts for OME synthesis reported in scientific literature

Catalyst (load wt%)	Educt (n_{DMM}:n_{TRI})	Y OME_{n-m} [wt%]	[meq H^+/g][d]
A36 (4.2) (*11*)	DMM/TRI (2:1)	31.5 (3-6)[a]	5.4
A15 (7.5) (*114*)	DMM/TRI (3:1)	51.2 (3-8)[b]	4.7
CT175 (7.5) (*114*)	DMM/TRI (3:1)	64.2 (3-8)[b]	4.9
p-toluenesulfonic acid (7.5) (*114*)	DMM/TRI (3:1)	30.2 (3-8)[c]	---
conc. sulfuric acid (7.5) (*114*)	DMM/TRI (3:1)	38.0 (3-8)[c]	---

[a] Heterogeneous catalyst, ion-exchange resin (Amberlyst 36); reaction conditions: 50 °C, 0.33 h, <5 bar
[b] Heterogeneous catalysts, ion-exchange resins (Amberlyst 15, CT175); reaction conditions: 90 °C, 0.5 h, 15 bar
[c] Homogeneous catalysts; reaction conditions: 90 °C, 0.5 h, 15 bar
[d] Exchange capacities

4.4.4.4. Recycling of the catalyst for OME synthesis

Utilization of heterogeneous catalysts exhibits the advantage of reusability, which has been reported for various solid acid catalysts utilized for OME production such as molecular sieves (*123*), ionic resins (*114*) and others (*115*) (see *2.6*). The catalytic stability of Deloxan® was examined by regeneration of the catalyst after each reaction. The reusability test was performed with a catalyst amount of 1.0 wt%, since higher Deloxan® loadings lead to longer chain OME production, which would hamper the filtration step. To obtain reliable data, the catalyst in the reaction mixture was firstly filtered from the reaction mixture by a glass frit (Por. 3), washed and lastly desiccated *in vacuo*. For comparable data, the moisture content of the solid catalyst was determined prior reusing for the next catalytic step and was kept again at 3 – 4 wt%, since the catalytic activity is strongly dependent on the wetness of Deloxan® as described previously.

The chain length *n* of the produced OME_n products was found to be in the range of n = 2 – 8. Upon reusing of the solid ionic resin, the OME_{2-8} mass fraction decreases on every recycling step, whilst the amounts of DMM and TRI are increasing as shown in **Figure 49**. Hence, the solid acid catalyst Deloxan® was found to lead to a significant decrease in the OME production upon reusability. In comparison, other acidic exchange resins and molecular sieves were reported to exhibit a high catalytic reactivity even after reusing as the structure of the recovered catalyst was found to remain stable (*114, 123*).

Therefore, further investigations might be relevant to develop a more sophisticated catalyst recovery technique or catalyst activation procedure aiming towards acceptable catalyst recoveries. Exemplarily, some catalyst can be recovered by rinsing with hydrochloric acid and subsequently by thoroughly washing with deionized water (*101, 114*).

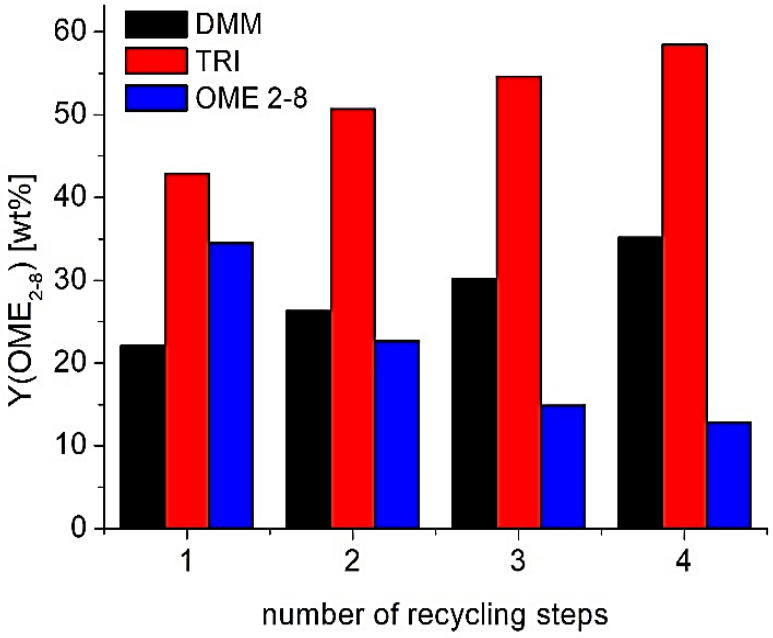

Figure 49 Mass fraction distribution within four repeated catalytic reaction runs after filtration and desiccation of Deloxan® for the synthesis of OME_{2-8} from trioxane and DMM (reaction conditions: 80 °C, 60 min, n_{DMM}/n_{TRI} = 1, cat. dosage 1.0 wt%; moisture content 3-4 wt%)

4.4.5. Variation of reaction time

The intention of this study was to identify the time-dependent reaction profile for reactions catalyzed by the catalysts sulfuric acid, MSA and Deloxan®. The corresponding reaction parameters are provided in **Table 30**, with the reaction time being the investigated variable. In the scope of the experiments, the liquid reaction mixture was investigated by GC-FID and samples were drawn in time intervals of 10 – 15 min (*3*).

Table 30 Reaction parameters for the investigations on the reaction time for OME synthesis (reaction conditions: 80°C, n_{DMM}/n_{TRI} = 1, moisture content in Deloxan® = 3 – 4 %)

	H_2SO_4	MSA	Deloxan®
Catalyst load [wt%]	1.0	3.2	1.7
Reaction time [min]	0 - 90	0 - 100	0 - 100

In **Figure 50** the corresponding mass selective fractions, *Y* (OME_{2-8}), are displayed as a function of reaction time (*left*). The reaction progress was found to match similar plots provided in literature for OME synthesis (*20*, *64*). For the investigated catalysts the OME_{2-8} product fraction is steadily increasing with prolonged reaction time until the limiting equilibrium of the reaction is reached, which makes an extension of reaction time rather inefficient for higher product yields. In other words, for the H_2SO_4 catalyzed reaction the maximum OME_{2-8} yield is observed after a reaction time of t = 90 min. It was experimentally found, that longer reaction times lead to an increased pFA formation at the given reaction parameters hampering the analytic procedure. This is why the reaction time was kept shorter with t = 90

min, compared to the reactions catalyzed by MSA and Deloxan®, with *t* = 100 min. Both, H_2SO_4 and Deloxan® exhibit a short induction period of approximately 5 – 10 min according to the interpolation lines in **Figure 50**. On the contrary, the MSA catalyzed reaction lacks an induction period. As previously noted, extension of reaction times for MSA and Deloxan® did not lead to pFA production but in a shift of the product distribution towards the production of longer molecules. This result is supported by the increasing $OME_{n>8}$ formation at longer reaction times (**Figure 50**, *right*).

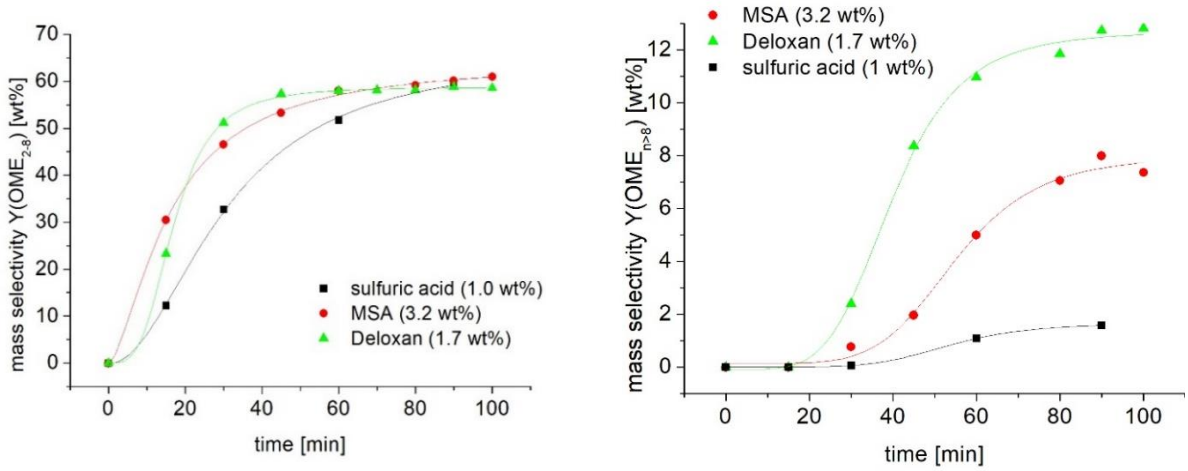

Figure 50 Mass selectivity *Y* of OME_{2-8} (*left*) and $OME_{n>8}$ (*right*) as a function of time for the catalysts sulfuric acid (load 1 wt%), MSA (load 3.2 wt%) and Deloxan® (1.7 wt%, moisture content 3-4 wt%) (reaction conditions: 80 °C, n_{DMM}/n_{TRI} = 1)

As indicated by the experimental results shown in **Figure 50**, terminating the OME synthesis after *t* = *60* min does not yield the highest observable mass fractions of OME_n. Moreover, to investigate the influence of a prolonged reaction time on the product distribution as a function of catalyst load, a catalyst screening was performed for the catalysts MSA and Deloxan®. The results are provided in **Figure 51** and **Figure 52**, respectively. All reactions were quenched after *t* = 70 min without altering other reaction parameters. It was found that prolonged reaction times shift the highest OME_n product fraction (n > 2) towards lower catalytic loadings, compared to the reactions performed at 60 min. In other words, the OME_{2-12} yields obtained after 70 min reaction time at a catalyst load of 3.2 wt% MSA and 1.5 wt% Deloxan® were found to be similar to the OME_{2-12} yields obtained for reactions performed with 3.5 wt% MSA and 1.7 wt% Deloxan® after 60 min reaction time. However, for reactions catalyzed by Deloxan® elongation in reaction time induces an increase of the $OME_{n>8}$ mass fraction, which is not advantageous in the context of OME employed as diesel additives (*11*, *101*).

Moreover, as it was determined that the OME_{2-8} and OME_{3-5} yields were not increased significantly by prolonging the reaction duration at a given temperature, the reaction time for further kinetic investigations on H_2SO_4, MSA and Deloxan® was chosen with *t* = 60 min.

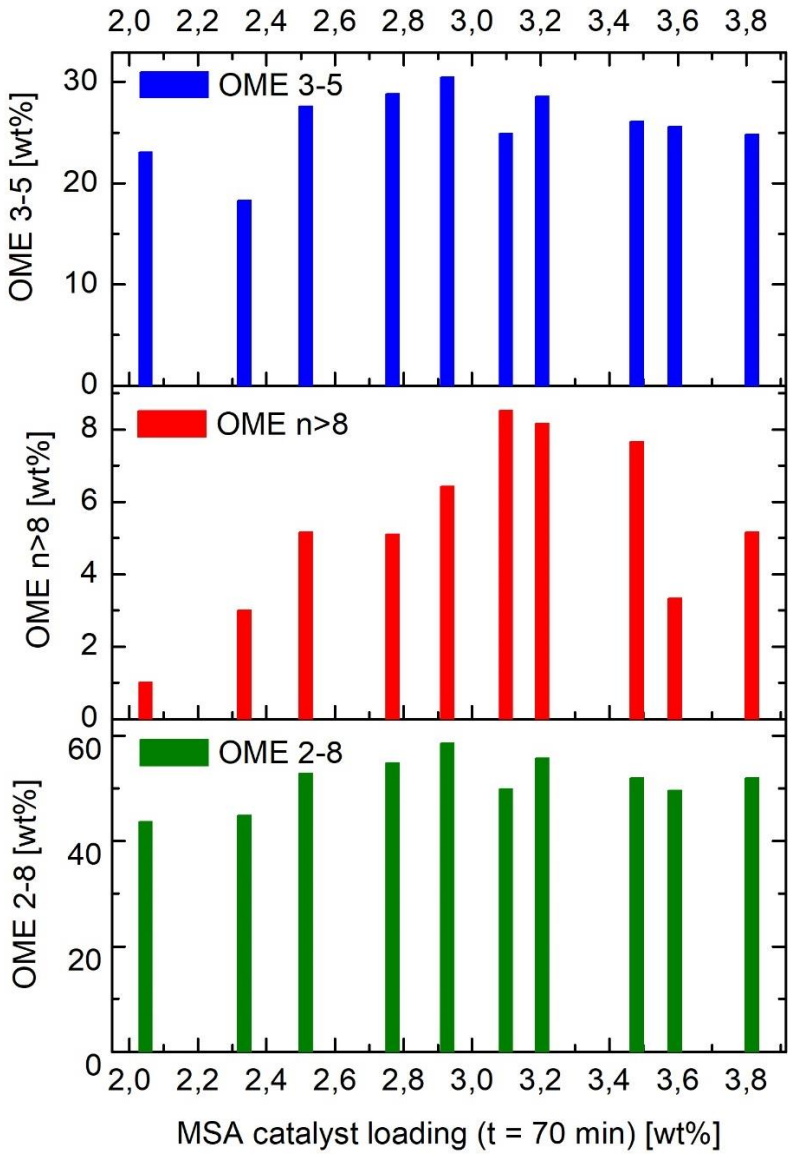

Figure 51 Mass selective yields for the OME_{2-8}, $OME_{n>8}$ and OME_{3-5} products as a function of different MSA loadings for the reaction time t = 70 min (reaction conditions: 80°C, n_{DMM}/n_{TRI} = 1)

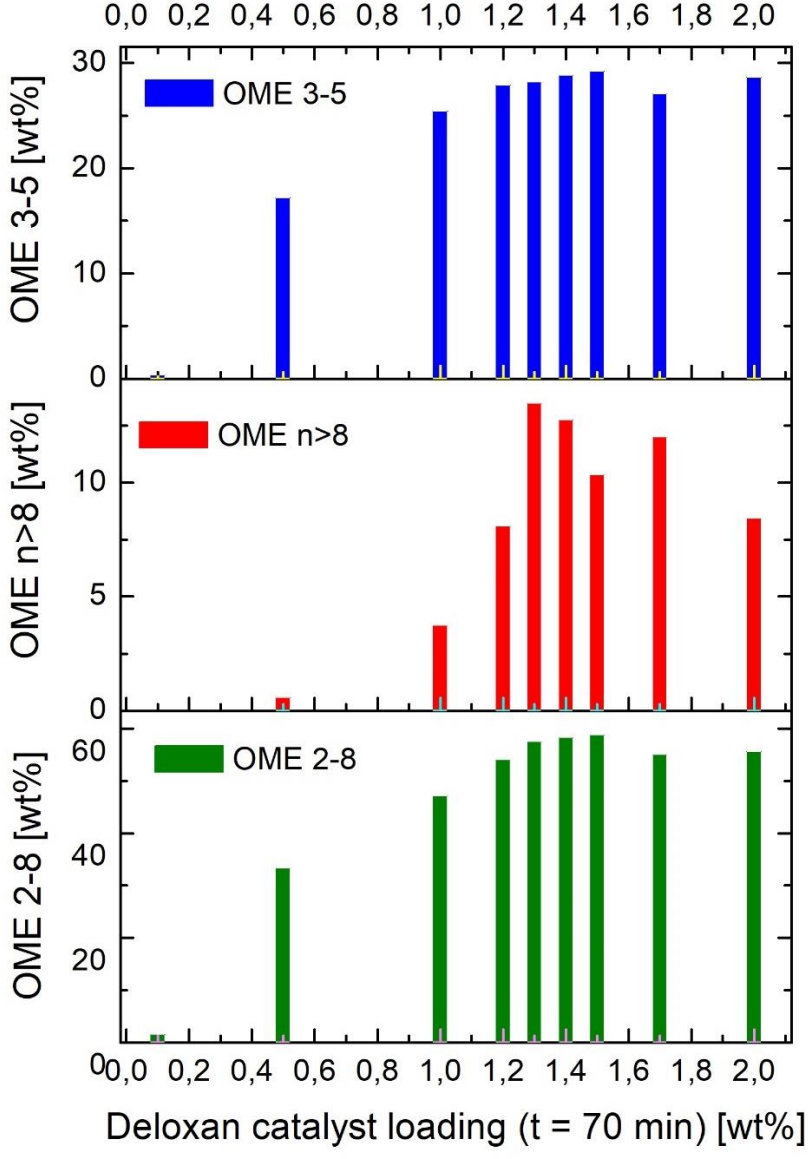

Figure 52 Mass selective yields for the OME_{2-8}, $OME_{n>8}$ and OME_{3-5} products as a function of different Deloxan® loadings for the reaction time t = 70 min (reaction conditions: 80°C, n_{DMM}/n_{TRI} = 1)

4.4.6. Variation of reaction temperature

Further studies focusing on the influence of the reaction temperature on the OME product formation were conducted predominantly to gather data on the molecular size distribution for reactions catalyzed by sulfuric acid, MSA and Deloxan®. Therefore, as depicted in **Figure 53 A-C**, the influence of temperature on the OME production was performed with the fixed catalyst dosages of 1.0 wt% H_2SO_4, 3.2 wt% MSA and 1.7 wt% Deloxan®, which correspond to the highest OME_n product formation as described earlier (see *4.4.2*, *4.4.3* and *4.4.4.3*). Moreover, the molar ratio was kept at 1 and the reactions were carried out within t = 60 min reaction time (*3*).

For the H_2SO_4 and Deloxan® catalyzed OME synthesis an increasing reaction temperature was accompanied by an enhanced OME_{2-8} product formation (**Figure 53 (D)**). Thus, both the H_2SO_4 and Deloxan® catalyzed reactions exhibit a maximum of OME_{2-8} production at 80 °C, whilst MSA was found to reach its OME production peak at 85 °C.

Furthermore, at higher temperatures the mass distribution shifted towards longer OME chain lengths for both, MSA and Deloxan® catalyzed reactions. Accordingly, at low reaction temperatures only short-chain OME products can be detected (**Figure 53 (B, C)**). Compared to the reaction performed at 80°C, H_2SO_4 was found to produce less OME at lower or higher temperatures accompanied by small changes in the mass product distributions (**Figure 53 (A)**). On the contrary, MSA and Deloxan® were found to lead to a significant drop of the OME_{2-8} mass yields at temperatures deviating from 80°C, with the corresponding product-profiles shown in **Figure 53 (D)**.

Moreover, all catalysts were found to exhibit a decrease of the OME product yield once the reaction temperature reaches 90°C. This is due to the fact that the production of OME as an exothermic reaction leads to an increase of temperature, which as a consequence reverses the chemical equilibrium towards the educts (*153*). However, MSA was found to reach its OME production peak at 85 °C. This result was accounted to the utilized catalyst load (3.2 wt%), which is slightly lower compared to the optimized MSA catalyst load but was chosen on purpose as previously described. Therefore, an increasing reaction temperature for the MSA catalysed reaction at the given reaction conditions still allowed an increase of the OME production, which was to decrease at 90°C as already discussed. Reduction of the reaction temperature to 60°C lead for all catalysts to an insufficient OME productions and consequently to a shift of the product distribution towards shorter OME chain length. Hence, the optimum operating temperature at 80°C was proven to be suitable for the herein investigated catalysts H_2SO_4, MSA and Deloxan® (*3*).

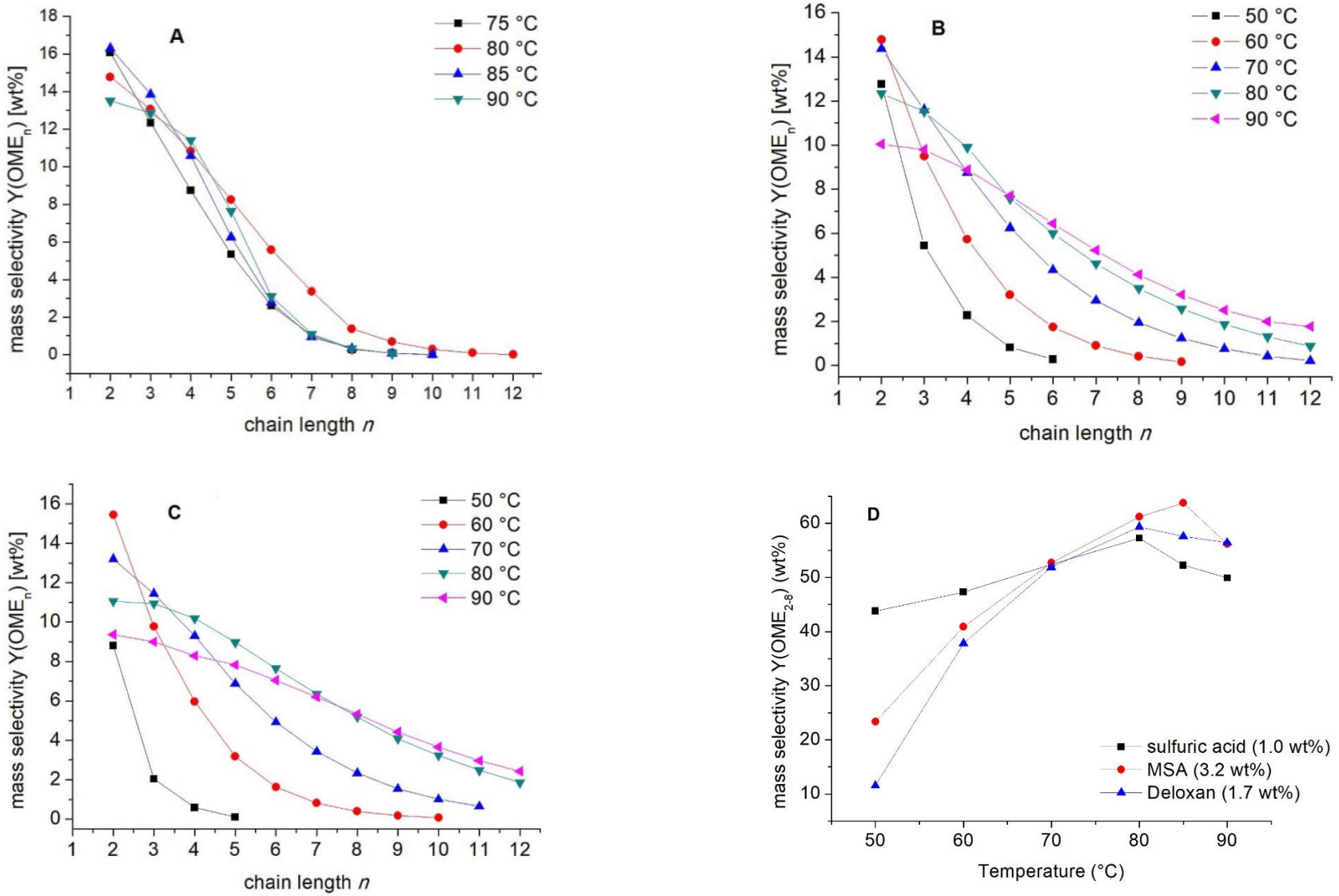

Figure 53 **A**: OME_{2-8} mass distribution for the 1.0 wt% H_2SO_4 catalyzed OME synthesis; **B**: OME_{2-8} mass distribution for the 3.2 wt% MSA catalyzed reaction and **C**: OME_{2-8} mass distribution for the 1.7 wt% Deloxan® catalyzed OME synthesis as a function of OME chain length *n*; **D**: Mass selective OME_{2-8} yield as a function of reaction temperature for the catalytic systems (reaction conditions: n_{DMM}/n_{TRI} = 1, t = 60 min, moisture content of Deloxan® = 3 – 4%)

4.4.7. Schulz-Flory distribution of OME_n products

The molecular size distribution of OME compounds catalyzed by sulfuric acid was reported to follow the Schulz-Flory distribution under equilibrium conditions as described in section *2.5.2* (*3, 74, 103, 124*). Herein, also the OME synthesis for the educts DMM and TRI catalyzed by MSA (3.2 wt%) or Deloxan® (1.7 wt%) were determined to follow the Schulz-Flory law (**Figure 58**) as indicated by the linear slopes characterized by the probability factor, α (*18*).

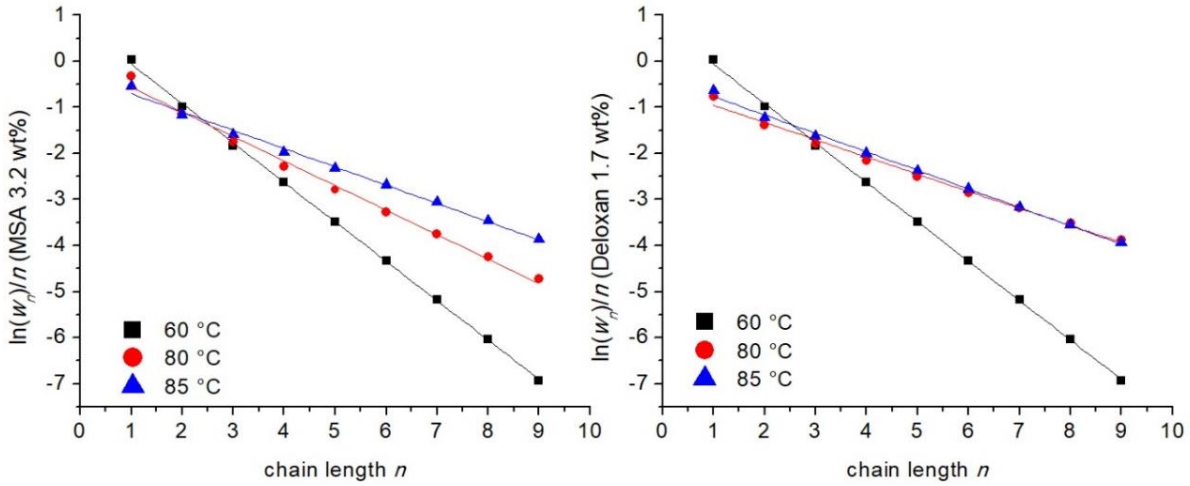

Figure 54 Schulz-Flory distribution of OME_n synthesized by the reaction of dimethoxymethane and trioxane catalyzed by (*left*) MSA (cat. load 3.2 wt%) and (*right*) Deloxan® (cat. load 1.7 wt%, moisture content 3-4 wt%) at different temperatures (*3*)

Hence, low values for α indicate that the OME product distribution is containing mainly low molecular weight molecules and *vice versa.* The corresponding values for α are provided in **Table 31**, which were obtained for the temperatures 60°C, 80°C and 85°C. Thus, the probability for the production of long-chain OME products is reduced at a lower reaction temperature and increases significantly with higher temperatures. Both, MSA and Deloxan® are prone to catalyze the production of long-chain OME at higher reaction temperatures. Hence, a reaction temperature of 80°C for the OME synthesis catalyzed by Deloxan® and MSA at ambient conditions might seem unfavorable for an efficient OME_{3-5} production for their application as diesel additives, as this product fraction will be more favored at lower reaction temperatures (60°C). For sulfuric acid catalyzed OME synthesis the reversed reaction behavior was found. However, an increase of the reaction temperature is accompanied by the formation of pFA by decreasing the overall product yield, whilst both MSA and Deloxan® were qualitatively found to exhibit low or none paraformaldehyde formation (*3*).

In literature the probability factors were reported in the range of 0.4 for reactions performed in autoclaves catalyzed by sulfuric acid. Although the herein derived values for the propagation probability are higher, DMM will always be present in the reaction mixture independently on the reactants and reaction conditions. Moreover, both MSA and Deloxan® will produce at higher reaction temperatures preferably longer-chain OME products, which are undesired for their application in diesel blends or fuel.

Hence, the separation of the desired OME_{3-5} product fraction will always be an required step for a large-scale OME production (*103*).

Table 31 Coefficient values of the propagation probability, α, from the reaction between DMM and trioxane (reaction conditions: 60 min, nDMM/nTRI = 1; moisture content of Deloxan® 3-4 wt%) (*3*)

Temperature	Catalyst and loading (wt%)[a]		
	H_2SO_4 (1.0)	MSA (3.2)	Deloxan® (1.7)
	Propagation probability (α)		
60 °C	0.66	0.45	0.44
80 °C	0.52	0.59	0.71
85 °C	0.43	0.68	0.69

[a] Catalyst loading refers to the values chosen for further investigations on the catalytic activity

4.4.8. Stochiometric ratio of educts

Variation of the educt stoichiometry on the OME synthesis was reported in literature for the acidic ionic resins catalysts CT175 (*114*), A36 (*11*) or NKC-9 (*101*). Hence, investigation regarding the influence of the educt ratio on the OME product distribution were mainly pursued to optimize the OME_{3-5} product yield. Therefore, in the next step, the influence of the stoichiometric molar educt ratio on the OME formation was investigated at ambient pressure, a reaction time of 60 min and a reaction temperature of 80°C (*3*). For this, MSA and Deloxan® were applied with catalyst amounts of 3.2 wt% and 1.7 wt%, respectively. The experimentally determined values for the OME product distributions according to the educt ratios n_{DMM}/n_{TRI} = 0.5, 1 and 2 are provided in **Table 32** (*3*).

Table 32 Mass selectivity Y of OME_{2-8} as a function of the educt ratios for the catalysts MSA (load 3.2 wt%) and Deloxan® (1.7 wt%; moisture content 3-4 wt%) (reaction conditions: 80 °C, 60 min)

cat. (load wt%)	Mass selective product distribution [wt%]									
	OME chain length *n*									
	n_{DMM}/n_{TRI}	2	3	4	5	6	7	8	2-8	>8
MSA (3.2)	0.50	8.73	8.13	6.88	6.07	5.08	4.18	3.39	42.47	8.06
	1.00	12.34	11.52	9.90	7.58	6.00	4.64	3.50	55.47	6.64
	2.00	9.80	1.94	0.41	0.00	0.00	0.00	0.00	12.15	0.00
Deloxan® (1.7)	0.50	6.21	6.54	6.17	6.13	5.56	5.00	4.42	40.03	11.94
	1.00	11.05	10.93	10.18	8.97	7.64	6.34	5.19	60.30	11.63
	2.00	9.49	1.82	0.45	0.00	0.00	0.00	0.00	11.77	0.00

Therefore, both MSA and Deloxan® produce higher $OME_{n>8}$ at a lower educt ratio, n_{DMM}/n_{TRI} = 0.5, which was observed in literature already for other heterogeneous catalysts (*64*). This property is due to the increased formaldehyde amount brought in by trioxane resulting in a creamy colorless paste, which might as well be due to an increased pFA formation (*150*). For the Deloxan® catalyzed reaction the product distribution was found to drop for short-chain OME compounds with n < 10, which is undesired especially in regard of high OME_{3-5} yields. At higher molar ratios (n_{DMM}/n_{TRI} = 2) no long-chain $OME_{n>4}$ products were formed for both catalysts as depicted in **Figure 55**, yielding a colorless liquid product-mixture**.** Thus, the product selectivity of OME_{2-8} was significantly lowered for molar ratios deviating from 1. Therefore, it is conducive to adjust the molar ratio to n_{DMM}/n_{TRI} = 1 as the OME_{2-8} and moreover the OME_{3-5} mass selective yield are maximized (*3*).

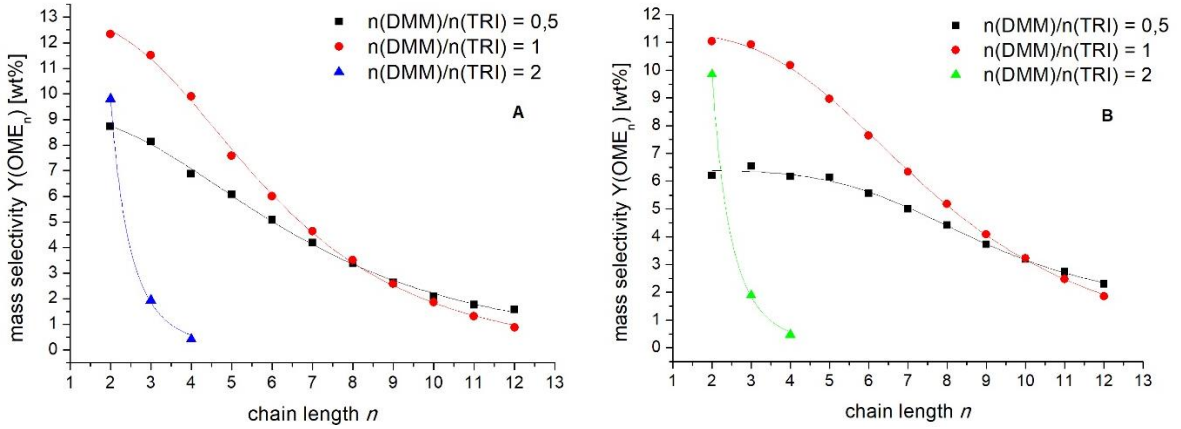

Figure 55 Mass selectivity *Y* of OME_n for different educt variation ratios as a function of the chain length *n* for the catalysts MSA (load 3.2 wt%) (**A**) and Deloxan® (1.7 wt%, moisture content 3-4 wt%) (**B**) (reaction conditions: 80 °C, t = 60 min) (*3*).

4.4.9. Reactions under pressurized conditions

In literature, many studies on the OME synthesis from volatile compounds such as DMM or MeOH struggle with low reactivity of DMM under atmospheric pressure due to its low boiling point (42 °C) (*3, 114*). Therefore, conducting the OME synthesis in autoclaves and thus increasing the gasification temperature of DMM by passing an inert gas into the reaction system leads mostly to an enhanced reactivity and consequently higher OME product formation (*3*). The experiments conducted for the OME synthesis from DMM and TRI catalyzed by H_2SO_4 (1.0 wt%), MSA (1.0 and 3.2 wt%) or Deloxan® (1.0 or 1.7 wt%) were carried out to determine the influence of the reaction pressure on the OME synthesis performed at 80°C and 60 min reaction time. Reaction termination was performed upon quenching of the autoclave in an ice bath to ambient temperature.

In **Figure 56** and **Figure 57** the neutralized liquid product fractions are depicted for the reactions catalyzed by 1.0 wt% H_2SO_4 and 3.2 wt% MSA, respectively, as well as for the Deloxan® (1.7 wt%) catalyzed reaction in **Figure 58** (*3*).

Figure 56 Reaction performed under N_2 pressure; reaction conditions: n_{DMM}/n_{TRI} = 1, 1.0 wt% H_2SO_4, t = 60 min; 80°C, 9.0 bar N_2

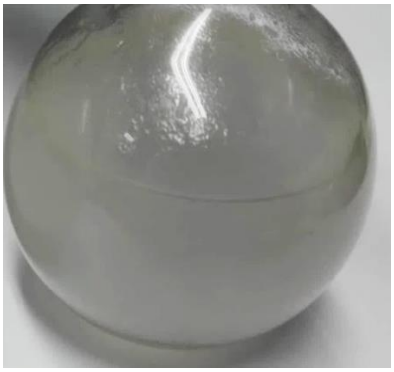

Figure 57 Reaction performed under N_2 pressure; reaction conditions: n_{DMM}/n_{TRI} = 1, 3.2 wt% MSA, t = 60 min; 80°C, 9.0 bar N_2

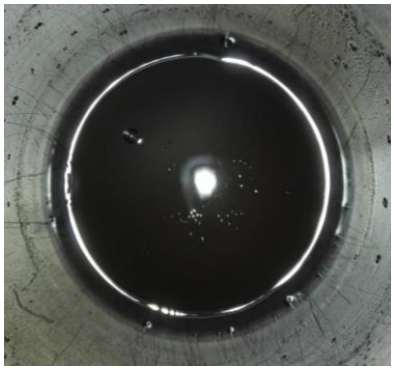

Figure 58 Reaction performed under N_2 pressure; reaction conditions: n_{DMM}/n_{TRI} = 1, 1.7 wt% Deloxan®, t = 60 min; 80°C, 9.0 bar N_2

In **Table 33** the obtained OME_n mass fractions, with n = 2 – 12, are provided for both, the pressurized and non-pressurized reactions. Pressurizing of the reaction mixtures catalyzed by H_2SO_4 or MSA lead to a decrease in the OME_{2-12} mass selective yields. On the contrary, reactions carried out by Deloxan® produced higher OME_{2-12} yields. This experimental result for the heterogeneously catalyzed OME synthesis supports the idea to conduct experiments with low-boiling point compounds in autoclaves (*114*). Moreover, to enable a more accurate comparability of the experimental findings, the relative fractions of the corresponding OME_{2-8}, OME_{3-5} and $OME_{n>8}$ to the overall OME_{2-12} mass selective yield were determined as given in **Table 33**.

Table 33 Mass ratios as a function of reaction pressure catalyzed by sulfuric acid (load 1 wt%), Deloxan® (1.0 and 1.7 wt%, moisture content 3-4 wt%) and MSA (load 1.0 and 3.2 wt%) (reaction conditions: 80 °C, 60 min, n_{DMM}/n_{TRI} = 1)

cat. (load wt%)	Pressure [bar]	$\frac{OME_{2-8}}{OME^{b}}$ [%]	$\frac{OME_{3-5}}{OME^{b}}$ [%]	$\frac{OME_{n>8}}{OME^{b}}$ [%]	OME_{3-5} [wt%]	OME^{b} [wt%]
H_2SO_4 (1.0)	ambient[a]	98.1	55.1	1.90	33.05	60.01
	9	94.6	50.3	5.39	27.95	55.61
MSA (1.0)	ambient[a]	c	28.9	0.00	3.65	12.66
	9	c	17.5	0.00	1.02	5.85
MSA (3.2)	ambient[a]	89.3	46.7	10.7	29.00	62.11
	9	96.2	51.1	3.79	25.81	50.48
Deloxan® (1.0)	ambient[a]	93.8	50.8	6.22	24.68	48.60
	9	97.7	52.6	2.30	25.98	49.39
Deloxan® (1.7)	ambient[a]	83.8	41.8	16.2	30.07	71.94
	9	88.1	45.4	11.8	34.09	75.10

[a] Refers to the atmospheric pressure present during OME synthesis performed in glass vessels. Reactions performed und N_2 pressure were conducted in pressure vessels.
[b] OME refers to OME with n = 2-12
[c] c denotes that no value for this ratio is provided, as only OME_{2-5} were produced which would be not accurate since the ratio refers to OME_{2-8}

The OME product distributions for the corresponding catalysts is provided in **Figure 59**. Pressurizing of reaction mixtures catalyzed by H_2SO_4 (1.0 wt%) lead to a slight increase of the production of longer chain OME products, while the MSA catalyzed reaction showed a reversed reaction behavior exhibiting less $OME_{n>8}$ formation for pressurized reactions. However, lowering of the catalyst loading to 1.0 wt% for both catalysts, MSA and Deloxan®, results in lower OME_{2-12} mass selectivity. However, according to the relative ratio OME_{3-5}/OME_n the production of shorter OME products, namely OME_{3-5}, is favored at lower Deloxan® loadings and thus, the solidification of the reaction mixture due to the increased amount of $OME_{n>8}$ products was prevented at lower Deloxan® loadings.

To sum up, upon pressurizing of the reaction mixture for reactions catalyzed by Deloxan® and MSA the OME_{3-5} fraction was found to increase, which is a desired product fraction for fuel additives and blends (*11*). It was found that for reactions catalyzed with 3.2 wt% MSA an increase of 4.4% in OME_{3-5} can be achieved and for catalyst loadings of 1.0 and 1.7 wt% of Deloxan® the product fraction is improved by 2.6% and 3.6%, respectively. Nevertheless, compared to some selected examples (*11*, *114*), the developed OME synthesis under ambient pressure catalyzed by Deloxan® and MSA led to even higher OME mass fractions. Moreover, Deloxan® exhibits a significantly lower exchange capacity clearly indicating good catalytic performance at the given reaction conditions (*3*).

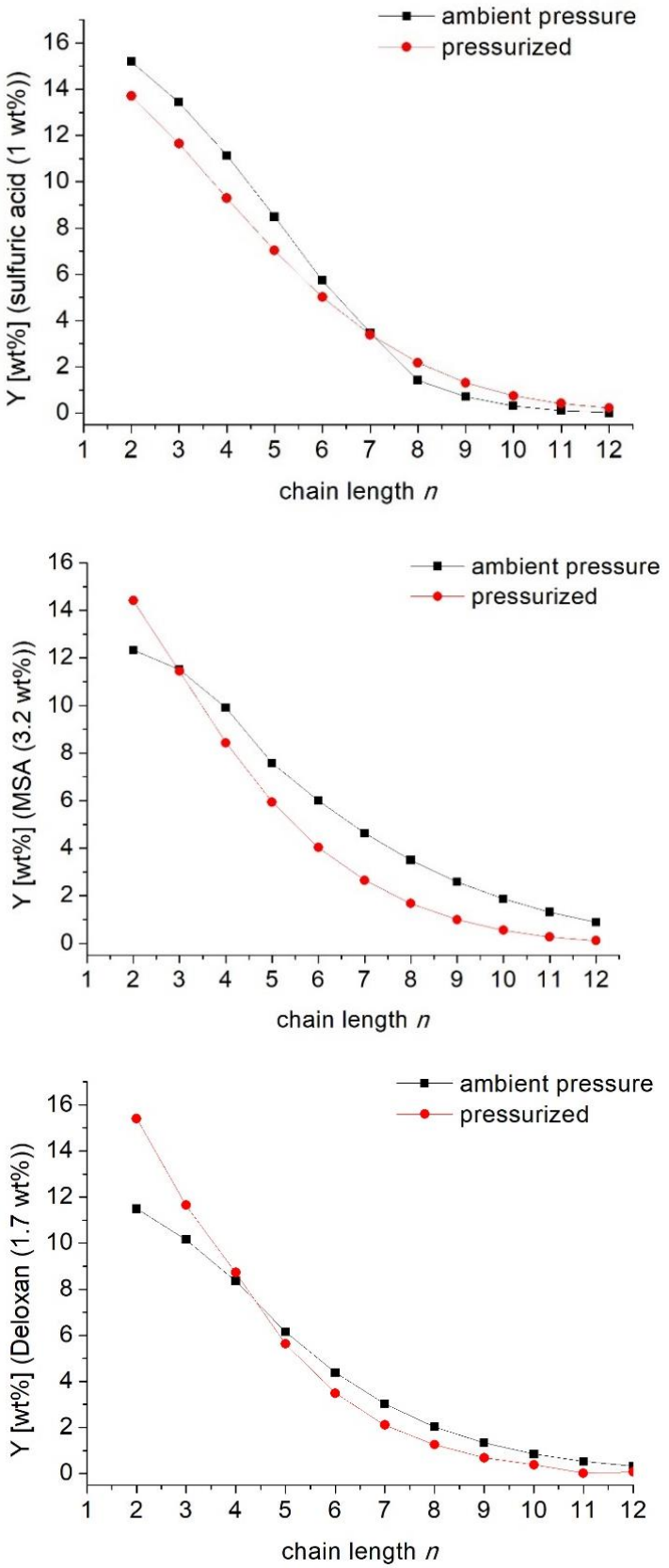

Figure 59 Mass distribution of OME product formation as a function of reaction pressure for the catalysts H_2SO_4 (load 1.0 wt%), Deloxan® (1.7 wt%) and MSA (load 3.2 wt%) (reaction conditions: 80 °C, n_{DMM}/n_{TRI} = 1, 60 min, 9 bar for pressurized reactions)

4.5. Alternative FA and methyl-cap sources

4.5.1. Dimethoxymethane and para-formaldehyde as educts

Gresham and Brooks (*125*) patented an OME preparation procedure catalyzed by 0.1 wt% H_2SO_4 from DMM and pFA at the stoichiometric ratio of n_{DMM}/n_{pFA} = 4 conducted in 60 min reaction time under pressurized conditions reporting good selectivity for short-chain OME (**Table 18**). It is known, that pFA can be activated either chemically by acids or bases, or thermally (*20*). Therefore, pFA as an alternative FA source to TRI was investigated at these reaction conditions to evaluate the OME product distribution for the catalysts sulfuric acid, MSA and Deloxan®. Reactions were performed in autoclaves at 80°C and a reaction time of 60 min by setting the molar educt ratio with n_{pFA}/n_{DMM} = 1.

Hence, the OME synthesis catalyzed by MSA and Deloxan® were conducted at a catalyst loading of 3.2 wt% and 1.7 wt%, respectively (see **Table 18**). The educt pFA was utilized without any pre-activation or pre-mixing in other chemicals. Typically, all OME synthesis reactions performed with pFA as the FA-source resulted in a solid-like product. Moreover, the non-converted pFA is after reaction completion (t = 60 min) still present at the autoclave bottom, which complicates the sampling procedure for the quantification of the product phase. Exemplarily, in **Figure 60** the product phase upon OME synthesis catalyzed by Deloxan® is depicted displaying a creamy highly viscous liquid. For a representative measurement, the reaction was allowed to cool to room temperature. The non-converted pFA was allowed to settle thus enabling an easier approach to the liquid product phase for the OME quantification.

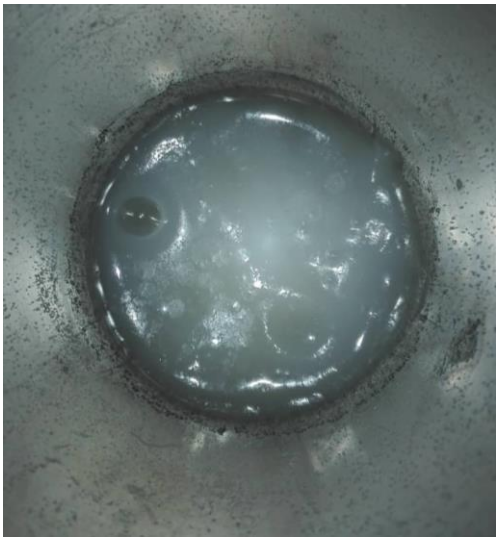

Figure 60 Reaction performed under N_2 pressure; reaction conditions: n_{DMM}/n_{pFA} = 1, 1.7 wt% Deloxan®, t = 60 min; 80°C, 9.0 bar N_2

The experimental results for the reactions at the corresponding catalyst loads are provided in **Table 34**. Compared to the product distribution obtained from the educts DMM and TRI for OME synthesis, almost no longer chain OME_n products were obtained, with n > 5. The highest OME_{2-5} mass selective

yields could be obtained from the 1.7 wt% catalyzed Deloxan® reaction with 28.9 wt%, which was moreover the only reaction yielding $OME_{n>5}$ products in 0.31 wt% product yield. Both the MSA and H_2SO_4 catalyzed OME synthesis were found to yield no $OME_{n>5}$ products. Higher H_2SO_4 catalyst loadings were found to lead to a further decrease in OME_{2-5} product formation.

Hence, the desired OME_{3-5} fraction for car manufacturers was found significantly lowered compared to patent literature for reactions performed with DMM and pFA as educts (*125*). This synthetic approach would only be economically feasible, if the educts were recycled for OME synthesis. In addition, further investigations should focus on the variation of the educt ratio for the MSA or Deloxan® catalyzed reactions and moreover on the catalytic screening of the catalyst dosages aiming to maximize the OME_{3-5} product fraction.

Table 34 Mass ratios for the OME synthesis from DMM and pFA catalyzed by H_2SO_4 (load 1, 1.5 wt%), Deloxan® (1.7 wt%, moisture content 3 – 4 wt%) and MSA (3.2 wt%) (reaction conditions: 9 bar N_2, 80 °C, 60 min, n_{DMM}/n_{TRI} = 1)

Catalyst	**Catalyst load [wt%]**	**Mass selectivity *Y* [wt%]**						
		OME chain length *n*						
		2	**3**	**4**	**5**	**2-5**	**3-5**	**n>5**
H_2SO_4	1.5	14.55	2.81	0.49	0.07	17.93	3.38	n.d.[a]
H_2SO_4	1.0	16.40	3.40	0.68	0.14	20.63	4.22	n.d.
MSA	3.2	18.74	4.32	0.89	0.16	24.11	5.36	n.d.
Deloxan®	1.7	19.96	6.28	2.04	0.70	28.98	9.02	0.31
H_2SO_4 (*125*)[b]	0.1	41.0	20.9	6.7	n.g.[c]	n.g.	n.g.	n.g.

[a] not detected
[b] reaction conditions of patent literature: n_{DMM}/n_{pFA} = 4, t = 60 min, 100°C, reaction pressure
[c] not given in (*125*)

4.6. Methanol and TRI as educts

Experiments performed with MeOH as an alternative to DMM providing the methyl-cap for OME synthesis was investigated widely in literature catalyzed by molecular sieves (*123*), sulfated solid acids (*144*), ionic liquids (*150*) and others (*115, 122*). Most Chinese authors reported high FA conversions for this reaction (*150, 122, 144*). However, Lautenschütz (*20*) associates MeOH derived OME products as less efficient, since water formed as the by-product induces the production of undesired side products (HF, Gly) and moreover the hydrolysis of OME_n products (see *2.4.2*). Hence, the high conversions of TRI, X_{TRI}, refer to both, the formation product and undesired side-products upon OME synthesis (see *4.4.1* for more details). Although OME synthesis from MeOH follows the aqueous synthesis route accompanied by the aforementioned drawbacks, this educt is economically more favorable for large-scale production as it can be derived in from biomass as a renewable feedstock (see *2.3.6*) (*62*).

Therefore, for the catalyst loadings of 3.2 wt% MSA and 1.7 wt% Deloxan® the OME synthesis was carried out with MeOH and TRI in the stoichiometric ratios n_{MeOH}/n_{TRI} = 0.5, 1, 3 and 5. The reactions were performed in autoclaves pressurized with 9 bar N_2 at a reaction temperature of 80°C. Exemplarily, the liquid product phase as well as the non-converted TRI after OME synthesis with 3.2 wt% MSA (molar educt ratio of 1) is depicted in **Figure 61**. It was conclusive that the TRI conversion for the experiments performed herein was omitted, as a large quantity was found to be non-converted upon reaction termination (t = 60 min). In this regard, Deloxan® was found to produce DMM as the only representative of OME products exhibiting one repeating unit (n = 1).

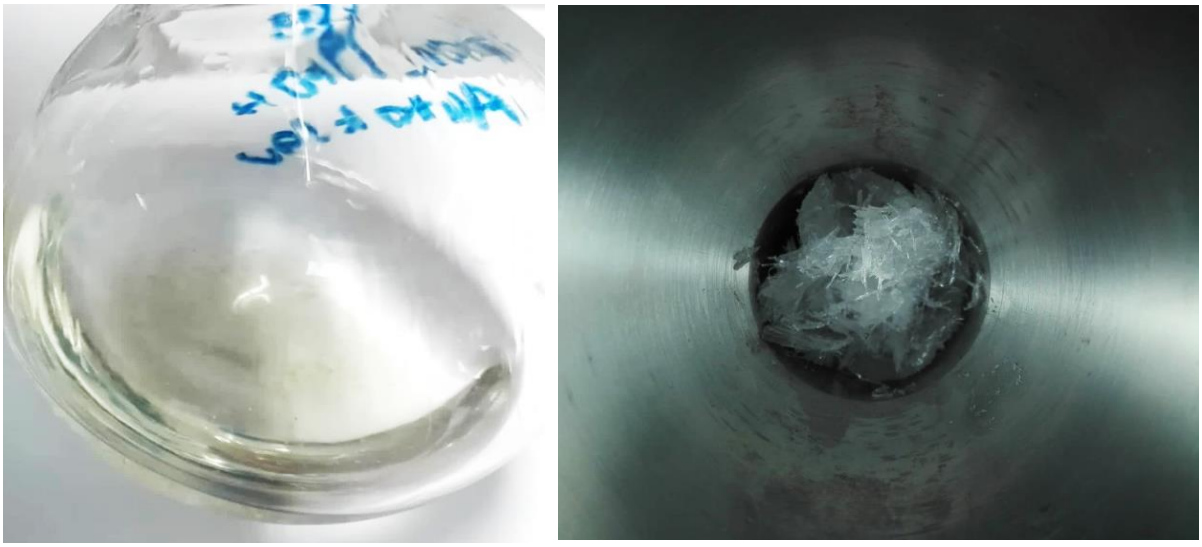

Figure 61 Reaction performed under N_2 pressure; reaction conditions: n_{DMM}/n_{TRI} = 1, 3.2 wt% MSA, t = 60 min; 80°C, 9.0 bar N_2

According to the experimental results are provided in **Table 35**, the solid acid exhibits a poor catalytic activity for the educt combination MeOH/TRI. Increasing the FA content consequently produces less water upon OME production and moreover reduces the DMM hydrolysis reactions. Similar behavior

was observed for the reactions catalyzed by MSA. A stoichiometric ratio of 0.5 was found to produce $OME_{2\text{-}12}$ products, which was scarcely observed for other catalysts in literature for the respective educts (*20*, *122*).

To sum up, the product yields for the OME synthesis from the educts methanol and TRI for any investigated stoichiometric ratio were found significantly less promising compared to the OME product yields obtained for reactions utilizing DMM and TRI. Moreover, DMM was found to be preferably produced for reactions catalyzed by MSA and Deloxan®, which could be employed as an educt itself once it was distilled from the liquid product mixture to remove all undesired side-products including hemiformals, water and such. Especially water will always be produced *via* the aqueous reaction route, as encountered for reactions employing methanol as educt, leading to low product yields containing short-chain OME products. However, this reaction route is very promising for large scale OME processes as methanol as an educt is cheaper compared to DMM and can be derived from renewable feedstocks. In this regard, further investigations should be conducted considering different catalyst loadings as a function of the molar educt ratio. Moreover, upon purification of the reaction mixture, the non-converted educts could be recycled for OME synthesis.

Table 35 Mass ratios for the OME synthesis from MeOH and TRI catalyzed by Deloxan® (1.7 wt%, moisture content 3-4 wt%) and MSA (3.2 wt%) (reaction conditions: 9 bar N_2, 80 °C, 60 min)

n_{MeOH}/n_{TRI}	MSA (3.2 wt%)		Deloxan (1.7 wt%)	
	DMM[a] [wt%]	OME (m-n) [wt%]	DMM[a] [wt%]	OME [wt%]
0.5	4.98	22.73 (2-12)	10.09	n.d.
1	32.07	2.92 (2-3)	5.09	n.d.
3	16.46	0.00	1.87	n.d.
5	9.83	0.00	0.93	n.d.

[a] DMM refers to either the non-converted educt or product formed upon OME transacetalization/product formation

4.7. Poly(oxymethylene) diethyl ethers (OEE_n)

Poly(oxymethylene) diethyl ethers (OEE) were thoroughly investigated by Lautenschütz (*20*) on their differences in reactivity compared to OME compounds. As earlier discussed (see *2.2.1*), the physico-chemical properties of the short chain OEE_n compounds with n = 2 – 4 (see **Scheme 1**) exhibit ignition points, flash points as well as high Cetane Numbers fulfilling the fuel requirements in their pure form. However, not much interest has been devoted for their application as additives in diesel fuels (*36*).

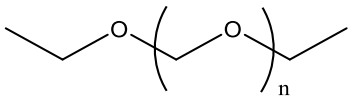

poly(oxymethylene) diethyl ether, OEE

Scheme 1 Structure of oly(oxymethylene) diethyl ether, OEE_n (*20*)

The oligomerization of OEE products was reported to be energetically hindered due to the high activation energy barrier for these reactions (*20*). Hence, OEE synthesis requires higher reaction temperatures to reach comparable reaction rates (*20*). One macroscopically observable difference between OME and OEE compounds is the different coloring of the products. Lautenschütz (*20*) associated the coloring to the presence of the catalyst A36, which could not be removed from the viscous OEE products. However, the OEE products obtained herein upon neutralization with ethanolic NaOH from a sulfuric acid catalyzed OME reaction, were found to yield a brownish coloring as shown in **Figure 63**. Hence, the difference in color can be associated to the formation of OEE compounds, as OME products are typically colorless (**Figure 62**). The obtained reaction mixture was measured by GC-MS with the chromatogram shown in **Figure 64**.

Figure 62 Acid catalyzed OME product mixture starting with DMM and TRI as educts after neutralization with aqueous NaOH

Figure 63 Acid catalyzed OEE product mixture starting with DMM and TRI as educts after neutralization with ethanolic NaOH

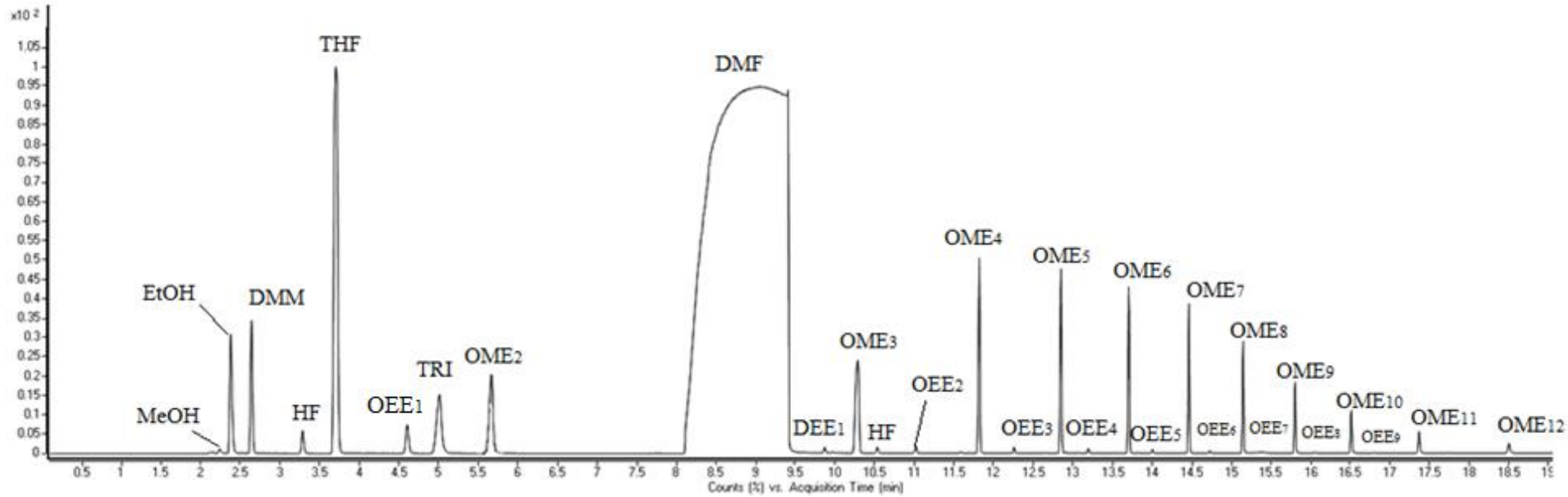

Figure 64 GC-MS chromatogram of the neutralized OME reaction with ethanolic NaOH yielding OEE_n, EMM_n, OME_n and HF_n compound (reaction conditions: 3.4 g DMM, 4.0 g TRI; 1.0 wt% sulfuric acid; 80°C; 60 min reaction time)

Hence, an OME synthesis was performed utilizing DMM (3.4 g) and TRI (4.0 g) at ambient pressure catalyzed by 1.0 wt% sulfuric acid at a reaction temperature of 80°C and 60 min reaction time. In the experimental section it was noted, that the neutralization step after completion of the OME product synthesis was typically carried out with aqueous NaOH (2.5 M) resulting in a colorless mixture (**Figure 62**). However, the ethanolic NaOH solution (2.5 M) was prepared with the intention to restrict the amount of water in the OME reaction mixture, which is increased if an aqueous NaOH solution is utilized for neutralization. For this, after reaction completion, this reaction mixture was neutralized accidentally by an excess of ethanolic NaOH at 80°C, which lead immediately to a brownish coloring of the mixture. Subsequently, the mixture was stirred further for 15 min and was then left to cool to ambient temperature yielding a brownish mixture as depicted in **Figure 63**, which corresponds to OEE products as previously introduced.

To quantify this class of oligomeric etheric compounds, a distillation procedure would have been required to yield the pure OEE products for the determination of the corresponding RRF values. However, since the OEE synthesis was not the focus of this work, no quantification by GC-FID measurements was further executed. Hence, a GC-MS measurement was performed to identify the products of the reaction mixture, and the retention times of the OEE products were assigned according to their boiling points. In **Table 36** the respective retention data are provided.

Table 36 GC-MS retention times for the OEE_n products and side products

Product[a]	Retention time [min]	**Side product**[b]	Retention time [min]
OEE_1	4.6	**MeOH**	2.1
OEE_2	11.0	**EtOH**	2.4
OEE_3	12.3	**HF_1 or OEE_1-OH**[c]	3.2
OEE_4	13.2	**DEE_1**	9.8
OEE_5	14.0	**DEE_2**	11.6
OEE_6	14.7	**DEE_3**	13.87
OEE_7	16.1	**HF_1**	n.d.[c]
OEE_8	16.8	**HF_2**	10.5
OEE_9	17.7	**HF_3**	n.d.

[a] OEE_{10-12} products could not be detected
[b] MeOH and HF retention times are in accordance to reported data in (*31*)
[c] Both structures are in principle possible, the MS chromatogram indicates a matching fragmentation pattern

The signals were identified either by the automated library search, or by analysis of the corresponding mass spectra. Hence, the OEE_n products with n = 1 – 9 were determined with the mass spectra provided in the *Appendix*. Also other products could be assigned, such as MeOH, diethoxyethane (DEE_n) and hemiformals (HF). The formation of these (side-)products will be discussed briefly in the following. Gresham et al. (*125*) and Lautenschütz (*20*) reported the acid catalyzed synthesis of OEE compounds from EtOH and monomeric FA with the reaction pathway for OEE synthesis provided in **Scheme 2**. As

EtOH was added in the reaction mixture for neutralization, it can be assumed that the OEE product formation was following this reaction pathway.

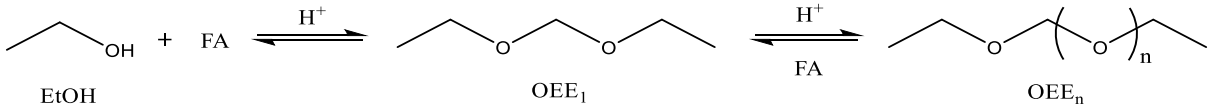

Scheme 2 Acid catalyzed OEE_1 synthesis from EtOH and monomeric FA and subsequent oligomerization to OEE_n compounds

Moreover, the presence of DMM in OEE_n mixtures containing an acidic catalyst were reported to lead to transacetalization reactions (*20*). In the case of n = 1 (OEE_1), the transacetalization product leads to the formation of ethoxymethoxymethane, EMM, which is shown in **Scheme 3** (*20*).

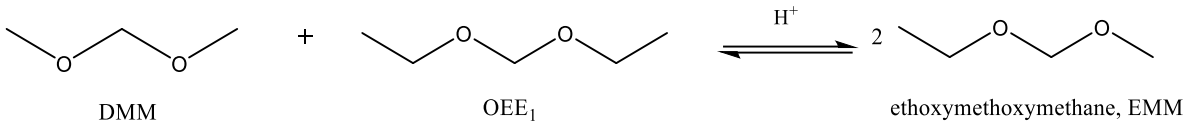

Scheme 3 Acid catalyzed transacetalization reaction of DMM and OEE_1 yielding EMM (*20*)

As proposed by Lautenschütz (*20*), it is important to consider that during the oligomerization reactions of DMM catalyzed in acidic media, in the first step an oxonium-DMM cation is formed which upon MeOH cleavage is in equilibrium with the carbenium cation, as depicted in **Scheme 4** (*20*).

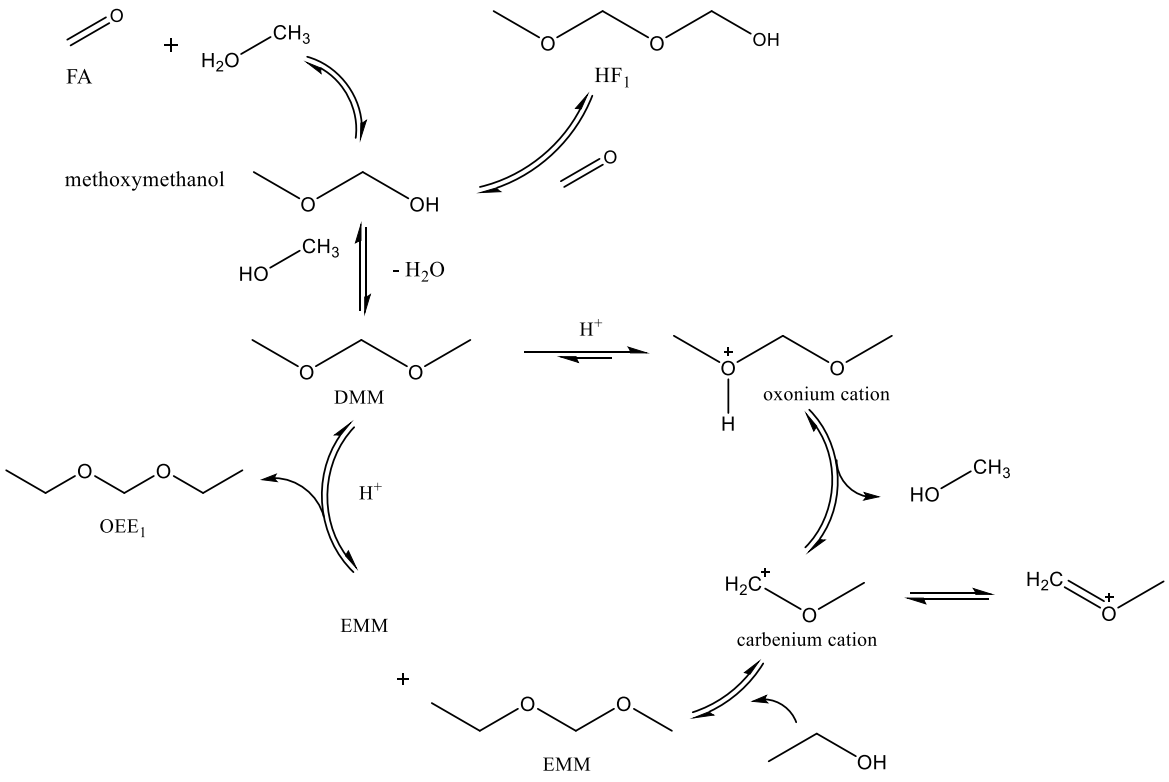

Scheme 4 Proposed reaction pathway for the acid catalyzed in situ formation of DEM and EMM as well as side-reactions to methoxymethanol and HF_1 (partly derived from (*20*))

As other species are in equilibrium as well, side-products such as OEE_1-OH/HF_1 can be formed, which were found in the herein investigated OEE reaction mixture. The theory regarding side-product formation during OEE synthesis is based on the detailed investigations by Lautenschütz (*20*). However, the EMM compounds could not be detected for the OEE reaction mixture, whereas oligomers of the diethoxyethane structuring, DEE_n, could be identified with the structures given in **Scheme 5**.

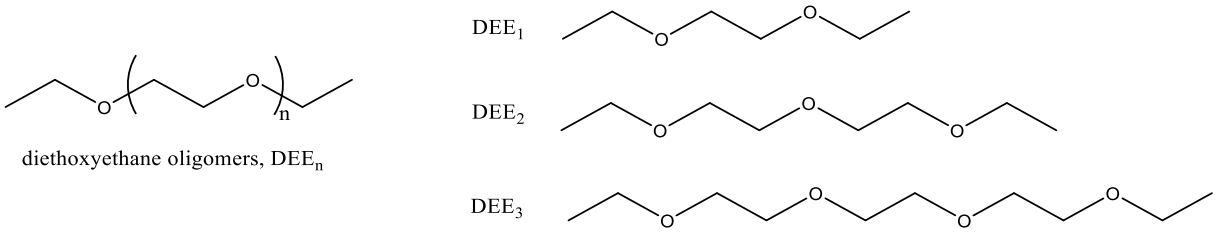

Scheme 5 Diethoxyethane oligomeric compounds, DEE_n, with n = 1, 2, 3

As the OEE products obtained herein were not intentionally produced by a synthetic procedure, these compounds will not be further discussed. Nevertheless, the conclusion could be drawn that employing the ethanolic NaOH to neutralize the OME reaction lead to a mixture of OEE_n and OME_n compounds. However, more undesired side-products were found for this approach including DME, HF, DEE and others. Purification of this reaction mixture by distillation, if possible, would be energy and time intensive as several distillation steps would be required due to compounds exhibiting similar boiling points. Hence, these products were not further investigated and the neutralization of the OME reaction mixture was performed for all other reactions discussed herein exclusively with an aqueous NaOH solution.

4.8. OME stability in water

Poly(oxymethylene) dimethyl ether (OME) compounds as well as trioxane were specified as stable compounds in neutral ambient conditions (*65*). However, the presence of water was found to influence the OME product distribution under acidic conditions as water reacts with ethers to form alcohols (see *2.4*) (*64*).

Hence, to investigate the stability of poly(oxymethylene) dimethyl ethers in the presence of water over a period of time, water dosages of 0.75 wt%, 1.50 wt% and 3.75 wt% were added to samples containing DMM and $OME_{2\text{-}7}$. In **Table 37** the mass selective fractions of OME and DMM are given as a function of the added water dosages. The samples were kept at ambient conditions and the influence of water on the etheric compounds was determined by GC-FID measurements by taking samples after 3, 24 and 48 hours. It was found, that the DMM and OME compounds are, as expected, stable in neutral conditions even with in presence of water (*140*). Interestingly, no MeOH could be detected for the sample at t = 0 hours without the addition of distilled water.

Table 37 Different water dosages to OME products leading to hydrolysis upon MeOH formation

t [h]	Added water [wt%]	$OME_{2\text{-}12}$ [wt%]	DMM [wt%]	MeOH [wt%]
0	0.00	24.49	15.63	0.00
3	0.75	22.47	13.79	0.95
	1.50	22.71	14.14	0.96
	3.75	21.69	13.56	0.95
24	0.75	22.38	13.07	1.22
	1.50	22.13	12.96	1.35
	3.75	21.83	12.69	1.33
48	0.75	22.54	12.37	1.19
	1.50	25.71	16.41	1.54
	3.75	21.84	12.16	1.15

However, as depicted in **Figure 65**, presence of water over a longer period resulted in an increased formation of MeOH. The sudden formation of MeOH upon the addition of water can be explained considering traces of an acidic catalyst in the sample. Hence, addition of H_2O induces the formation of MeOH, which might be due to the acid catalyzed equilibrium given in **Eq. 6**.

$$OME_n + H_2O \leftrightharpoons MeOH + HF_n \qquad \textbf{Eq. 6}$$

Interestingly, a direct relationship between the different dosages of water could not be derived, as 3.75 wt% did not necessarily lead to the highest MeOH formation. Therefore, the experimental imply that in order to ensure the stability of OME compounds over time, the exclusion of water prior storage is essential to reduce the formation of MeOH.

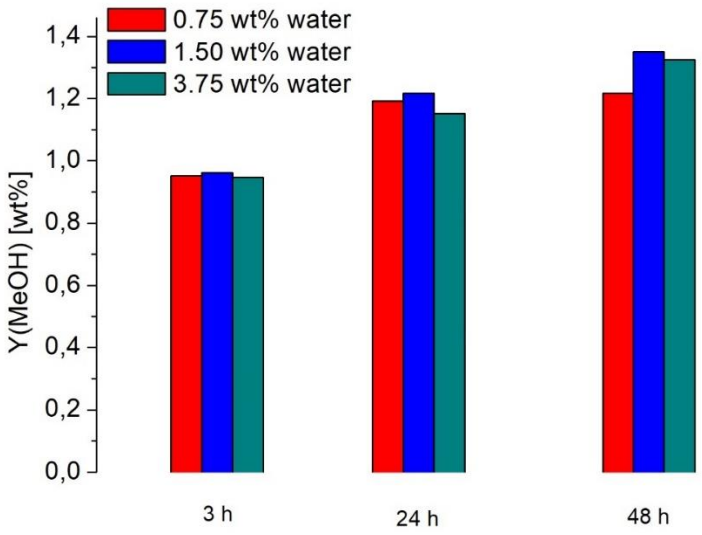

Figure 65 MeOH formation given as mass selective yield *Y* upon added water dosages as a function of time

4.9. Purification of OME

Upon synthesis of OME_n products, the removal of both, catalyst and trioxane, is crucial to stop the reaction mixture (i) from further oligomerization and (ii) to purify OME for blending purposes. Distillation of the reaction mixture to purify OME_n has been reported in scientific literature as the state-of-the-art procedure. For calibration and quantification purposes, pure OME_{1-4} can be directly injected for the determination of relative response factors (RRF) (*69*), whilst longer-chain OME_n compounds, with $n > 4$ can be obtained upon linear extrapolation of the RRF values (*69, 140*). However, regarding the OME purification procedure a major drawback is the presence of trioxane or undesired side-products in the reaction mixture. To overcome the difficulty of its removal, either extraction or multi-step distillation has to be conducted.

4.9.1. Extraction methods

In literature, Oestreich (*31*) proposed an extraction concept for the purification of OME compounds from polar side-products (hemiformals, glycols, MeOH and H_2O) using diesel or n-decan with water as extracting solvents. Therefore, extraction of OME products with an appropriate solvent combination (polar/apolar) is advantageous to remove unwanted side-products while concentrating OME compounds in the organic phase (*39*). Utilizing diesel as such is advantageous as the major objective of short-chain OME_{3-5} is their blending with diesel fuels. However, it was not reported if the organic phase could be removed to obtain pure OME compounds by subsequent distillation (*31*). Therefore, the aim of the extraction experiments reported herein was to remove trioxane, purify the OME products from undesired polar side products and subsequently to isolate pure OME compounds upon removal of the extracting solvent by distillation.

Solubility testing of DMM, trioxane and OME_{2-n} in various organic solvents has been conducted by Lautenschütz (*20*). Based on this, the extraction procedure has been carried out using n-hexane and cyclohexane for OME extraction and distilled water for the removal of trioxane and polar compounds. In principle, other organic solvents would be as well of interest however, the main selection criteria were the insolubility of trioxane in the organic phase and a low boiling point of the extracting solvent to simplify its removal by distillation. Therefore, the extraction was carried out in four steps using an aliquot of 2 mL distilled OME_{2-12} product with 2 mL of both, distilled water and n-hexane or cyclohexane. The watery phase was removed, and each extraction step was repeated thrice. Subsequently, the organic phase was measured by GC-FID to determine the mass fractions of the extracted compounds. As depicted in **Figure 66**, the amount of TRI dropped significantly after the first extraction step and a complete removal was obtained after four steps. Similar behavior was found for MeOH. Disadvantageously, after every extraction step, the amount of OME decreases significantly and upon complete removal of TRI the mass selectivity of OME decreased by around 30 wt% (**Figure 66**).

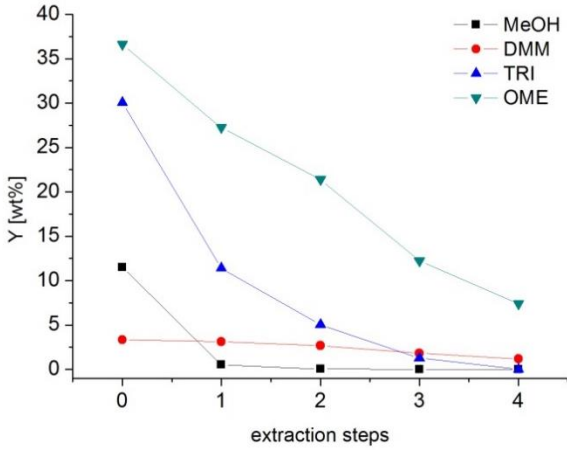

Figure 66 Mass selective yield Y of DMM, TRI, MeOH and OME upon four step extraction with hexane

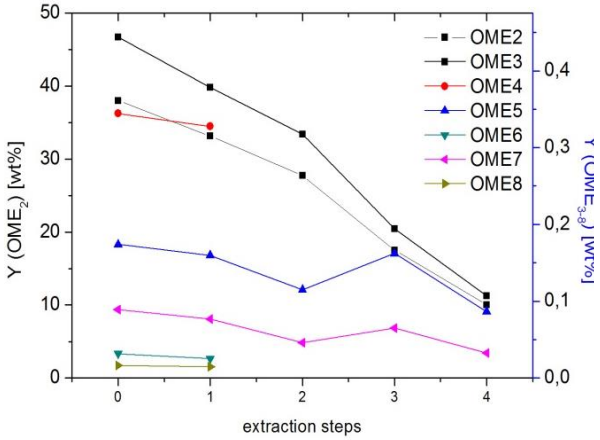

Figure 67 Mass distribution of OME_{2-8} products as a function of extraction steps (with hexane)

The hydrophilic property of longer-chain OME_n (n > 6) has been reported in literature (*31*). It was experimentally found, that extraction with polar solvents lead to a significant decrease of this product fraction, which is shown in **Figure 67**. Furthermore, multi-step extractions for a complete removal of trioxane was accompanied by a reduction of shorter-chain OME products. Some OME products (n = 4, 6 and 8) were below the detection limit and were therefore not detected after a single-step extraction, however, no explanation could be found for this result. In this context it must be noted, that the represented data were calculated from a single experiment. To obtain pure OME compounds, in a first attempt the organic solvents could not be removed under reduced pressure (water bath temperature 40°C, 235 mbar). Another approach was attempted by distillation, however, neither hexane nor cyclohexane could be removed from the reaction mixture. Changing the distillation columns from 20 cm to 45 cm, covering the column in alumina foil or upon distillation under reduced pressure always led to the presence of hexane or cyclohexane in the obtained distillate, which was confirmed by GC-MS measurement (**Figure 68**, *top to bottom*).

Therefore, purification of OME compounds *via* the extraction procedure led to (i) loss of longer-chain $OME_{n>6}$ products, (ii) presence of the extraction solvent and consequently to (iii) unsatisfying purity of the OME products. To obtain purified OME standards the purification of OME was not further pursued by an extracting technique. Instead a *via* multi-step distillation under reduced pressure was established, which will be discussed in the following.

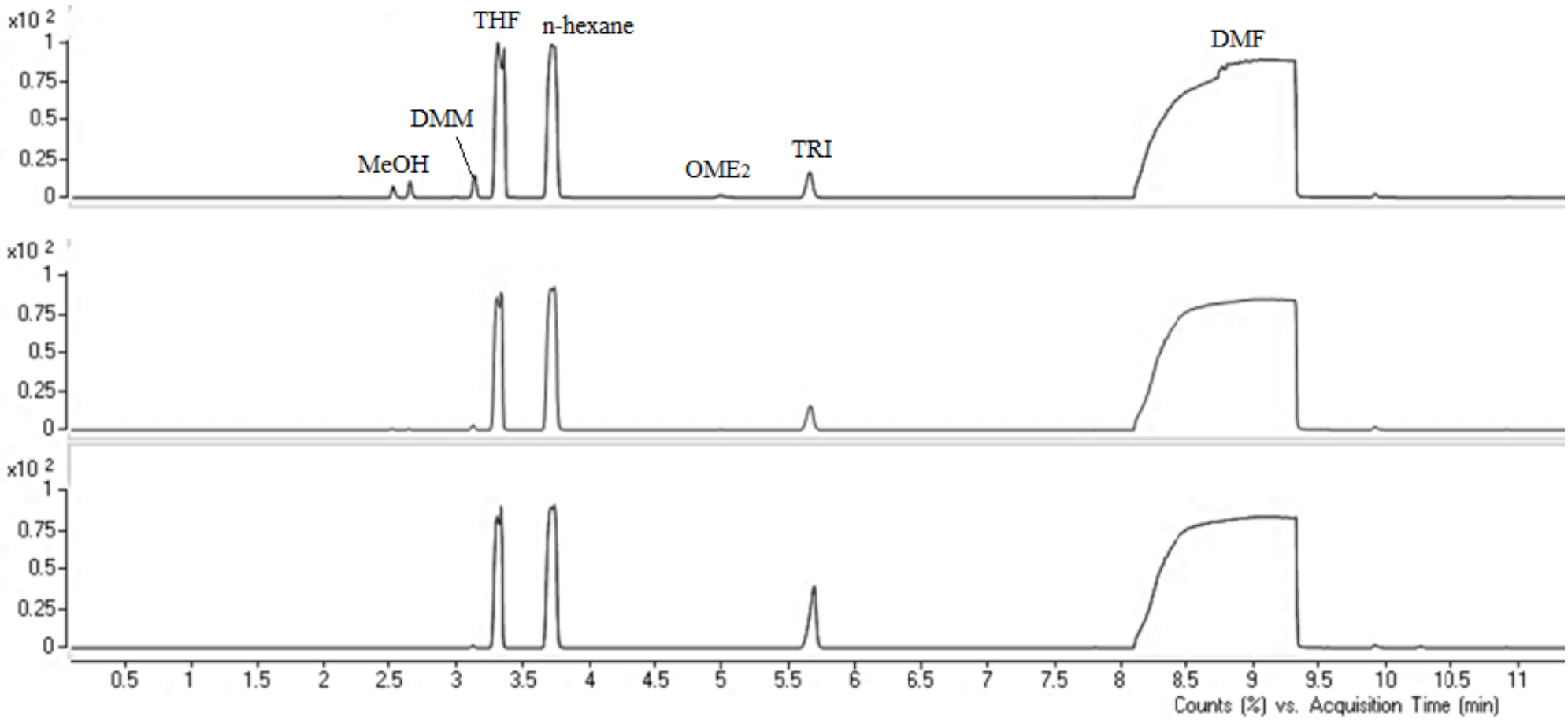

Figure 68 From top to bottom: GC-MS chromatrograms of the multi-step distillation procedure after a hexane extraction containing DMM (3.2 min), TRI (5.6 min), and OME_2 (5.2 min); hexane (3.7 min) is present in significant amount after every distillation step (in DMF (8.0 – 9.4 min) and THF (3.3 min))

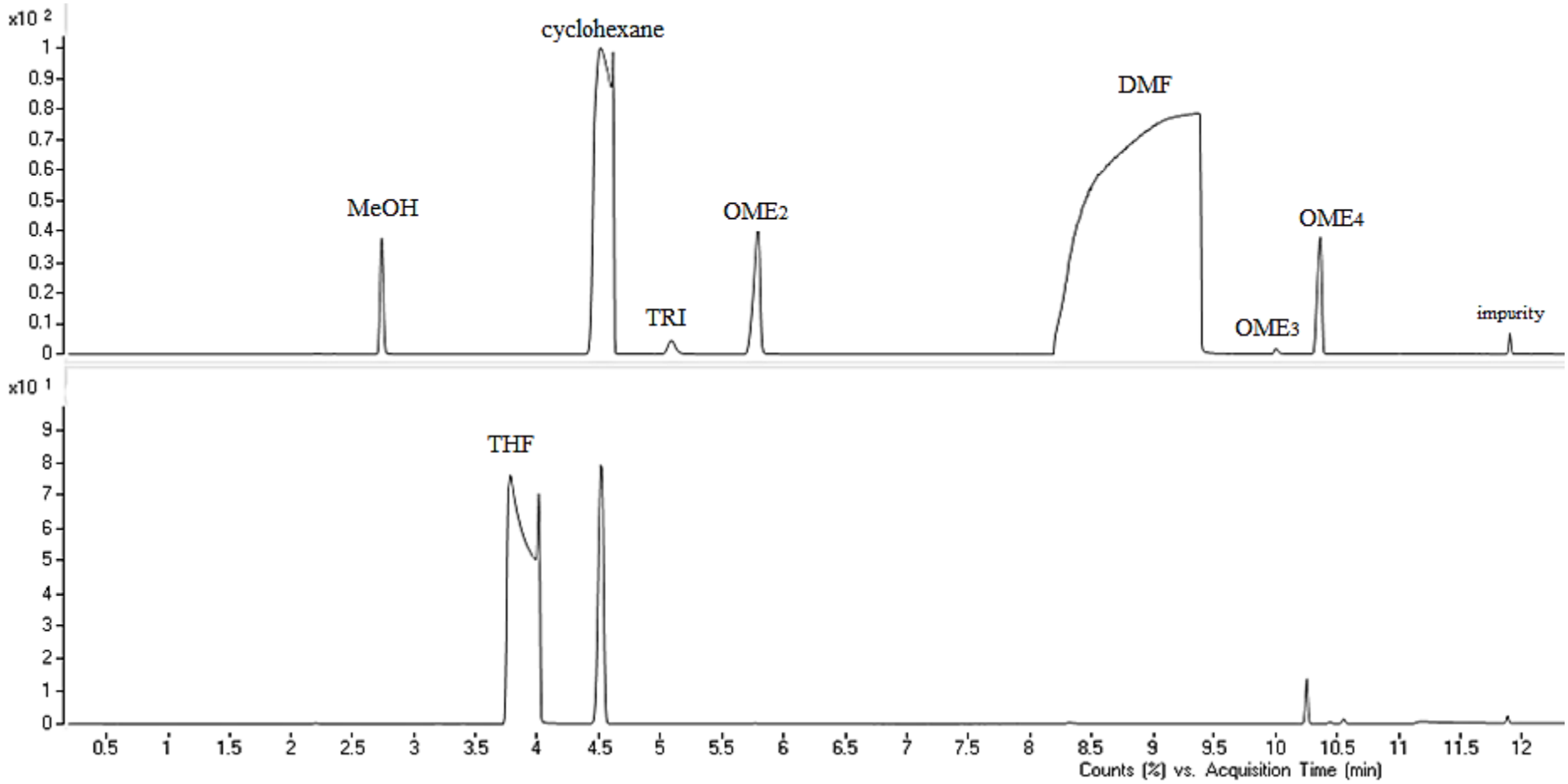

Figure 69 From top to bottom: : GC-MS chromatograms of the multi-step distillation procedure after a cyclohexane extraction; cylcohexane (4.5 min); upper diagram initial composition containing MeOH (2.6 min), TRI (5.6 min), OME_2 (5.2 min), OME_3 (10.3 min), OME_4 (11.8 min) measured in DMF (8.0 – 9.4 min) and THF (3.3 min) (*upper diagram*); remained distillate with non-distilled cyclohexane measured in THF (*lower diagram*)

4.9.2. Multi-step distillation procedure

Aiming for the quantification of the produced OME_{2-12} products, the OME_n (n = 2 – 4) compounds were purified by fractionated distillation under reduced pressure, which was already introduced in literature (*20*). Moreover, the distillation procedure has to be repeated several times to achieve a GC peak area of at least >97% for OME_{2-4} (*36*). Longer-chain OMEs (n > 5) are typically not possible to purify *via* distillation as they are solids at ambient temperature (*64*).

For this, a crude five-step distillation procedure under reduced pressure was performed utilizing the combined neutralized OME reaction mixtures, which were catalyzed by 0.7 – 1.0 wt% sulfuric acid. The progress of the distillation was controlled by GC-MS measurement of a small quantity of both, the distillate and the sump product after every distillation step. In **Figure 70** the GC-MS measurement (upper diagram) is shown for the neutralized reaction mixture prior distillation containing DMM, TRI and OME_{2-12}. In the first distillation step, DMM and traces of MeOH were successfully removed at ambient pressure and at 40°C column head temperature and would be recycled on a large-scale for OME synthesis (*154*). The corresponding GC-MS measurement of the sump product is shown in **Figure 70** (lower diagram). After the second and third distillation step, OME_2 and TRI could be removed under reduced pressure, whilst OME_{3-4} were obtained after the last two distillations (**Figure 73**). However, the obtained fractions of the subsequent distillation steps were contaminated with OME_{n+1} products. In other words, it was impossible to isolate a pure OME_n compound, e.g. OME_2, following this distillation procedure as longer-chain OME_{n+1} compounds (e.g. OME_3) will always be present in the distillate. To reduce the amount of the undesired OME_{n+1} products in the distillate, the distillation must be performed with caution avoiding both, rapid heating and a fast pressure reduction. In sum, to remove DMM and OME_{2-4} from the reaction mixture, five distillation steps were performed with the distillation data provided in **Table 39**.

Table 38 Distillation parameters including the oil bath temperature, column head temperature and pressure for the multi-step distillation

No. of distillation steps	Distillate content[a]	T (head) [°C]	p [mbar]
1	MeOH, DMM	36 – 52	930 – 608
2	OME_2, TRI	62 – 66	580 – 367
3	TRI (OME_2)[b]	67 – 72	480
4	OME_3, OME_4, TRI	40 – 64	410 – 460
5	OME_3, OME_4	62 – 68	121 – 143

[a] According to GC-FID measurements
[b] traces of OME_2 present after the second distillation step

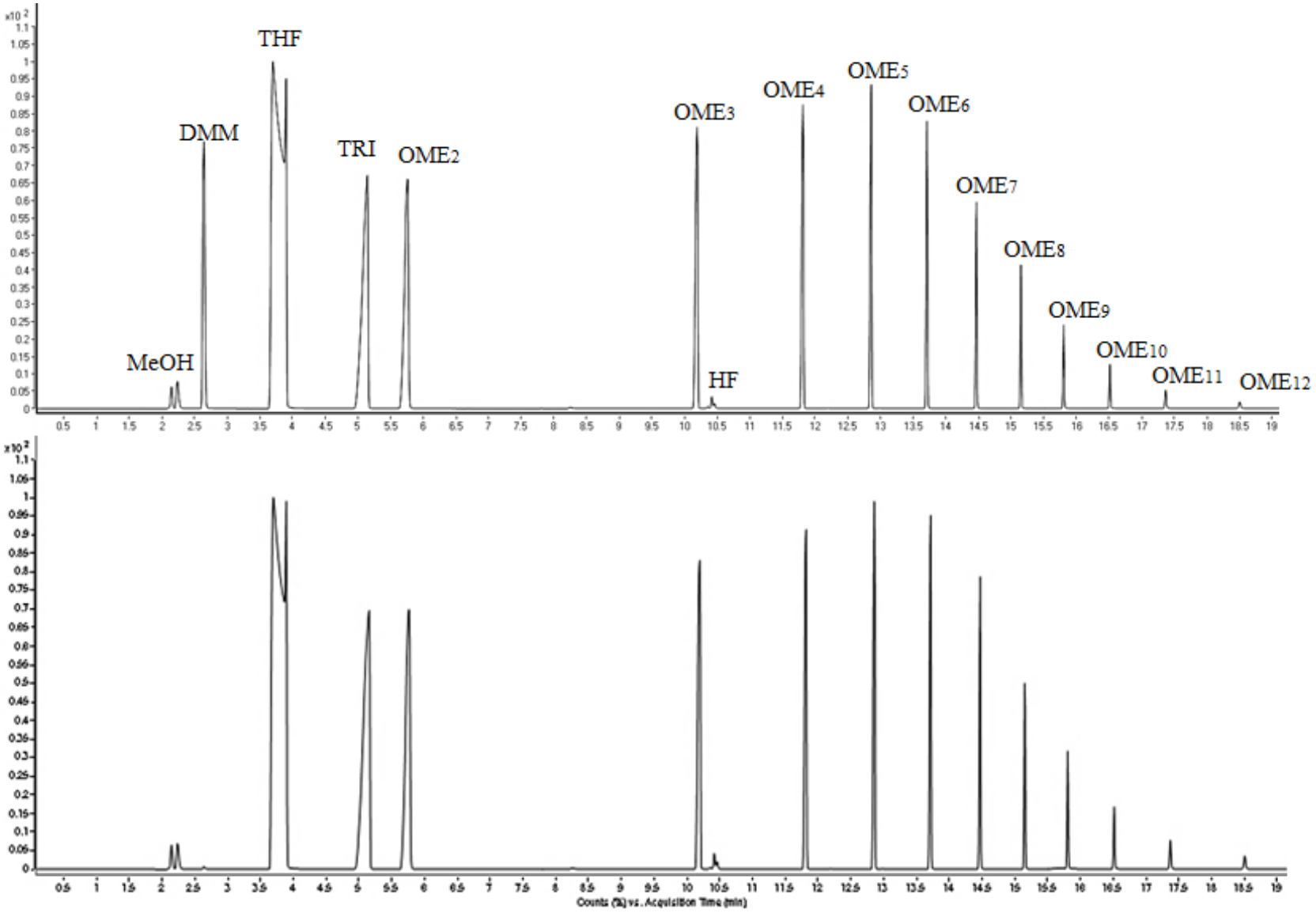

Figure 70 GC-MS chromatogram of the non-distilled neutralized reaction mixture (upper diagram) and upon single-step distillation (lower diagram)

Removal of short chain OME products resulted in the solidification of the distillation residue containing the products OME_{3-12} (**Figure 71**, right). These were impossible to separate upon distillation at temperatures below 130°C and reduced pressure, due to their high boiling points and solidification at a certain temperature (*11*). The corresponding GC-MS measurement is given in **Figure 73** (lower diagram), proofing that the products DMM, TRI and OME_2 were removed from the product mixture, whereas only a small quantity of OME_3 and OME_4 was possible to separate from the solidified distillation residue.

Figure 71 (*from left to right*) (a) DMM (98% purity), (b) OME_2 (97% purity), (c) OME_3 (96% purity with small amount of OME_4),(d) pFA and (e) OME_{8-12}

Furthermore, to purify the OME_{2-4} compounds to obtain GC-standards, another distillation step was necessary, which was performed for OME_2 and a mixture comprising OME_{3-4}. As the boiling-point difference between OME_2 and TRI is small, the latter was always present in distillates containing OME_2 (*65*). The removal of TRI was successfully completed by another, yet time intensive multi-step distillation procedure. In this regard, to remove a large quantity of TRI from the distillates of the second distillation step, the mixture was cooled in an ice bath to solidify TRI resulting in a sharp-edged needle-like solid (**Figure 72**, *right*). The remaining OME_2 rich liquid was removed *via* syringe or decantation for further purification. Therefore, for the distillation of the OME_2 compound, the heating and the applied pressure must be slowly increased or reduced to avoid dragging of TRI into the pure OME_2 fraction.

According to this, another distillation of the OME_{3-4} rich fraction was performed for the OME_{3-4} rich distillates, which were obtained after the last crude-distillation step. Hence, the OME_2 and $OME_{3,4}$ products were purified in small quantities with a purity of 97% (200.1 mg) and 96% (167.8 mg) respectively (**Figure 71**). The latter exhibits a slight turbidity, which is due to low amounts of OME_4. The herein experimentally found distillation data for the OME purification including DMM, TRI and OME_{2-4} is summarized in **Table 39**.

As proofed by GC-FID measurement a product mixture comprising DMM, TRI and OME_{2-7} can be isolated as a colorless liquid upon a single-step distillation from the neutralized reaction mixture as shown in **Figure 72** (*left*).

Table 39 Distillation data for OME purification

	T b.p. [°C]	T_{head} [°C]	$T_{oil\ bath}$ [°C]	p [mbar]
DMM	42 (*155*)	< 40[a]	< 100	930
OME_2[b]	105 (*42*)	44 – 48	100	600
TRI[c]	114 (*11*)	70 – 72	130	480
OME_3	156 (*42*)	62 – 64	130	400
OME_4[d]	202 (*42*)	70	130	400

[a] refers to a temperature region of 36-40°C

[b] OME_2 must be further purified, as it was not possible to separate from trioxane with the noted distillation set-up.

[c] The given temperature region does not indicate, that TRI is removed upon distillation; TRI is dragged through several distillation fractions, which have to be further purified; boiling temperature provided by Sigma-Aldrich

[d] Can be obtained upon distillation of fractions containing only OME_3 and OME_4

The remaining non-distillable colorless solid was found to comprise longer-chain OME products with n > 7 (**Figure 72**, middle), neutralized acidic catalyst as well as small amounts of pFA as an unwanted side product (**Figure 71**) (*18*, *45*). The latter was confirmed by determination of the decomposition temperature, which was in the temperature range as provided by the manufacturer for pFA in 97% purity.

In sum, a multi-step distillation procedure was successfully performed to isolate purified $OME_{2\text{-}4}$ compounds for their application as GC-standards. In the first step, the purification procedure comprised a crude five-step distillation to separate the corresponding OMEs, which were subsequently further purified in a distillation procedure. However, if pure OME standards for GC quantification are not required, a one-step distillation procedure was successfully employed yielding $OME_{2\text{-}7}$ as the distillate, whilst longer-chain $OME_{n>7}$ remained in the distillation sump.

Figure 72 Left: $OME_{2\text{-}7}$ products upon single-step distillation**; middle:** colorless solid residual upon single-step distillation containing $OME_{8\text{-}12}$, neutralization precipitate and pFA**; right:** TRI in small amount of OME product

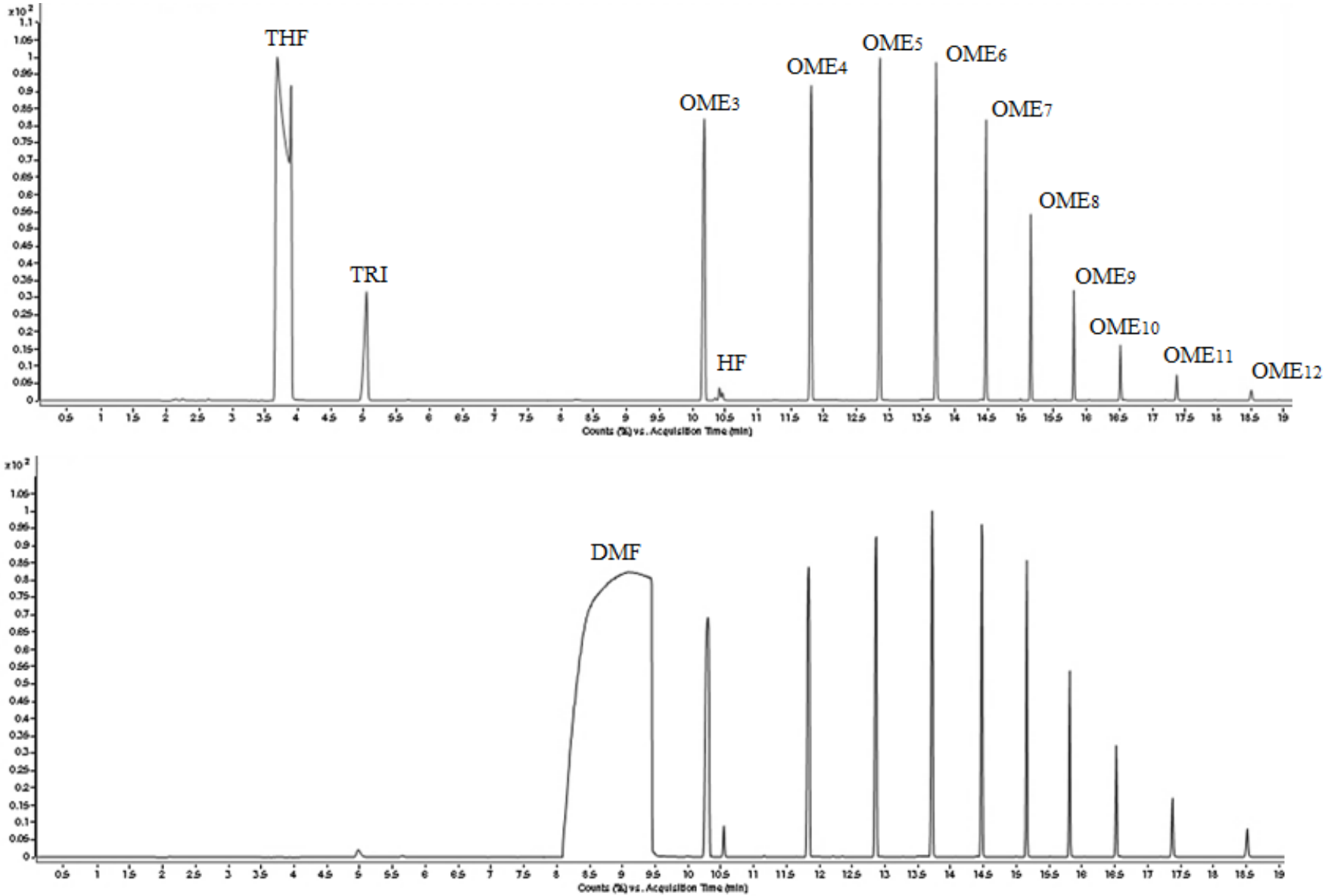

Figure 73 GC-MS chromatogram performed after two-step distillation (upper diagram) and upon five-step distillation (lower diagram)

4.10. A comparison of the resulting OME_{3-5} mass fractions for different catalysts and educts

The desired product fraction, OME_{3-5}, was found to be the most suitable regarding specified fuel characteristics and regulations (see *2.2*) (*11, 101*). Therefore, for the herein discussed reactions for OME production, the experimental results are summarized in **Table 40** focusing on the OME_{3-5} product mass fraction. As expected, the obtained yields are indicating that the reactions conducted from DMM and TRI as educts (anhydrous reaction pathway, see *2.4.1*), lead to the highest OME_{3-5} mass yields and are thus more advantageous compared to other educts.

Hence, the highest OME_{3-5} yield was obtained for the 3.5 wt% MSA catalyzed reaction, performed at ambient condition. Similarly, Deloxan® with 1.7 wt% catalyst loading produces good results, although this heterogeneous acid catalyst was found to exhibit a much lower exchange capacity, compared to other catalysts as discussed earlier (see **Table 29**). The educt combinations MeOH/TRI and DMM/pFA were determined to produce unsatisfying OME_{3-5} yields. The experimental results for the different reactions are given in **Table 40**. Thus, the catalysts examined in this work were found to be highly suitable catalysts for OME synthesis yielding moreover a promising OME_{3-5} product fraction for diesel applications.

In conclusion, the reactions performed with TRI and DMM were found to be superior to alternative FA and methyl-cap sources, employing a low educt ratio at mild reaction conditions. Furthermore, lower side-product formation, e.g. pFA, was achieved even for reactions catalyzed by sulfuric acid. Hence, it can be concluded that the reactions performed at ambient pressure were found comparable, if not better results to the synthetic procedure of Li and co-workers (*18*).

Table 40 Overview of the reactions for the production of OME products from the educt variations DMM/TRI (ambient conditions), pFA/DMM, MeOH/TRI (pressurized conditions) for different educt ratios

	Educt ratio	**Catalyst**	**Catalyst loading [wt%]**	**OME_{3-5} [wt%]**	**OME (m-n) [wt%]**
TRI/DMM[a]	1.0	H_2SO_4	1.0	32.1	58.3 (2 – 12)
		MSA	3.2	29.0	62.1 (2 – 12)
		MSA	3.5	32.7	76.2 (2 – 12)
		Deloxan®	1.0	24.7	48.6 (2 – 12)
		Deloxan®	1.7	30.1	71.9 (2 – 12)
pFA/DMM[b]	1.0	H_2SO_4	1.0	4.3	21.0 (2 – 5)
	1.5	H_2SO_4	1.5	3.4	17.9 (2 – 5)
	1.0	MSA	3.2	5.4	24.1 (2 – 5)
		Deloxan®	1.7	9.0	29.3 (2 – 5)
MeOH/TRI[c]	0.5	MSA	3.2	10.9	22.7 (2 – 12)

[a] reaction conditions: 80°C, 60 min, atmospheric pressure
[b] reaction conditions: 80°C, 60 min, 9 bar N_2 pressure
[c] reaction conditions: 80°C, 60 min, 9 bar N_2 pressure

5. Summary and conclusion

This study aimed towards an environmentally friendly production route of poly(oxymethylene) dimethyl ethers (OME_n) from the educts DMM, TRI, MeOH and pFA, catalyzed by sulfuric acid, MSA and Deloxan®. A detailed kinetic survey for OME synthesis on the variation of the reaction temperature, reaction time, stochiometric ratio of the reactants DMM and TRI at ambient pressure has been conducted. Furthermore, detailed OME work-up procedures and stability testing have been surveyed and developed, including extraction procedures with n-hexane and cylcohexane as solvents, as well as a multi-step distillation procedure. The latter was conveyed aiming for purified OME standards regarding OME quantification using THF as the internal standard. In this regard, the OME sample preparation prior GC measurement was conducted neutralizing the OME product phase with aqueous NaOH. However, addition of an ethanolic NaOH solution lead to the formation of OEE products, which was regarded with minor importance compared to OME products.

For the optimized reaction conditions at ambient pressure (80°C, n_{DMM}/n_{TRI} = 1, 60 min), both MSA (3.2 wt%) and Deloxan® (1.7 wt%) were found to catalyze $OME_{2\text{-}12}$ product formation more efficiently, compared to sulfuric acid (1.0 wt%). Hence, the $OME_{3\text{-}5}$ yields were determined for the corresponding catalysts with 29.0 wt%, 30.1 wt% and 32.1 wt%, respectively. However, elongation of the reaction time lead to longer-chain OME product formation for MSA and Deloxan®, whereas for sulfuric acid a preferred pFA side-product formation was observed. Thus, at 70 min reaction time the highest $OME_{2\text{-}8}$ yields at the given conditions were obtained at even lower MSA and Deloxan® catalyst loadings, with 2.9 wt% and 1.5 wt%, respectively. Similarly, both MSA and Deloxan® are prone to catalyze preferably longer-chain OME products, whilst sulfuric acid lead to the production of pFA. At 80°C both sulfuric acid (1.0 wt%) and Deloxan® (1.7 wt%) reach the maximum $OME_{2\text{-}12}$ yield, whilst MSA (3.2 wt%) reaches its maximum at 85°C. All catalysts reported herein were found to follow the Schulz-Flory distribution implying a sequential OME chain growth. The stoichiometric educt ratio $n_{DMM/TRI}$ = 1.0 at ambient pressure lead to the highest OME product yield, whilst lower ratios lead to the production of longer-chain OME products.

Furthermore, the influence of the reaction pressure on the OME synthesis catalyzed by MSA (3.2 wt%) and Deloxan® (1.7 wt%) was found to exhibit a higher relative $OME_{3\text{-}5}$ fraction, compared to the sulfuric acid (1.0 wt%) catalyzed OME synthesis. However, reactions performed under pressurized conditions with MeOH/TRI and pFA/DMM lead to unsatisfying OME product yields.

To sum up, the anhydrous OME synthesis with DMM and TRI as educts at ambient conditions with an advantageously low pFA side-product formation, lead for reactions catalyzed by 1.0 wt% sulfuric acid to comparable $OME_{2\text{-}12}$ yields reported in literature for sulfuric acid catalyzed OME reactions. Furthermore, at the optimized catalyst load of 3.5 wt% of MSA, the $OME_{2\text{-}8}$ product yield was found to reach significantly higher product formation (64.9 wt%) compared to sulfuric acid and other liquid

catalysts reported in literature. At present, the acid catalyst La^{3+}/SO_4^{2-} was reported to achieve the highest OME product yield (75.5 wt%, n = 2 – 8).

Even more promising OME yields were obtained for the reactions catalyzed by 1.7 wt% Deloxan®. Compared to other heterogeneously catalyzed reactions in literature, a significantly lower catalyst load of Deloxan® (1.7 wt%) and a far lower exchange capacity (0.659 mmol H^+/g dry catalyst) lead to an OME_{2-8} product yield of 60.3 wt%. This result is comparable to at the present most promising ion-exchange resin regarding OME synthesis, CT175, which was reported to produce 64.2 wt% of OME_{2-8} at a catalyst load of 7.5 wt%. However, poor recyclability of the heterogeneous catalyst Deloxan® might hamper its application in a large-scale OME process chain and further investigations on the re-activation of the catalyst would be required. In contrast, the aqueous synthesis route lead to non-promising results, and further investigations would be required on different educt ratios for the educt combinations MeOH/TRI and pFA/DMM.

Additionally, utilizing DMM and TRI as educts for the anhydrous reaction pathway catalyzed by sulfuric acid, MSA and Deloxan® lead to OME_{3-5} yields in the range of 29 – 33 wt%. This OME fraction was reported to lead to a smokeless combustion if applied as pure OME fuel and to a significant reduction of soot if blended with diesel fuel. Blending of OME_{3-5} with diesel fuel is at current the most promising technological application due to its good fitting physicochemical properties, regarding Cetane Number, autoignition point and others. In this regard, to make the OME_{3-5} product yield economically more feasible, a catalytic process chain would be required with recycled streams containing DMM, trioxane, OME_2 and longer-chain OME products with n > 5. Employing fixed bed reactors, the heterogeneous solid acid Deloxan® could be employed as this catalyst was found to produce almost no undesired side-products, such as hemiformals, pFA and others. Thus, for a large-scale OME process-development the aforementioned advantageous properties including mild reaction conditions, low catalyst load and reduced side-product formation abolish the cost of OME downstream processing rendering this pathway to be more attractive, compared to the aqueous approach with MeOH or pFA as educts.

In this regard, the direct one-step OME synthesis reported herein was developed for comparably low homogeneous and heterogeneous catalyst loadings, mild reaction conditions, high OME yields and a plain workup, thus providing a more attractive and advantageous OME production as potential diesel fuel.

List of tables

List of figures

List of schemes

References

1. Baranowski, C. J.; Bahmanpour, A. M.; Kröcher, O. Catalytic synthesis of polyoxymethylene dimethyl ethers (OME): A review. *Applied Catalysis B: Environmental*, 407–420.
2. Maus, W.; Jacob, E.; Härtl, M.; Seidenspinner, P. Synthetic fuels - ome1: a potentially sustainable diesel fuel**,** *2014*.
3. Klokic, S.; Hochegger, M.; Mittelbach, M.; Schober, S. *Process development for an efficient one-step poly(oxymethylene) dimethyl ether (OME) fuel production*, 2019.
4. Lumpp, B.; Rothe, D.; Pastötter, C.; Lämmermann, R.; Jacob, E. Oxymethylenether als Dieselkraftstoffzusätze der Zukunft. *MTZ Motortech Z [Online]* **2011,** *72* (3), 198–203.
5. Richter, G.; Zellbeck, H. Oxymethylene Ethers as an Alternative for Passenger Car Diesel Engines. *MTZ Worldw [Online]* **2017,** *78* (12), 60–67.
6. Zhang, Y.; Boehman, A. L. Impact of Biodiesel on NOx Emissions in a Common Rail Direct Injection Diesel Engine. *Energy Fuels [Online]* **2007,** *21* (4), 2003–2012.
7. Geyer, S. M.; Jacobus, M. J.; Lestz, S. S. Comparison of Diesel Engine Performance and Emissions from Neat and Transesterified Vegetable Oils. *Transactions of the ASAE [Online]* **1984,** *27* (2), 375–381.
8. Liu, H.; Wang, Z.; Wang, J.; He, X.; Zheng, Y.; Tang, Q.; Wang, J. Performance, combustion and emission characteristics of a diesel engine fueled with polyoxymethylene dimethyl ethers (PODE3-4)/ diesel blends. *Energy [Online]* **2015,** *88*, 793–800.
9. Miyamoto, N.; Ogawa, H.; Nurun, N. M.; Obata, K.; Arima, T. Smokeless, Low NOx, High Thermal Efficiency, and Low Noise Diesel Combustion with Oxygenated Agents as Main Fuel [Online] **1998**.
10. Chavanne, G. Procedure for the transformation of vegetable oils for their uses as fuels.**1937,** US 422,877.
11. Burger, J.; Siegert, M.; Ströfer, E.; Hasse, H. Poly(oxymethylene) dimethyl ethers as components of tailored diesel fuel: Properties, synthesis and purification concepts. *Fuel [Online]* **2010,** *89* (11), 3315–3319.
12. Härtl, M.; Seidenspinner, P.; Wachtmeister, G.; Jacob, E. Synthetischer Dieselkraftstoff OME1 — Lösungsansatz für den Zielkonflikt NOx-/Partikel-Emission. *MTZ Motortech Z [Online]* **2014,** *75* (7), 68–73.
13. Tan, Y. R.; Botero, M. L.; Sheng, Y.; Dreyer, J. A.H.; Xu, R.; Yang, W.; Kraft, M. Sooting characteristics of polyoxymethylene dimethyl ether blends with diesel in a diffusion flame. *Fuel [Online]* **2018,** *224*, 499–506.
14. Liu, J.; Shang, H.; Wang, H.; Zheng, Z.; Wang, Q.; Xue, Z.; Yao, M. Investigation on partially premixed combustion fueled with gasoline and PODE blends in a multi-cylinder heavy-duty diesel engine. *Fuel [Online]* **2017,** *193*, 101–111.
15. Bhatelia, T.; Lee, W. J.; Samanta, C.; Patel, J.; Bordoloi, A. Processes for the production of oxymethylene ethers: Promising synthetic diesel additives. *Asia-Pac. J. Chem. Eng. [Online]* **2017,** *12* (5), 827–837.
16. Wieland, S.; Panster, P. Replacing liquid acids in fine chemical synthesis by sulfonated polysiloxanes as solid acids and as supports for precious metal catalysts [Online]**,** *SAE Technical Paper Series***, 1997**, 108, 67–74.

17. International Symposium on Acid Base Catalysis; International Symposium on Acid-Base Catalysis. *Acid-base catalysis II. Proceedings of the International Symposium on Acid-Base Catalysis II, Sapporo, December 2 - 4, 1993*; Studies in surface science and catalysis 90; Kodansha: Tokyo, **1994**.

18. Li, H.; Song, H.; Zhao, F.; Chen, L.; Xia, C. Chemical equilibrium controlled synthesis of polyoxymethylene dimethyl ethers over sulfated titania. *Journal of Energy Chemistry [Online]* **2015,** *24* (2), 239–244.

19. Prasad, R.; Bella, V. R. A Review on Diesel Soot Emission, its Effect and Control. *Bull. Chem. React. Eng. Catal.* **2011,** *5* (2). DOI: 10.9767/bcrec.5.2.794.69-86.

20. Ludger Peter Lautenschütz. Neue Erkenntnisse in der Syntheseoptimierung oligomerer Oxymethylendimethylether aus Dimethoxymethan und Trioxan. Inaugural-Dissertation; Ruprecht-Karls-Universität Heidelberg, **2015**.

21. Singh, P.; Varun; Chauhan, S. R. Carbonyl and aromatic hydrocarbon emissions from diesel engine exhaust using different feedstock: A review. *Renewable and Sustainable Energy Reviews [Online]* **2016,** *63*, 269–291.

22. Reif, K. *Dieselmotor-Management. Systeme, Komponenten, Steuerung und Regelung*, 5., überarbeitete und erweiterte Auflage; SpringerLink Bücher; Vieweg+Teubner Verlag: Wiesbaden, **2012**.

23. Delphi. Worldwide emission standards - Passenger cars and light duty. delphi.com. *Accessed: 17.05.2019*

24. Brussels, Belgium: CEN. *EN590: Automotive fuels - Diesel - Requirements and test methods*. *EN590*, **2014** (EN590).

25. West Conshohocken. *ASTM-D975, Standard specification for diesel fuel oils (PA: ASTM)*, **2014**.

26. Dörmer, W.; Neumann, N.; Clasen, V.; Pfisterer, U.; Busch, O. Betriebsstoffe. In *Handbuch Verbrennungsmotor*: *Grundlagen, Komponenten, Systeme, Perspektiven*, 7., vollst. überarb. und erw. Aufl.; van Basshuysen, R., Schäfer, F., Eds.; ATZ/MTZ-Fachbuch; Springer Vieweg: Wiesbaden, **2015**; pp 892–958.

27. Fessmann, J.; Orth, H. *Angewandte Chemie und Umwelttechnik für Ingenieure*. *Handbuch für Studium und betriebliche Praxis*, 2. Aufl.; Ecomed Sicherheit; Ecomed: Landsberg, **2002**.

28. Dabelstein, W.; Reglitzky, A.; Schütze, A.; Reders, K. Automotive Fuels. *Ullmann's encyclopedia of industrial chemistry*; Wiley: Chichester, **2010**; p 1.

29. S. P. Srivastava and J. Hancsók, Ross, J. Fuels and Fuel-Additives. *Energy Technology [Online]* **2014,** *2* (11), 934–935.

30. Russell, A.; Epling, W. S. Diesel Oxidation Catalysts. *Catalysis Reviews [Online]* **2011,** *53* (4), 337–423.

31. Oestreich, D. Prozessentwicklung zur Gewinnung von Oxymethylenethern (OME) aus Methanol und Formaldehyd. Hochschulschrift; Fakultät für Chemieingenieurwesen und Verfahrenstechnik (CIW), **2017**.

32. Ambs, J. L.; McClure, B. T. The Influence of Oxidation Catalysts on NO2 in Diesel Exhaust [Online], *SAE Technical Paper Series*, **1993**.

33. Guan, B.; Zhan, R.; Lin, H.; Huang, Z. Review of state of the art technologies of selective catalytic reduction of NOx from diesel engine exhaust. *Applied Thermal Engineering [Online]* **2014,** *66* (1-2), 395–414.

34. van Setten, B. A. A. L.; Makkee, M.; Moulijn, J. A. Science and technology of catalytic diesel particulate filters. *Catalysis Reviews [Online]* **2001,** *43* (4), 489–564.

35. Zheng, M.; Reader, G. T.; Hawley, J.G. Diesel engine exhaust gas recirculation—a review on advanced and novel concepts. *Energy Conversion and Management [Online]* **2004,** *45* (6), 883–900.

36. Lautenschütz, L.; Oestreich, D.; Seidenspinner, P.; Arnold, U.; Dinjus, E.; Sauer, J. Physico-chemical properties and fuel characteristics of oxymethylene dialkyl ethers. *Fuel [Online]* **2016,** *173*, 129–137.

37. Liebl, J.; Beidl, C. Internationaler Motorenkongress 2017 [Online] **2017**.

38. Shamsul, N. S.; Kamarudin, S. K.; Rahman, N. A.; Kofli, N. T. An overview on the production of bio-methanol as potential renewable energy. *Renewable and Sustainable Energy Reviews [Online]* **2014,** *33*, 578–588.

39. Oestreich, D.; Lautenschütz, L.; Arnold, U.; Sauer, J. Production of oxymethylene dimethyl ether (OME)-hydrocarbon fuel blends in a one-step synthesis/extraction procedure. *Fuel [Online]* **2018,** *214*, 39–44.

40. Härtl, M.; Gaukel, K.; Pélerin, D.; Wachtmeister, G. Oxymethylene Ether as Potentially CO2-neutral Fuel for Clean Diesel Engines Part 1: Engine Testing. *MTZ Worldw [Online]* **2017,** *78* (2), 52–59.

41. Han, D. Y.; Cao, Z. B.; Shi, W. W.; Deng, X. D.; Yang, T. Y. Influence of polyoxymethylene dimethyl ethers on diesel fuel properties. *Energy Sources, Part A: Recovery, Utilization, and Environmental Effects [Online]* **2016,** *38* (18), 2687–2692.

42. Boyd, R. H. Some physical properties of polyoxymethylene dimethyl ethers. *J. Polym. Sci. [Online]* **1961,** *50* (153), 133–141.

43. KANG, M.-r.; SONG, H.-y.; JIN, F.-x.; Chen, J. Synthesis and physicochemical characterization of polyoxymethylene dimethyl ethers. *Journal of Fuel Chemistry and Technology [Online]* **2017,** *45* (7), 837–845.

44. Liu, H.; Wang, Z.; Wang, J.; He, X. Improvement of emission characteristics and thermal efficiency in diesel engines by fueling gasoline/diesel/PODEn blends. *Energy [Online]* **2016,** *97*, 105–112.

45. Oestreich, D.; Lautenschütz, L.; Arnold, U.; Sauer, J. Reaction kinetics and equilibrium parameters for the production of oxymethylene dimethyl ethers (OME) from methanol and formaldehyde. *Chemical Engineering Science [Online]* **2017,** *163*, 92–104.

46. Feiling, A.; Münz, M.; Beidl, C. Potential of the Synthetic Fuel OME1b for the Soot-free Diesel Engine. *ATZextra Worldw [Online]* **2016,** *21* (S11), 16–21.

47. Iannuzzi, S. E.; Barro, C.; Boulouchos, K.; Burger, J. Combustion behavior and soot formation/oxidation of oxygenated fuels in a cylindrical constant volume chamber. *Fuel [Online]* **2016,** *167*, 49–59.

48. Liu, H.; Wang, Z.; Zhang, J.; Wang, J.; Shuai, S. Study on combustion and emission characteristics of Polyoxymethylene Dimethyl Ethers/diesel blends in light-duty and heavy-duty diesel engines. *Applied Energy [Online]* **2017,** *185*, 1393–1402.

49. Härtl, M.; Seidenspinner, P.; Jacob, E.; Wachtmeister, G. Oxygenate screening on a heavy-duty diesel engine and emission characteristics of highly oxygenated oxymethylene ether fuel OME1. *Fuel [Online]* **2015,** *153*, 328–335.

50. Sarathy, S. M.; Oßwald, P.; Hansen, N.; Kohse-Höinghaus, K. Alcohol combustion chemistry. *Progress in Energy and Combustion Science [Online]* **2014,** *44*, 40–102.

51. Park, S. H.; Lee, C. S. Applicability of dimethyl ether (DME) in a compression ignition engine as an alternative fuel. *Energy Conversion and Management [Online]* **2014,** *86*, 848–863.

52. Arteconi, A.; Mazzarini, A.; Di Nicola, G. Emissions from Ethers and Organic Carbonate Fuel Additives: A Review. *Water Air Soil Pollut [Online]* **2011,** *221* (1-4), 405–423.

53. Beatrice, C.; Bertoli, C.; D'Alessio, J.; Del Giacomo, N.; Lazzaro, M.; Massoli, P. Experimental Characterization of Combustion Behaviour of New Diesel Fuels for Low Emission Engines. *Combustion Science and Technology [Online]* **1996,** *120* (1-6), 335–355.

54. Westbrook, C. K.; Pitz, W. J.; Curran, H. J. Chemical kinetic modeling study of the effects of oxygenated hydrocarbons on soot emissions from diesel engines. *The journal of physical chemistry. A [Online]* **2006,** *110* (21), 6912–6922.

55. Liu, J.; Wang, H.; Li, Y.; Zheng, Z.; Xue, Z.; Shang, H.; Yao, M. Effects of diesel/PODE (polyoxymethylene dimethyl ethers) blends on combustion and emission characteristics in a heavy duty diesel engine. *Fuel [Online]* **2016,** *177*, 206–216.

56. McEnally, C. S.; Pfefferle, L. D. Experimental study of fuel decomposition and hydrocarbon growth processes for practical fuel components in nonpremixed flames: MTBE and related alkyl ethers. *Int. J. Chem. Kinet. [Online]* **2004,** *36* (6), 345–358.

57. Sun, W.; Wang, G.; Li, S.; Zhang, R.; Yang, B.; Yang, J.; Li, Y.; Westbrook, C. K.; Law, C. K. Speciation and the laminar burning velocities of poly(oxymethylene) dimethyl ether 3 (POMDME 3) flames: An experimental and modeling study. *Proceedings of the Combustion Institute [Online]* **2017,** *36* (1), 1269–1278.

58. Oscar C. Bridgeman; Hobart S. White. Automobile Fuel-System Design and Vapor Lock. *SAE Transactions [Online]***, 1932** (27), 129-135, 142, 184. https://www.jstor.org/stable/44436651.

59. Barro, C.; Parravicini, M.; Boulouchos, K.; Liati, A. Neat polyoxymethylene dimethyl ether in a diesel engine; part 2: Exhaust emission analysis. *Fuel [Online]* **2018,** *234*, 1414–1421.

60. D. A. Pierpont, D. T. Montgomery and R. D. Reitz. Reducing Particulate and NOx Using Multiple Injections and EGR in a D.I. Diesel: SAE Transactions. *Journal of Fuels and Lubricants [Online]* **1995,** No. 104, 171–183.

61. Iannuzzi, S. E.; Barro, C.; Boulouchos, K.; Burger, J. POMDME-diesel blends: Evaluation of performance and exhaust emissions in a single cylinder heavy-duty diesel engine. *Fuel [Online]* **2017,** *203*, 57–67.

62. Schmitz, N.; Burger, J.; Ströfer, E.; Hasse, H. From methanol to the oxygenated diesel fuel poly(oxymethylene) dimethyl ether: An assessment of the production costs. *Fuel [Online]* **2016,** *185*, 67–72.

63. Burger, J.; Hasse, H. Multi-objective optimization using reduced models in conceptual design of a fuel additive production process. *Chemical Engineering Science [Online]* **2013,** *99*, 118–126.

64. Burger, J.; Ströfer, E.; Hasse, H. Chemical Equilibrium and Reaction Kinetics of the Heterogeneously Catalyzed Formation of Poly(oxymethylene) Dimethyl Ethers from Methylal and Trioxane. *Ind. Eng. Chem. Res. [Online]* **2012,** *51* (39), 12751–12761.

65. Burger, J.; Ströfer, E.; Hasse, H. Production process for diesel fuel components poly(oxymethylene) dimethyl ethers from methane-based products by hierarchical optimization

with varying model depth. *Chemical Engineering Research and Design [Online]* **2013,** *91* (12), 2648–2662.

66. Schelling, H.; Stroefer, E.; Pinkos, R.; Haunert, A.; Tebben, G.-D.; Hasse, H.; Blagov, S. Verfahren zur herstellung von polyoxymethylendimethylethern, **2004**, WO 2006/045506 A1.
67. Grützner, T.; Hasse, H.; Lang, N.; Siegert, M.; Ströfer, E. Development of a new industrial process for trioxane production. *Chemical Engineering Science [Online]* **2007,** *62* (18-20), 5613–5620.
68. Drunsel, J.-O. Entwicklung von Verfahren zur Herstellung von Methylal und Ethylal; TU Kaiserslautern, Kaiserslautern, **2012**.
69. Schmitz, N.; Homberg, F.; Berje, J.; Burger, J.; Hasse, H. Chemical Equilibrium of the Synthesis of Poly(oxymethylene) Dimethyl Ethers from Formaldehyde and Methanol in Aqueous Solutions. *Ind. Eng. Chem. Res. [Online]* **2015,** *54* (25), 6409–6417.
70. Stroefer, E.; Hasse, H.; Blagov, S. Verfahren zur Herstellung von polyoxymethylendimethylethern aus methanol und formaldehyd.
71. Hagen, G. P.; Spangler, M. J. Preparation of polyoxymethylene dimethyl ethers by catalytic conversion of dimethyl ether with formaldehyde formed by oxy-dehydrogenation of dimethyl ether. **1998**. US 5959156.
72. Hagen, G. P.; Spangler, M. J. Preparation of polyoxymethylene dimethyl ethers by acid-activated catalytic conversion of methanol with formaldehyde formed by dehydrogenation of methanol. US6437195.
73. Stroefer, E.; Schelling, H.; Hasse, H.; Blagov, S. Method for the production of polyoxymethylene dialkyl ethers from trioxan and dialkylethers. **2006**. US 7999140
74. Zheng, Y.; Tang, Q.; Wang, T.; Wang, J. Kinetics of synthesis of polyoxymethylene dimethyl ethers from paraformaldehyde and dimethoxymethane catalyzed by ion-exchange resin. *Chemical Engineering Science [Online]* **2015,** *134*, 758–766.
75. Burger, J.; Schmitz, N.; Hasse, H.; Stroefer, E. Process for preparing polyoxymethylene dimethyl ethers from formaldehyde and methanol in aqueous solutions. US 20180134642.
76. G. Reuss, W. Disteldorf, A. O. Gamer, A. Hilt. Formaldehyde: in Ullmann's Encyclopedia of Industrial Chemistry. *Wiley-VCH Verlag GmbH & Co. KGaA [Online]* **2000**.
77. Laird, T. Ullmann's Encyclopedia of Industrial Chemistry, 5th Edition VCH: Weinheim, Germany. 1996/1997. Section A, 28 vols. Section B, 8 vols. DM 19 400. *Org. Process Res. Dev. [Online]* **1997,** *1* (5), 391–392.
78. Lang, N.; Stroefer, E.; Stammer, A.; Friese, T.; Siegert, M.; Hasse, H.; Grützner, T.; Blagov, S. Integriertes Verfahren zur Herstellung von Trioxan aus Formaldehyd. **2007**. WO2007017479A1
79. Lang, N.; Stroefer, E.; Stammer, A.; Friese, T.; Siegert, M.; Hasse, H.; Grützner, T.; Blagov, S.; Ott, M. Verfahren zur abtrennung von trioxan aus einem trioxan/formaldehyd/wasser-gemisch. **2003**. WO 2005063353
80. Siegert, M.; Lang, N.; Stroefer, E.; Friese, T.; Hasse, H. Verfahren zur Abtrennung von Trioxan aus einem Trioxan/Formaldehyd/Wassergemisch mittels Druckwechselrektifikation. **2003**. WO 2005063733
81. Siegert, M.; Lang, N.; Thiel, J.; Stroefer, E.; Sigwart, C. Verfahren zur Herstellung von Roh-trioxan. **2007**. WO 2009077416
82. Cheremisinoff, N. P. *Industrial Solvents Handbook*, 2nd ed.; Taylor & Francis: Milton, **2004**.

83. Masamoto, J.; Matsuzaki, K. Development of Methylal Synthesis by Reactive Distillation. *J. Chem. Eng. Japan / JCEJ [Online]* **1994,** *27* (1), 1–5.

84. Masamoto, J., Ohtake, J. Kawamura, M. Process for producing formaldehyde and derivatives thereof. **1994**

85. Hasse, H.; Drunsel, J.-O.; Burger, J.; Schmidt, U.; Renner, M.; Blagov, S. Process for the production of pure methylal. **2010**. US20140187823A1

86. E. Fiedler, G. Grossmann, D. B. Kersebohm, G. Weiss, C. Witte. Methanol: in Ullmann's Encyclopedia of Industrial Chemistry. *Wiley-VCH Verlag GmbH & Co. KGaA [Online]* **2002**.

87. Niethammer, B.; Wodarz, S.; Betz, M.; Haltenort, P.; Oestreich, D.; Hackbarth, K.; Arnold, U.; Otto, T.; Sauer, J. Alternative Liquid Fuels from Renewable Resources. *Chemie Ingenieur Technik [Online]* **2018,** *90* (1-2), 99–112.

88. Reuss, G.; Disteldorf, W.; Gamer, A. O.; Hilt, A. Formaldehyde [Online]**, 2012,** *Ullman's Encylopedia of Industrial Chemistry*, *19*, 377.

89. Heim, L. E.; Konnerth, H.; Prechtl, M. H. G. Future perspectives for formaldehyde: pathways for reductive synthesis and energy storage. *Green Chem. [Online]* **2017,** *19* (10), 2347–2355.

90. Vita, A.; Italiano, C.; d. Previtali; Fabiano, C.; Palella, A.; Freni, F.; Bozzano, G.; Pino, L.; Manenti, F. Methanol synthesis from biogas: A thermodynamic analysis. *Renewable Energy [Online]* **2018,** *118*, 673–684.

91. Bahmanpour, A. M.; Hoadley, A.; Tanksale, A. Formaldehyde production via hydrogenation of carbon monoxide in the aqueous phase. *Green Chem. [Online]* **2015,** *17* (6), 3500–3507.

92. Bahmanpour, A. M.; Hoadley, A.; Mushrif, S. H.; Tanksale, A. Hydrogenation of Carbon Monoxide into Formaldehyde in Liquid Media. *ACS Sustainable Chem. Eng. [Online]* **2016,** *4* (7), 3970–3977.

93. Jin, G.; Werncke, C. G.; Escudié, Y.; Sabo-Etienne, S.; Bontemps, S. Iron-Catalyzed Reduction of CO2 into Methylene: Formation of C-N, C-O, and C-C Bonds. *Journal of the American Chemical Society [Online]* **2015,** *137* (30), 9563–9566.

94. Galat Alexander. Preparation of paraformaldehyde. **1953**. US 2775619

95. Alexander F Maclean. Concentration of formaldehyde by distillation and fractional condensation. **1954**. US2675346A

96. Baerns, M. *Technische Chemie*, 2nd ed.; Wiley: Hoboken, **2013**.

97. Festel, G.; Würmseher, M.; Rammer, C.; Boles, E.; Bellof, M. Modelling production cost scenarios for biofuels and fossil fuels in Europe. *Journal of Cleaner Production [Online]* **2014,** *66*, 242–253.

98. EIA. U.S. refinery prices of petroleum products to end users excluding taxes. https://www.eia.gov/petroleum/marketing/monthly/pdf/pmmtab2.pdf. (accessed: 18.05.2019)

99. WANG, H.; Shen, J. Decomposition of polyoxymethylene dimethyl ethers and synthesis of bisphenol F. *Catalysis Today [Online]* **2017,** *298*, 263–268.

100. Ai, Z.-J.; Chung, C.-Y.; Chien, I.-L. Design and control of poly(oxymethylene) dimethyl ethers production process directly from formaldehyde and methanol in aqueous solutions. *IFAC-PapersOnLine [Online]* **2018,** *51* (18), 578–583.

101. Zheng, Y.; Tang, Q.; Wang, T.; Liao, Y.; Wang, J. Synthesis of a Green Fuel Additive Over Cation Resins. *Chem. Eng. Technol. [Online]* **2013,** *36* (11), 1951–1956.

102. Haltenort, P.; Hackbarth, K.; Oestreich, D.; Lautenschütz, L.; Arnold, U.; Sauer, J. Heterogeneously catalyzed synthesis of oxymethylene dimethyl ethers (OME) from dimethyl ether and trioxane. *Catalysis Communications [Online]* **2018,** *109*, 80–84.

103. Wang, F.; Zhu, G.; Li, Z.; Zhao, F.; Xia, C.; Chen, J. Mechanistic study for the formation of polyoxymethylene dimethyl ethers promoted by sulfonic acid-functionalized ionic liquids. *Journal of Molecular Catalysis A: Chemical [Online]* **2015,** *408*, 228–236.

104. Schmitz, N.; Burger, J.; Hasse, H. Reaction Kinetics of the Formation of Poly(oxymethylene) Dimethyl Ethers from Formaldehyde and Methanol in Aqueous Solutions. *Ind. Eng. Chem. Res. [Online]* **2015,** *54* (50), 12553–12560.

105. Fetters, L. J.; Lohse, D. J.; Richter, D.; Witten, T. A.; Zirkel, A. Connection between Polymer Molecular Weight, Density, Chain Dimensions, and Melt Viscoelastic Properties. *Macromolecules [Online]* **1994,** *27* (17), 4639–4647.

106. Tobita, H. Molecular Weight Distribution of Living Radical Polymers. *Macromol. Theory Simul. [Online]* **2006,** *15* (1), 12–22.

107. Zheng, Y.; Tang, Q.; Wang, T.; Wang, J. Molecular size distribution in synthesis of polyoxymethylene dimethyl ethers and process optimization using response surface methodology. *Chemical Engineering Journal [Online]* **2015,** *278*, 183–189.

108. Painter, P. C.; Coleman, M. M. *Essentials of Polymer Science and Engineering;* DEStech Publications, Incorporated, **2008**.

109. Kissin, Y. v. Molecular weight distributions of linear polymers: Detailed analysis from GPC data. *J. Polym. Sci. A Polym. Chem. [Online]* **1995,** *33* (2), 227–237.

110. Elias, H.-G. *Macromolecules. Volume 1 · Structure and Properties;* Springer: Boston, MA, **1977**.

111. Lee, W.; Lee, H.; Cha, J.; Chang, T.; Hanley, K. J.; Lodge, T. P. Molecular Weight Distribution of Polystyrene Made by Anionic Polymerization. *Macromolecules [Online]* **2000,** *33* (14), 5111–5115.

112. Zhao, Y.; Xu, Z.; Chen, H.; Fu, Y.; Shen, J. Mechanism of chain propagation for the synthesis of polyoxymethylene dimethyl ethers. *Journal of Energy Chemistry [Online]* **2013,** *22* (6), 833–836.

113. Crabtree, R. H. *The organometallic chemistry of the transition metals*, Sixth edition; Wiley: Hoboken, New Jersey, **2014**.

114. Wang, L.; Wu, W.-T.; Chen, T.; Chen, Q.; He, M.-Y. Ion-exchange resin-catalyzed synthesis of polyoxymethylene dimethyl ethers: A practical and environmentally friendly way to diesel additive. *Chemical Engineering Communications [Online]* **2014,** *201* (5), 709–717.

115. Wang, R.; Wu, Z.; Qin, Z.; Chen, C.; Zhu, H.; Wu, J.; Chen, G.; Fan, W.; Wang, J. Graphene oxide: An effective acid catalyst for the synthesis of polyoxymethylene dimethyl ethers from methanol and trioxymethylene. *Catal. Sci. Technol. [Online]* **2016,** *6* (4), 993–997.

116. Shi, G.-F.; Miao, J.; Wang, G.-Y.; Su, J.-M.; Liu, H.-X. Synthesis of Polyoxymethylene Dimethyl Ethers Catalyzed by Rare Earth Compounds. *Asian J. Chem. [Online]* **2015,** *27* (6), 2149–2153.

117. Wu, Q.; Li, W.; Wang, M.; Hao, Y.; Chu, T.; Shang, J.; Li, H.; Zhao, Y.; Jiao, Q. Synthesis of polyoxymethylene dimethyl ethers from methylal and trioxane catalyzed by Brønsted acid ionic liquids with different alkyl groups. *RSC Adv. [Online]* **2015,** *5* (71), 57968–57974.

118. Yang, Z.; Hu, Y.; Ma, W.; Qi, J.; Zhang, X. Synthesis of Polyoxymethylene Dimethyl Ethers Catalyzed by Pyrrolidinonium-Based Ionic Liquids. *Chem. Eng. Technol.*, **2017**, *40*, 1784–1791.

119. Ghandi, K. A Review of Ionic Liquids, Their Limits and Applications. *GSC [Online]* **2014,** *04* (01), 44–53.

120. Liu, Y.; Lotero, E.; Goodwinjr, J. A comparison of the esterification of acetic acid with methanol using heterogeneous versus homogeneous acid catalysis. *Journal of Catalysis [Online]* **2006,** *242* (2), 278–286.

121. Zhang, J.; Shi, M.; Fang, D.; Liu, D. Reaction kinetics of the production of polyoxymethylene dimethyl ethers from methanol and formaldehyde with acid cation exchange resin catalyst. *Reac Kinet Mech Cat [Online]* **2014,** *113* (2), 459–470.

122. Fang, X.; Chen, J.; Ye, L.; Lin, H.; Yuan, Y. Efficient synthesis of poly(oxymethylene) dimethyl ethers over PVP-stabilized heteropolyacids through self-assembly. *Sci. China Chem. [Online]* **2015,** *58* (1), 131–138.

123. Zhao, Q.; Wang, H.; Qin, Z.-f.; Wu, Z.-w.; Wu, J.-b.; Fan, W.-b.; Wang, J.-g. Synthesis of polyoxymethylene dimethyl ethers from methanol and trioxymethylene with molecular sieves as catalysts. *Journal of Fuel Chemistry and Technology [Online]* **2011,** *39* (12), 918–923.

124. Wu, J.; Zhu, H.; Wu, Z.; Qin, Z.; Yan, L.; Du, B.; Fan, W.; Wang, J. High Si/Al ratio HZSM-5 zeolite: An efficient catalyst for the synthesis of polyoxymethylene dimethyl ethers from dimethoxymethane and trioxymethylene. *Green Chem. [Online]* **2015,** *17* (4), 2353–2357.

125. William F. Gresham, Lindamere and Richard E. Brooks, Edgemoore Terrace. Preparation of Polyformals. **1954**. US2449469

126. Chen, W.; Li, F.; Yang, W.; Gao, H. Method for preparing polyoxymethylene dimethyl ether. **2009**. CN101768058A

127. Schelling, H.; Stroefer, E.; Pinkos, R.; Haunert, A.; Tebben, G.-D.; Hasse, H.; Blagov, S. Verfahren zur Herstellung von Plyoxymethylendimethylethern. **2005**. WO2006045506-A1

128. P. Panster to Degussa AG. European Patent. EP 548 821.

129. P. Panster to Degussa AG. European Patent. DE 42 23 589.

130. Amandi, R.; Licence, P.; Ross, S. K.; Aaltonen, O.; Poliakoff, M. Friedel−Crafts Alkylation of Anisole in Supercritical Carbon Dioxide: A Comparative Study of Catalysts. *Org. Process Res. Dev.*, **2005**, *4*, 451–456.

131. Article OME Made in Germany- ome. http://www.ome-technologies.de/news/article/article/ome-made-in-germany.html. Accessed: 12.12.2018

132. Xia, C.; Song, H.; Chen, J.; Jin, F.; Kang, M. System and method for continuously producing polyoxymethylene dimethyl ethers. **2012**. US 20140114092 A1

133. Chen, J.; Song, H.; Xia, C.; Kang, M.; Jin, R. System and method for continuously producing polyoxymethylene dialkyl ethers. **2012**. US 9067188

134. John A. Marsella. Dimethylformamide - Kirk-Othmer Encyclopedia of Chemical Technology. *Inc, John Wiley &. Sons [Online]* **2000**.

135. Buncel, E.; Symons, E. A. The inherent instability of dimethylformamide–water systems containing hydroxide ion. *J. Chem. Soc. D [Online]* **1970,** *0* (3), 164–165.

136. Heaney, H.; Papageorgiou, G.; Wilkins, R. The Generation Of Iminium Ions Using Chlorosilanes And Their Reactions With Electron Rich Aromatic Heterocycles. *Tetrahedron [Online]* **1997,** No. 53, 2941–2958.

137. Mori, S.; Barth, H. G. *Size Exclusion Chromatography*. *(Springer Laboratory)*, 1999th ed.; Springer Science & Business Media, **1999**.

138. Saint Laumer, J.-Y. de; Leocata, S.; Tissot, E.; Baroux, L.; Kampf, D. M.; Merle, P.; Boschung, A.; Seyfried, M.; Chaintreau, A. Prediction of response factors for gas chromatography with flame ionization detection: Algorithm improvement, extension to silylated compounds, and application to the quantification of metabolites. *Journal of separation science [Online]* **2015,** *38* (18), 3209–3217.

139. Alzahrani, A.; Mirallai, S. I.; Chalmers, B. A.; McArdle, P.; Aldabbagh, F. Synthesis of N-(dialkylamino)methylacrylamides and N-(dialkylamino)methylmethacrylamides from Schiff base salts: useful building blocks for smart polymers. *Organic & biomolecular chemistry [Online]* **2018,** *16* (22), 4108–4116.

140. Zhu, G.; Zhao, F.; Wang, D.; Xia, C. Extended effective carbon number concept in the quantitative analysis of multi-ethers using predicted response factors. *Journal of chromatography. A [Online]* **2017,** *1513*, 194–200.

141. Wang, M.; Wang, C.; Han, X. Selection of internal standards for accurate quantification of complex lipid species in biological extracts by electrospray ionization mass spectrometry-What, how and why? *Mass spectrometry reviews [Online]* **2017,** *36* (6), 693–714.

142. Meerwein, H.; Delfs, D.; Morschel, H. Die Polymerisation des Tetrahydrofurans. *Angew. Chem. [Online]* **1960,** *72* (24), 927–934.

143. Harris, D. C. *Lehrbuch der Quantitativen Analyse*, 8., vollst. überarb. erw. Aufl. 2014; Springer Spektrum: Berlin, **2014**.

144. Li, H.; Song, H.; Chen, L.; Xia, C. Designed SO42−/Fe2O3 -SiO2 solid acids for polyoxymethylene dimethyl ethers synthesis: The acid sites control and reaction pathways. *Applied Catalysis B: Environmental [Online]* **2015,** *165*, 466–476.

145. Deutsch, D.; Oestreich, D.; Lautenschütz, L.; Haltenort, P.; Arnold, U.; Sauer, J. High Purity Oligomeric Oxymethylene Ethers as Diesel Fuels. *Chemie Ingenieur Technik [Online]* **2017,** *89* (4), 486–489.

146. Sigma Aldrich. Product Information of Paraformaldehyde (No. P6148 and 441244).

147. Roitman, D. B.; McAlister, J.; Oaks, F. L. Composition characterization of methanesulfonic acid. *J. Chem. Eng. Data [Online]* **1994,** *39* (1), 56–60.

148. http://www.hygroscopiccycle.com/industrial-reference/. Hygroscopic compounds (Accessed 24.03.2019).

149. Li, H.; Li, Y.; Guo, T.; Zhang, J.; He, L. The green and expeditious synthesis of sulfated titania with enhanced catalytic activity in polyoxymethylene dimethyl ethers synthesis. *Reac Kinet Mech Cat [Online]* **2018,** *124* (1), 139–151.

150. Deng, X.; Cao, Z.; Li, X.; Han, D.; Zhao, R.; Li, Y. The Synthesis of Polyoxymethylene Dimethyl Ethers for New Diesel Blending Component. *Synthesis and Reactivity in Inorganic, Metal-Organic, and Nano-Metal Chemistry [Online]* **2015,** *46* (12), 1842–1847.

151. Zhang, J.; Liu, D. Preparation of a hydrophobic-hydrophilic adjustable catalyst surface for the controlled synthesis of polyoxymethylene dimethyl ethers: A potential replacement of diesel fuel. *Int J Energy Res [Online]* **2018,** *42* (3), 1237–1246.

152. Gaur, B.; Srinivasan, H. S. Corrosion of metals and alloys in methane sulphonic acid. *British Corrosion Journal [Online]* **2013,** *34* (1), 63–66.

153. Lei Y H, Sun Q, Chen Z X, Shen J Y. Theoretical calculations on the thermodynamics for the synthesis reactions of polyoxymethylene dimethyl ethers. *Acta Chim. Sinica [Online]*, **2009**, No. 67, 767–772.

154. Schmitz, N.; Ströfer, E.; Burger, J.; Hasse, H. Conceptual Design of a Novel Process for the Production of Poly(oxymethylene) Dimethyl Ethers from Formaldehyde and Methanol. *Ind. Eng. Chem. Res. [Online]* **2017,** *56* (40), 11519–11530.

155. Lide, D. R. *CRC handbook of chemistry and physics;* CRC Boca Raton, **2012**.

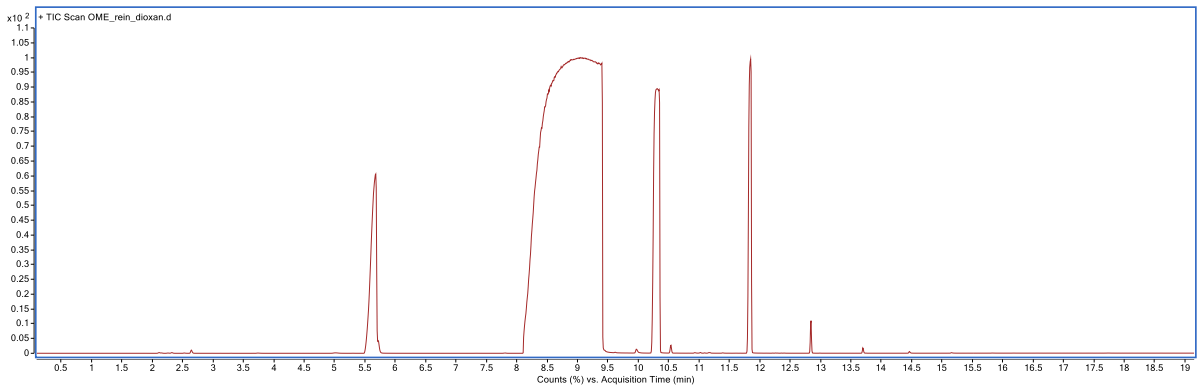

Figure 74 OME with 1,4-Dioxane as internal standard (ISTD)

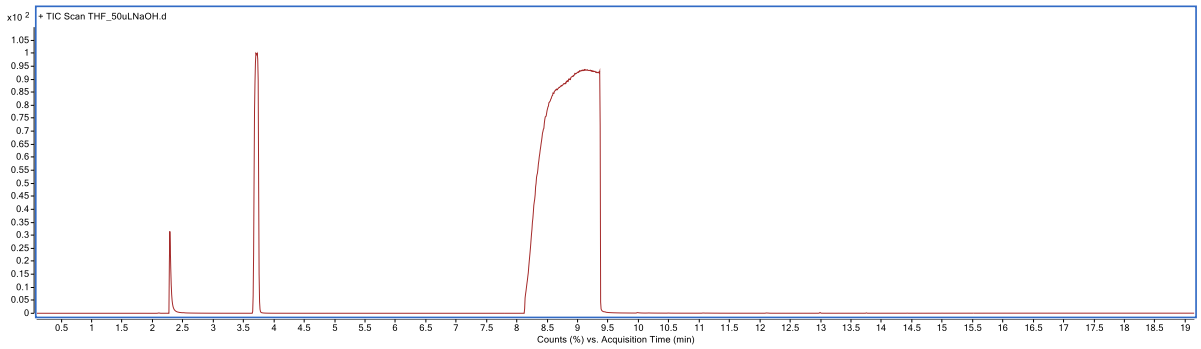

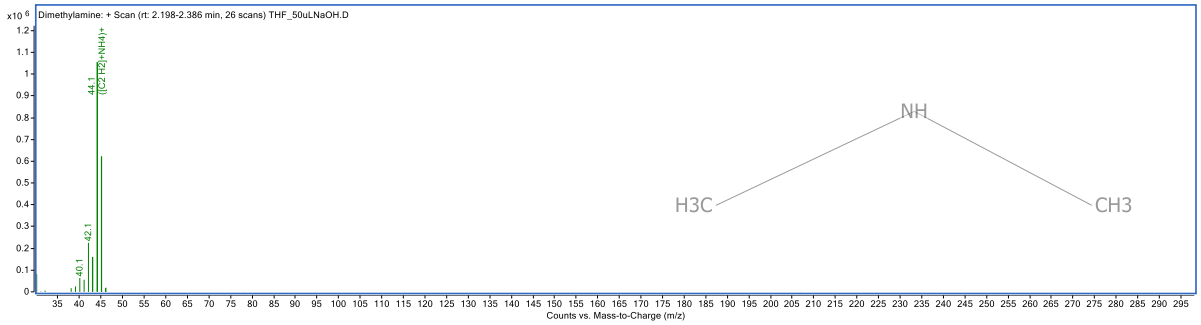

Figure 75 Dimethyl amine confirmation by GC-FID (DMF in basic media)

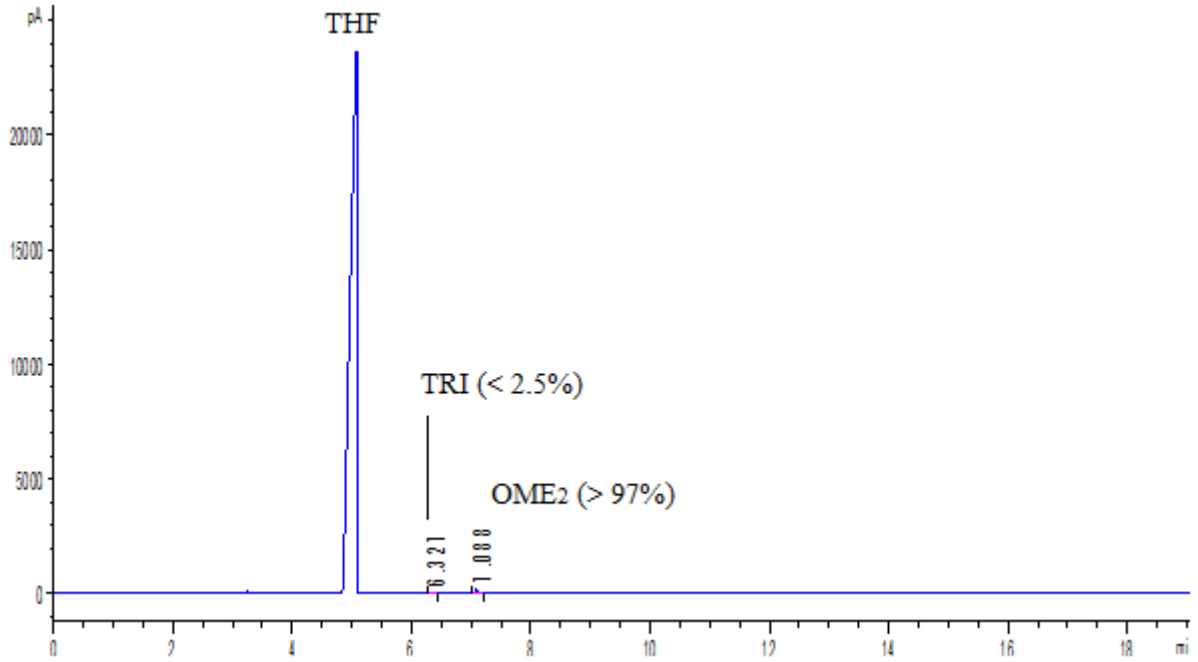

Figure 76 GC-FID of the purified OME_2 product in >97% purity

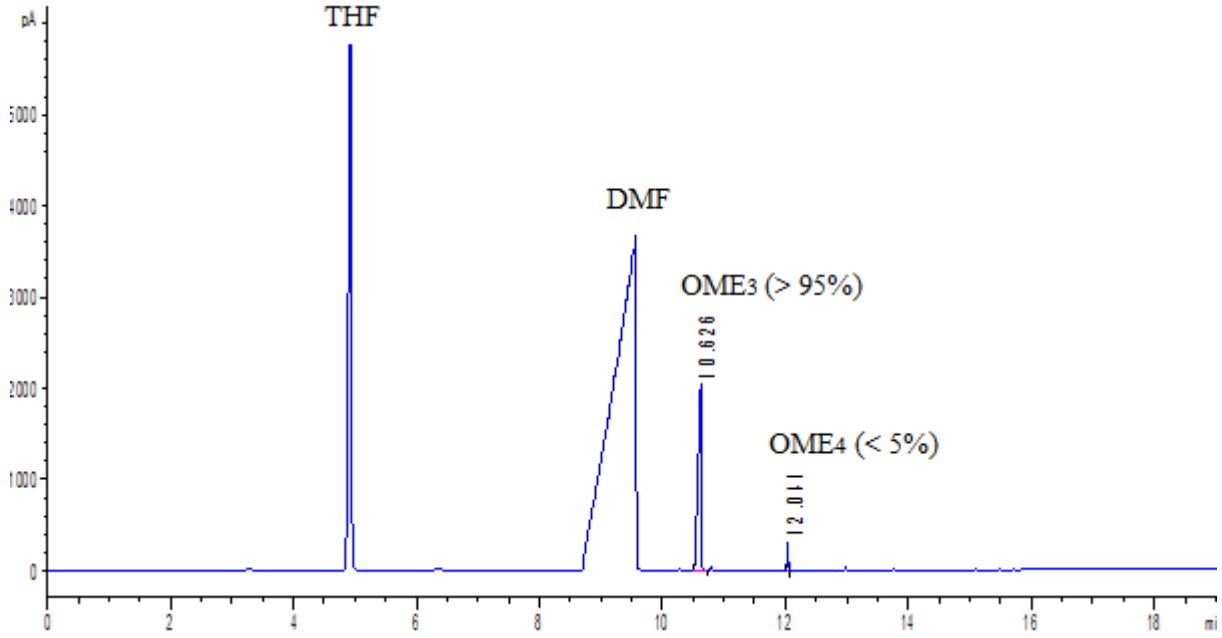

Figure 77 GC-FID of the purified $OME_{3\text{-}4}$ product in >95% purity

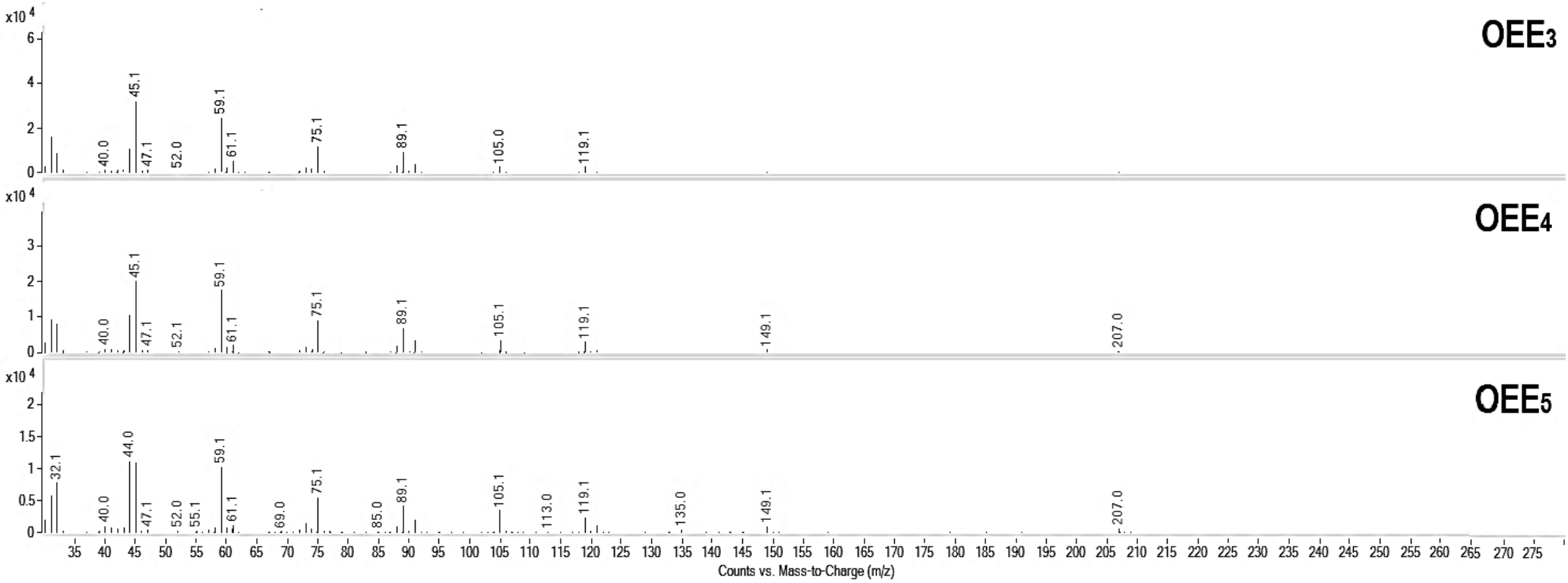

Figure 78 Mass spectra obtained upon GC-MS measurement for the OEE_3, OEE_4 and OEE_5 products

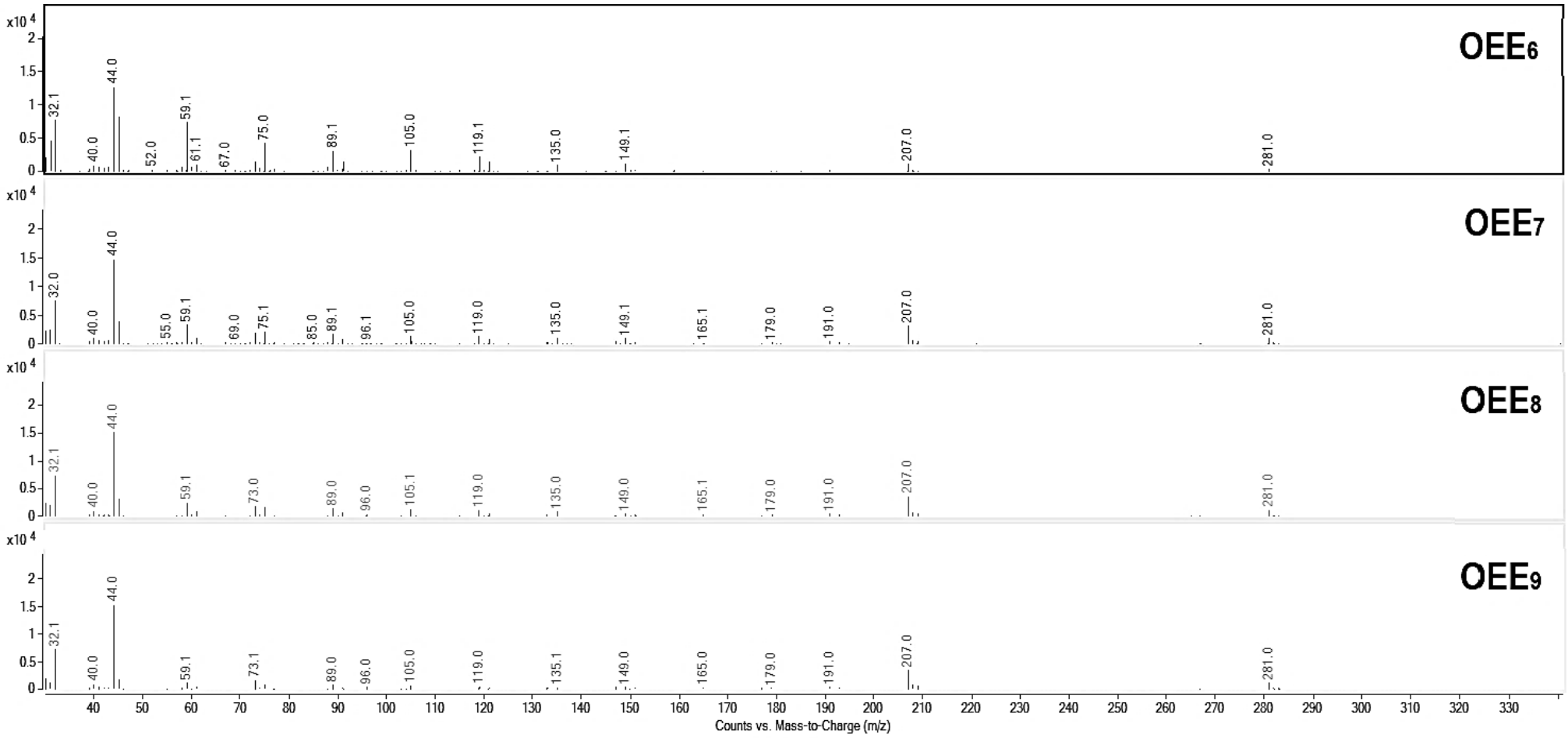

Figure 79 Mass spectra obtained upon GC-MS measurement for the OEE_6, OEE_7, OEE_8 and OEE_9 products

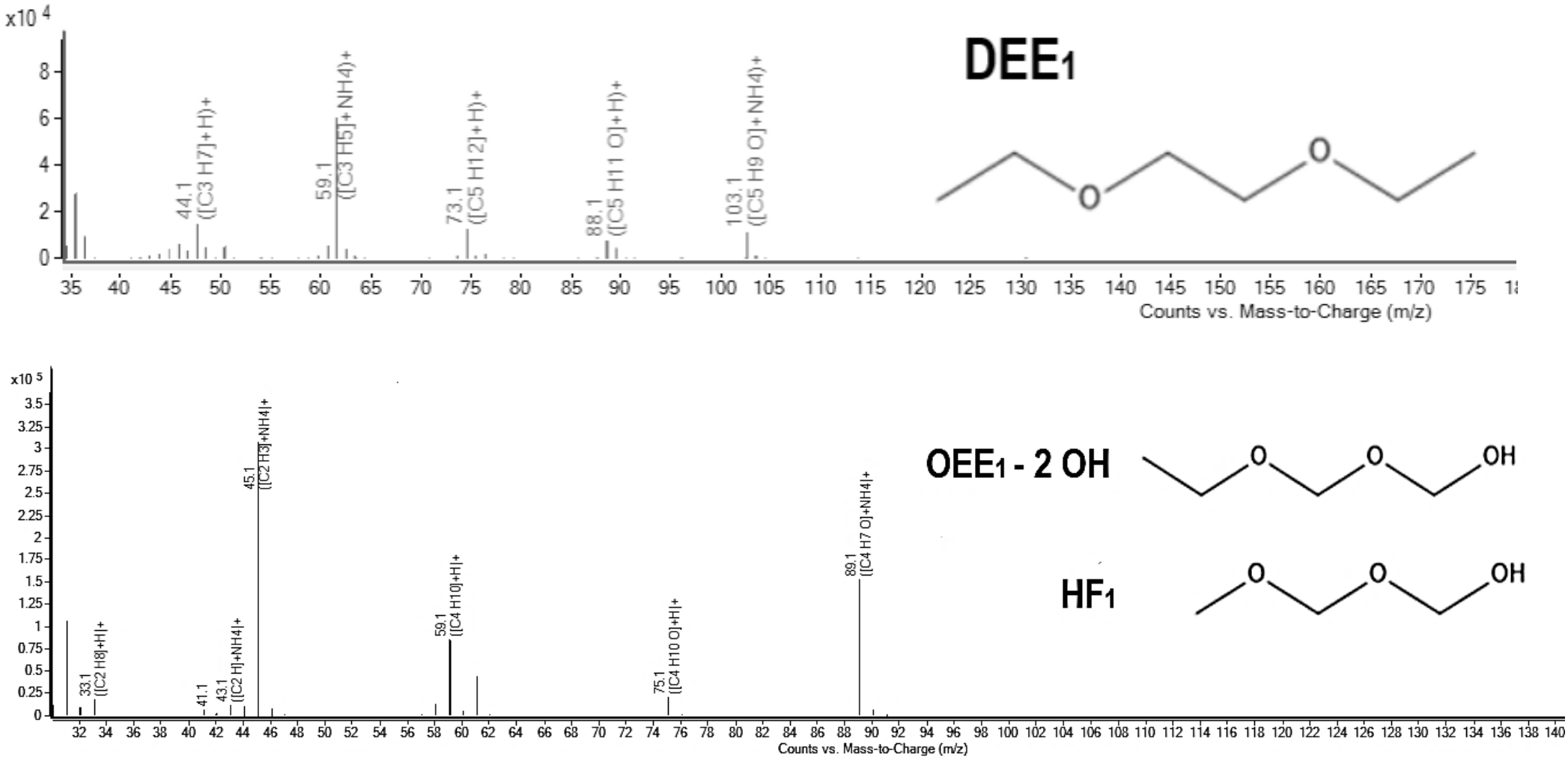

Figure 80 Mass spectra obtained upon GC-MS measurement for the DEE_1 (*upper spectrum*) and OEE_1 – 2OH or HF_1 (*lower spectrum)* product

Table 41 Overview of patents reported for OME synthesis comprising patent number, catalyst and educt

Patent No.	catalysts	educts
US9447355B2	DTBP	DME, DMM
	Amberlyst 36	pFA/MeOH
EP2987781 A1	Amberlyst 36	pFA/MeOH/Dodecan
	Amberlyst 36	pFA/EtOH
WO2006/045506 A1	H_2SO_4/sulfonic acids/CF_3SO_3H/p-toluenesulfonic acid/heteropolyacids/acidic ion-exchangers (Amberlite IR 120)/TiO2/ZrO2	DMM/TRI/pFA
US2449469	H_2SO_4	DMM/pFA
	H_2SO_4	DMM/konz. FA Lösung
US5746785	HCOOH	DMM/pFA
US6392102	metal oxide catalysts	MeOH/FA
EP-A1070755	CF_3SO_3H	DMM/pFA
DE102005027702A1	water-free sulfuric acid, sulfonic acids such as CF_3SO_3H und para-toluenesulfonic acid, heteropolyacids, acidic ion-exchangers, zeoliths, alumosilicates, SiO_2, aluminium oxides, TiO_2 und ZrO_2	MeOH/pFA
US6392102B1	aluminosilicate	MeOH/pFA
US4341069	Cu, Zn, Cr	DME - synthesis
US2882243	Zeolite A	
US2882244	Zeolite X	
US313007	Zeolite Y	
US3702886	ZSM-5	
US3709979	ZSM-11	
US3832449	ZSM-12	
US5746785	formic acid	pFA/MeOH or DMM
WO2000029365A3	bentonites, montmorillonites, cation-exchange resins, sulfonated fluoroalkylene resins	FA/MeOH
	Cu-salt, Zn-salt	TRI/DMM
US7999140B2	sulfuric acid, Amberlyte IR 120	TRI/DMM/DME
US20180134642A1	ion-exchange resins, zeolites, aluminosilicates, aluminium dioxide, titanium dioxideAmberlyst® 15, Amberlyst® 46	FA/MeOH
US6534685	CF3SO3H	DMM/pFA
US7671240	mineral acids such as substantially anhydrous sulfuric acid, sulfonic acids such as trifluoromethanesulfonic acid and para-toluenesulfonic acid, heteropolyacids, acidic ion exchange resins, zeolites, aluminosilicates, silicon dioxide, aluminum oxide, titanium dioxide and zirconium dioxide. Oxidic catalysts may, in order to increase their acid strength, be doped with sulfate or phosphate groups	FA/MeOH
US2011/0313202	ionic liquids (two - step reaction)	aq. FA/MeOH

EP2987781A1	mineral acids, acidic ion-exchangers, zeoliths, alumosilicates, SiO_2, aluminium oxides, TiO_2 und ZrO_2	FA/MeOH
US5746785	formic acid	FA/MeOH
US2014/0114093	ionic liquids (two - step reaction)	FA/MeOH
US2015/0094497	ionic liquid	FA/MeOH
DE102005027701A1	mineral acids such as substantially anhydrous sulfuric acid, sulfonic acids such as trifluoromethanesulfonic acid and para-toluenesulfonic acid, heteropolyacids, acidic ion exchange resins, zeolites, aluminosilicates, silicon dioxide, aluminum oxide, titanium dioxide and zirconium dioxide. Oxidic catalysts may, in order to increase their acid strength, be doped with sulfate or phosphate groups	FA/MeOH
GB603872A	H_2SO_4	FA/dicycloalkyl or dialkyl formal (DMM, diethylformal, dicyclohexylformal, diisopropylformal, di-n-propyl formal, dibutylformal)
US6160174	anion exchange resin	MeOH/FA/DMM
US62655284	anion exchange resin	MeOH/FA/DMM
WO2006045506A1	H_2SO_4/Amberlite IR 120//Trifluormethan sulfonsäure/	DMM/TRI
US6160174A	molecular sieve	DME/MeOH
US5959156A	anion exchange resin	DME/FA
CA2581502A1	H_2SO_4/Amberlite IR 120//Trifluormethan sulfonsäure/	DMM/TRI
DE102016222657A1	acidic catalyst	FA/MeOH
WO2000029365A2	heterogeneous acidic catalyst (comprising formic acid, acetic acid); sulfonated/styrene-divinylbenzene copolymer, an acrylic acid-divinylbenzene copolymer, a methacrylic acid- divinylbenzene copolymertetrafluoroethylene resin derivative (trade name, Naflon H); CuZnTeO or CuZnSeO	FA/MeOH
CA25811502A1	Amberlyte IR 120/Trifluormethansulfuric acid/H2SO4/	DMM/TRI/OME2
US7560599B2	ionic liquid	MeOH/TRI
DE102009039437A1	sauren ionischen Flüssigkeit	DMM/TRI
WO2011067229A1	hydrophober Zeolit	TRI/FA
DE112011100027T5	ionic liquid	TRI/MeOH/DMM
US8987521B2	ionic liquid	FA/MeOH
US9067188B2	acid ionic liquid	FA/aliphatic alcohol
US9169186B2	ionic liquid	aq. FA/DMM
US2015/0094497	aicidic ionic liquid	pFA/MeOH

US20080207954A1	mineral acids such as substantially anhydrous sulfuric acid, sulfonic acids such as trifluoromethanesulfonic acid and para-toluenesulfonic acid, heteropolyacids, acidic ion exchange resins, zeolites, aluminosilicates, silicon dioxide, aluminum oxide, titanium dioxide and zirconium dioxide	FA/MeOH
US1315439	ionic liquid	TRI/MeOH
US6265528B1	anion exchange resin	MeOH/FA
EP3323800A1	acidic ion exchange resins (e.g. Amberlyst® 15, Amberlyst® 46), zeolites, aluminosilicates, silicon dioxide, aluminum oxide, titanium dioxide and zirconium dioxide	FA/MeOH/DMM
US6160174	ion exchangers	MeOH/DMM
CN102372613B	molecular sieve SAP0-34/ZSM-5/Fe-oxides, sulfates/MCM-22 (zeolite)/ionic liquid	MeOH/TRI
CN102372611B	molecular sieve SAP0-34/ZSM-5/Fe-oxides, sulfates/MCM-22 (zeolite)/ionic liquid	MeOH/TRI
CN102372615B	molecular sieve SAP0-34/ZSM-5/Fe-oxides, sulfates/MCM-22 (zeolite)/ionic liquid	TRI/DMM
CN102432441A	acidic styrene cation A-70	DMM/TRI
CN104086380B	graphene oxide	MeOH/TRI
CN105294411B	conjugated polymeric support	pFA/MeOH/DMM
CN104177237B	aluminosilicate	TRI/DMM
CN104292084B	molecular sieve	DMM/TRI
CN101182367A	ionic liquid	MeOH/TRI
CN101768058B	ZSM-5/MCM-22/MCM-56	MeOH/
CN103664549A	SBA-15/MCM-41/MCM-22	MeOH/DMM/pFA
CN103880612A	HZSM-5/Mg/HZSM-5/Al-/Zn-/Cu-P/Zn-P/Mo/Mo-P	MeOH/DMM/pFA
CN103420815A	SBA-15/MCM-41/MCM-22 addition of SO42-/ZrO2	
CN102040491	solid zeolite catalyst	pFA
CN101768057A	H_2SO_4/HCl/peroxosulfuric acid + carrier (ZrO2, TiO2..)	MeOH/TRI
CN200710018474.9	ionic liquid cation (quarternary phosphonium salt, triflurormethanesulfonate anion)	MeOH/pFA/TRI
CN101972644A	Nb-oxided catalyst	DMM/TRI
CN102180778A	p-toluenesulfonic acid	lower alcohols/pFA
CN102249870A	MCM-22	MeOH/TRI
CN102320941	solid super acids	DMWT%eOH
CN102372615A	SAP0-34 molecular sieve and other strongly acidic resins	DMM/TRI
CN102372613A	SAP0-34/zeolite MCM-22/X-type zeolite/cationic acidic ionic liquid portion to 1-methyl-3- (4-sulfonato-butyl) imidazolium ion, anionic moiety selected bisulfate	MeOH/TRI

CN1031121924A	SAP0-34/zeolite MCM-22/X-type zeolite/cationic acidic ionic liquid portion to 1-methyl-3- (4-sulfonato-butyl) imidazolium ion, anionic moiety selected bisulfate	MeOH/TRI
CN103664547A	S042_ / Zr02 / SBA-15	MeOH/DMM/TRI
CN104276932A	amorphous aluminosilicate	MeOH/DMM/pFA
CN101665414A	ionic liquid	TRI/DMM
CN102040488A	beta-zeolum, ZSM-5/MCM-22/MCM-56	carbinol/TRI
CN103420813A	ZSM-5/ZSM-11	MeOH/DME/FA/TRI
CN103420814A	ZSM-11	MeOH/DME/FA/TRI
CN103420818A	molecular sieve MEL)	MeOH/DME/FA/TRI
CN103664545A	ionic exchange resin	MeOH/DMM/FA
CN103664546A	ZSM-5 (different preparation of the catalyst)	MeOH/DME/FA/TRI
CN103739459A	molecular sieve	MeOH/DME/FA/TRI
CN103739460A	H4PWMo6O4 tungsten heteropoly acid	MeOH/TRI
CN103772161A	molecular sieve + heteropolyacid	MeOH/DMM/pFA
CN103772162A	acidic ion exchange resin	MeOH/DMM/TRI
CN104151148A	activated carbon carrier	MeOH/DMM/pFA
CN106397142A	molecular sieves structures of H-MFI, H-Y and H-beta	DMM/TRI
CN104549443B	strong ion modified acidic zeolite; the modified metal selected from Sn, Mn, Cu, Ti	FA
CN102040490A	SO4<2->/ZrO2, SO4<2->/Fe2O3, Cl<->/TiO2, Cl<->/Fe2O3, SO4<2->/Al2O3 and S2O8<2->/ZrO2	DMM/TRI
CN103848730A	stron acidic resins	pFA/DMM
CN102040491A	beta zeolite, X zeolite, Y zeolite, ZSM-5 molecular sieve, MCM-22, MCM-56, UZM-8 or SAPO-34	MeOH/TRI/pFA/DMM
CN101768058A	Beta zeolite, ZSM-5 molecular sieve, MCM-22 and MCM-56 zeolite molecular sieve	MeOH/TRI/MeOH
CN102786397A	stron acidic resins	pFA melt with DMM
CN102964227A	elected modified styrene - divinylbenzene based resins/sulfonated tetrafluoroethylene resin/acrylic/molecular sieves is selected from zeolite 3A, 4A molecular sieves, 5A molecular sieves , 13X molecular sievesdivinylbenzene based resinsmethacrylic acid - divinylbenzene resin, a sulfonated tetrafluoroethylene resin;	pFA/DMM
CN102000559A	Nb-oxided catalyst	DMM/TRI
CN102295734A	molecular sieve	pFA/DMM
CN 200910201661	Beta zeolum, ZSM-5 molecular sieve and MCM-22 or MCM-56 zeolum molecular sieve	DMM/TRI
CN101182367A	acidic ionic liquid	FA/MeOH

CN101962318A	ionic liquid	FA/MeOH
CN 200910056819.9	solid superacids	MeOH/TRI
CN103420816A	SAPO-5 molecular sieve	MeOH/DME/FA/TRI
CN103420814A	ZSM-11	MeOH/DME/FA/TRI
CN102249868A	ionic liquid	TRI/MeOH
CN102786396A	cyclic amide ionic liquid	TRI/MeOH/DMM
CN102786395A	pyrrolidine ionic liquid	pFA/DMM/TRI/MeOH
CN104016838A	ionic liquids	DMWT%eOH/FA
CN104722249A	acidic catalyst (reactor column with catalyst packed section)	DMM/FA
CN103772164A	ionic liquid	FA/alcohol
CN104513141A	ionic liquid	pFA/MeOH
CN104045530A	ionic liquid catalysts	conc. FA/MeOH
CN103121924A	WO3/ZrO2-SiO2 or MoO3/ZrO2-SiO2	MeOH/DME/FA/TRI
CN103739458B	Al-MCM-41, Al-MCM-48, Al-SBA-15, Al-HMS, Al -MSU-1 or Al-MSU-2	MeOH/DME/FA/TRI
CN103664550B	strongly acidic cation exchange resin, sold currently strongly acidic market listing cation exchange resin	FA/DMM
CN104447237B	fixed bed reactor	MeOH/FA
CN104971667B	fluidized bed reactor /molecular sieves, ion exchange resins	pFA/DMM
CN104974025B	cation exchange resin, molecular sieves and silica	pFA/DMM